TABLE OF MAGNETIC DIPOLE ROTATIONAL BANDS

AMITA and ASHOK KUMAR JAIN

Department of Physics, University of Roorkee

Roorkee - 247667, India

and

BALRAJ SINGH

Department of Physics & Astronomy, McMaster University

Hamilton, Ontario L8S 4M1, Canada

The experimentally observed level structures which appear to support the newly proposed magnetic rotation phenomenon in weakly deformed nuclei are classified according to their intrinsic structures and other measured properties such as $B(M1)/B(E2)$ values, lifetimes, etc. A total of 120 magnetic dipole-rotational bands are observed in 56 nuclei spread over four mass regions, namely, $A = 80$ ($Z = 35$–37), 110 ($Z = 48$–51), 135 ($Z = 54$–64), and 195 ($Z = 80$–86); 42 such bands are observed in Pb isotopes alone. Interpretation of these bands in terms of shears mechanism and other possibilities are briefly discussed. A number of high-spin features such as signature splitting, signature inversion, and backbending are also discussed. The literature cutoff date for the data is August 1999. © 2000 Academic Press

CONTENTS

INTRODUCTION

Experimental observation of features like rotational bands and enhanced transition probabilities usually signify the presence of nonsphericity in nuclei. Normally one observes enhanced electric quadrupole transitions connecting $\Delta I = 2$ levels in a rotational band. Observation of quasirotational bands based on configurations which are known to be nearly spherical is therefore quite unexpected. Nuclear structure physics has in recent times been witness to the observation of many such groups of levels which appear to have rotational character and display enhanced magnetic dipole transitions connecting $\Delta I = 1$ levels. Such bands have therefore been termed in the literature "magnetic dipole" or "magnetic rotational" bands and subsequently also "shears" bands. Observation of such structures has given rise to much excitement, and one hopes that many new and exotic coupling schemes may be identified [1]. In this paper we present a Table of the established as well as the most likely candidates of magnetic rotation (MR) bands. The literature cutoff date for the data is August 1999.

Most MR-band nuclei are either even–even or odd–A; only a few odd–odd nuclei are known to have such bands. The largest aggregate of data occurs in the $A \approx 195$ mass region, where 12 lead isotopes having $191 \leq A \leq 202$ display as many as 42 MR bands. All the nuclei included in the compiled Table are shown in Fig. 1. Each nucleus is assigned a box that exhibits the total number of

MR bands, the minimum excitation energy, the minimum and maximum spins assigned in these bands, the corresponding parities, and the number of bands which exhibit backbending. It should be noted that a critical evaluation of the experimental data is not the aim of this paper and most of the information has been gleaned from the references cited for each band; a total of 81 references have been cited.

Salient Features of Magnetic Dipole Rotational Bands

Based on observations made so far and on theoretical calculations, MR bands are expected to display the following properties:

1. The bands exhibit a $\Delta I = 1$ structure rather than a $\Delta I = 2$ structure and have a somewhat rotational character.

2. They are typically observed in nearly spherical nuclei, most having a very small oblate deformation, although many are also known to have small prolate deformation.

3. The bandhead lies at a high excitation energy (a few MeV) and has a high spin ($I \sim 10$–$15\ \hbar$) and a high value of K (the projection of I on the symmetry axis), both indicative of a multi-quasiparticle character.

4. Intraband transitions are predominantly magnetic dipole (M1) in nature, with B(M1) values being of the order

FIG. 1. Isotope chart of Z vs N for the magnetic dipole rotational bands included in this compilation. See key (inset) for the interpretation of the entries in each box.

Chart entries (by element row and neutron number N):

Top block — N = 109–120

- $_{86}$Rn: N=119: 1, ~2.3, $21/2^+$ $41/2^+$, BB(1)
- $_{83}$Bi: N=114: 1; N=115: 1; N=116: 2; N=119: 3; N=120: 1
- $_{82}$Pb: N=109: 2, 2.4, $27/2^+$ $45/2^+$, BB(1); N=110: 2, 4.2, 15^- 25^-, BB(1); N=111: 5, ~2.7, $29/2^+$ $61/2^+$, BB(2); N=112: 3, 4.1, 13^+ 31, BB(2); N=113: 3, 3.0, $27/2^-$ $55/2^-$, BB(2); N=114: 4, 16^- 30, BB(2); N=115: 3, 3:3, $27/2^-$ $65/2^-$, BB(2); N=116: 5, 18^- 28, BB(1); 3; N=117: 5, 3.6, $25/2^+$ $73/2^+$, BB(3); N=119: 5, $35/2$ $51/2$; N=120: 2
- $_{80}$Hg: N=112: 2, 6.3, 22^+ 34^+, BB(2); N=113: 3, 5.3, $47/2^-$ $75/2^-$, BB(3); N=115: 3, 5.2, $43/2^+$ $71/2^-$, BB(2); N=116: 1, ≥ 6.4, 22^+ 30^+, BB(1)

Second block — N = 70–80

- $_{64}$Gd: N=78: 2, 4.8, 12 21^+, BB(2); N=79: 1, 5.4, 14^+ 23^+, BB(1)
- $_{62}$Sm: N=77: 1, 3.3, $25/2^-$ $41/2$, BB(1)
- $_{60}$Nd: N=74: 3, 2.3, 8^- 27^-, BB(3); N=76: 5, 3.8, 9^- 29^+, BB(2); N=77: 3, 3.9, $27/2^-$ $53/2^+$, BB(2); N=78: 1, 5.6, 14 21, BB(1)
- $_{59}$Pr: N=74: 3, 2.1; N=78: 1, 3.4, $25/2^-$ $41/2^-$, BB(1)
- $_{58}$Ce: N=77: 3, 3.2, $23/2^+$ $43/2^-$, BB(2); N=78: 1, 5.6, 14^- 22^-
- $_{57}$La: N=74: 2, 2.1, $19/2^-$ $43/2^-$
- $_{56}$Ba: N=76: 2, 4.1, 10^+ 15^-
- $_{54}$Xe: N=70: 1, 5.1, 12 24, BB(1)

Third block — N = 55–64

- $_{51}$Sb: N=57: 2, 2.1, 7^- 20^-, BB(1); N=61: 2, 1.7, 7^- 19^+, BB(1)
- $_{50}$Sn: N=55: 1, 7.0, $29/2^+$ $43/2^+$, BB(1); N=56: 2, 8.0, 15^- 22^-, BB(1); N=58: 2, 6.7, 12^- 22^-
- $_{49}$In: N=62: 3, 3.5, $19/2^-$ $43/2^+$, BB(2); N=63: 2, 2.2, $15/2^-$ $33/2^+$, BB(1)
- $_{48}$Cd: N=59: 2, 5.6, 11^- 21^-, BB(1); N=60: 2, 3.3, $21/2^-$ $39/2^-$, BB(1); N=61: 3, 5.8, 13^- 24

Fourth block — N = 42–48

- $_{37}$Rb: N=42: 1, 3.3, $19/2^-$ $27/2^-$; N=44: 1, 2.6, $15/2^-$ $25/2^-$; N=45: 1, 2.6, 11^- 16^-; N=46: 1, 2.3, $13/2^-$ $21/2^-$; N=47: 1, 3.4, 11^- 17^-; N=48: 1, 3.2, $17/2^-$ $23/2^-$, BB(1)
- $_{36}$Kr: N=43: 1, 2.9, $17/2^-$ $23/2^-$
- $_{35}$Br: N=42: 1, 2.9, $17/2^-$ $23/2^-$; N=44: 1, 2.4, $13/2^-$ $21/2^-$; N=46: 1, 2.5, $13/2^-$ $21/2^-$

Key (inset):

No. of Bands	$E_{\min}$(MeV)
I^π(min.)	I^π(max.)

BB = Backbending

---

of several Weisskopf units. Crossover E2 transitions are either very weak or absent, so that B(E2) values are $\lesssim 0.1$ (eb)^2. The ratio B(M1)/B(E2) is therefore quite large, with values $\sim$10–100 (μ_N/eb)^2. In normal rotational bands this ratio is less than 1 (μ_N/eb)^2. In a number of MR bands in the $A = 110$ and 195 mass region, a decrease in the B(M1) values with increasing spin has been observed.

5. These bands have generally weak connections to other yrast states.

6. These bands carry a dynamical moment of inertia of the order of $\Im^{(2)} = 10$–$25\ \hbar^2$MeV^{-1}, smaller than the dynamical moments of inertia of normal-deformed and superdeformed nuclei. The ratio $\Im^{(2)}/B$(E2) is larger than 150 $\hbar^2$MeV^{-1}(eb)$^{-2}$ here, in comparison to a value of 15

$\hbar^2 \mathrm{MeV}^{-1}(\mathrm{eb})^{-2}$ in well-deformed nuclei and 5 $\hbar^2 \mathrm{MeV}^{-1}(\mathrm{eb})^{-2}$ in superdeformed nuclei.

Keeping these characteristics in mind, we have been able to extract from the published literature on experimentally observed level structures 120 MR bands in 56 nuclei. These are spread over four mass regions, namely $A = 77–85$, $105–113$, $124–144$, and $191–205$. While most of these bands have been assigned oblate many-quasiparticle configurations, several prolate configurations have also been assigned to bands in the lighter mass regions.

We find that in addition to the above-mentioned characteristics, the experimentally observed bands also exhibit the following features:

1. Some of these cascades do not display an $I(I + 1)$ behavior and are irregular in their structure.
2. Many MR bands display signature splitting.
3. A large number of cases display backbending.

Physical Mechanism of Magnetic Rotation

The largest number of MR bands has been identified in Pb nuclei, and these, therefore, constitute the foremost testing ground for the various physical mechanisms which could give rise to rotation-like features with strong magnetic dipole transitions connecting $\Delta I = 1$ states. A configuration assignment for the bands has been possible in most of the cases in Pb nuclei based on considerations such as (i) the excitation energies and angular momenta, (ii) comparisons with the known excitations in neighboring nuclei, and (iii) estimates from model calculations. Unlike the superdeformed bands, the linking transitions have been seen in a large number of cases; the excitation energies and the angular momenta are therefore known with greater certainty in many instances.

The low-lying excitations of neutron-deficient Pb isotopes are known to consist of spherical states arising from neutron hole excitations, and further higher-lying excitations are formed on weakly oblate states built on broken-pair proton (particle–hole) excitations across the core. As an example, the 0^+ state at 931 keV in $^{194}\mathrm{Pb}$, having a small oblate deformation [2], is built on the $\{\pi 9/2^-[505]\}^2$ configuration of the $h_{9/2}$ orbital. Two high-spin isomeric excitations are observed at 2438 and 2934 keV, having $I^\pi = 8^+$ and 11^-, respectively [3]; these are interpreted as $(2p2h)$ broken proton-pair shell model configurations given by $[\{\pi h_{9/2},\ 9/2^-[505]\} \otimes \{\pi h_{9/2},\ 7/2^-[514]\}]_{K^\pi = 8^+}$ and $[\{\pi h_{9/2},\ 9/2^-[505]\} \otimes \{\pi i_{13/2},\ 13/2^+[606]\}]_{K^\pi = 11^-}$. Both these configurations are also known to be associated with a small oblate deformation $\beta_2 \sim -0.18$ as suggested by some calculations. However, no regular collective bands built on these states have been observed.

The $\Delta I = 1$ bands observed in the lead isotopes have been assigned configurations consisting of the $K^\pi = 11^-$ excitation coupled to low-Ω one/three quasineutrons (in odd–A nuclides) or two/four quasineutrons (in even–A nuclides). Since the protons occupy high-Ω states, their density distribution is like a torus with angular momentum pointing along the symmetry axis. The low-Ω neutron hole states, on the other hand, have a dumbbell-like density distribution, with angular momentum pointing along a direction perpendicular to the symmetry axis [4, 5]. Maximum overlap between the two density distributions is therefore obtained when the angular momenta of proton particle and neutron hole are perpendicular to each other, and the resultant angular momentum lies somewhere between the proton and the neutron angular momenta, as shown in Fig. 2a. Frauendorf [4, 6, 7] suggested that these two angular momenta are like the two blades of a pair of shears, and that the unusual properties of MR bands, such as the generation of high angular momenta at such low deformation, predominance of regular M1 transitions, lack of signature splitting, etc., can be explained if the two blades simultaneously align toward the resultant total angular momentum to generate higher angular momentum states (cf. Fig. 2b). This mechanism has hence been named the "shears mechanism." A tilted-axis version of the Cranking model (TAC) was proposed [4] which incorporates this shears mechanism quite successfully and gives a good estimate of the excitation energies, spins, and $B(\mathrm{M1})/B(\mathrm{E2})$ values of many such bands.

A similar mechanism is seen to work in the $A = 110$ and 135 mass regions although different orbitals are involved. In the $A = 110$ mass region the active orbitals are high-Ω proton $g_{9/2}$ holes, driving the nucleus toward a slightly prolate shape of $\beta_2 \sim 0.13$, and low-Ω neutron $h_{11/2}$ particles [7]. Due to the shape of their density distribution, the proton angular momentum vector aligns itself toward the nuclear symmetry axis while the neutron angular momentum vector aligns toward an axis perpendicular to it. In the $A = 135$ mass region, $h_{11/2}$ proton particles and $h_{11/2}$ neutron holes are involved in the configuration of MR bands [8]; sometimes $g_{7/2}$ protons are also assigned a role. The coexistence of prolate and oblate shapes is predicted in different bands in a few nuclei. However, the interpretations are not as firm in these mass regions as in the $A = 195$ mass region. It may be noted that the high-j intruder orbitals, which are known to play an important role in many high-spin phenomena such as superdeformation, also play an important role in generating MR bands.

Recent calculations based on the spherical shell model with a reasonable configuration space for protons and neutrons have also been able to reproduce regular MR bands and confirm the shears mechanism of generating magnetic dipole rotational bands [9].

A suggestion has recently been made that the shears mechanism may arise due to a residual interaction between the protons and neutrons in the two blades [10]. An interaction of the $P_2(\theta)$ kind can be mediated through the core by particle–vibration coupling acting in second order. This
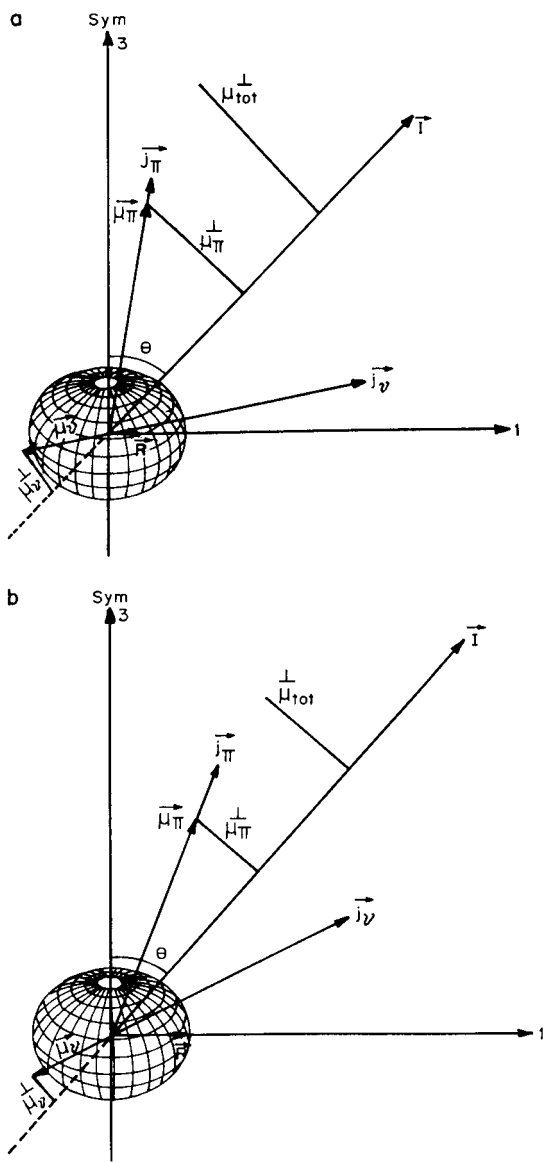
a

b

FIG. 2. Schematic coupling scheme of shears mechanism for a small oblate deformation in the Pb region at (a) small rotational frequency and (b) large rotational frequency. For details see text.

kind of physical mechanism may not require the presence of a deformed mean field for nearly spherical nuclei.

Application of Tilted-Axis Cranking Model

A general TAC Hamiltonian for a single particle is given by [4]

$$h'_{TAC} = h_{sp} - \omega(j_1 \sin\theta \cos\varphi + j_2 \sin\theta \sin\varphi + j_3 \cos\theta),$$ (1)

where h_{sp} is the single particle Hamiltonian in a deformed field (e.g., a deformed oscillator or a deformed Woods–

Saxon potential); ω is the rotational frequency, and (θ, φ) are the tilting angle and the azimuthal angle of the total angular momentum, respectively; and (j_1, j_2, j_3) are the components of particle angular momentum j along the (1, 2, 3) axes, respectively, where the 3-axis is the symmetry axis.

Detailed calculations have been reported in the literature for the MR bands, where, using the multiparticle version of the TAC, pairing and residual interactions have also been included (for example see [11, 12] and references therein). Within the pairing plus quadrupole–quadrupole model, the quasiparticle Routhian is given by [5]

$$h' = h_{sp} - \hbar\omega_0\beta\left(\cos\gamma q_0 - \frac{\sin\gamma}{\sqrt{2}}(q_2 + q_{-2})\right)$$
$$- \Delta(P^+ + P) - \lambda n - \omega(j_1 \sin\theta + j_3 \cos\theta), \quad (2)$$

where $\varphi = 0°$ has been substituted to reduce the three-dimensional problem to a planar one. Here, $\hbar\omega_0 = 41A^{-1/3}$; β and γ are the usual deformation parameters; and q_0, q_2, and q_{-2} are the expectation values of the respective components of the quadrupole tensor Q. The operator P^+ creates the pair field, the strength of which is fixed by the gap parameter Δ. The Fermi level λ is fixed to give the correct particle number. As an example, we have performed calculations for the MR band in ^{105}Sn by using the TAC code [13]. The proton pairing was neglected in these calculations because the proton $Z = 50$ shell is closed. For the neutrons, pairing was taken into account using a constant $\Delta_\nu = 0.80$ MeV. The neutron Fermi level λ was calculated to give the appropriate particle number. We have done calculations for a series of deformation parameters to minimize the total energy in the lab frame and found that the most suitable deformation in this case is $\beta = 0.137$ and $\gamma = 10°$. Single proton and single quasineutron Routhians were then calculated. Taking the bandhead spin and parity into consideration, we chose the configuration $\pi(g_{9/2}^{-1}g_{7/2}) \otimes \nu[h_{11/2}^2(g_{7/2}d_{5/2})^1]$ and calculated the total quantities (like spin, energy, equilibrium tilt angle θ). In order to compare the experimental results with the calculated ones, we transform the experimental energies $E(I)$ into rotational frequencies by using the relation

$$\hbar\omega(I) = E(I) - E(I - 1). \quad (3)$$

The results of our calculations along with the experimental results [14] are shown in Fig. 3, where the total angular momentum I vs $\hbar\omega$ is plotted. The TAC curve differs slightly from the observed values but exhibits the same trend. The observed values also show a backbending that has been attributed in [14] to the alignment of a $(g_{7/2}d_{5/2})$ neutron pair. The wavefunctions so obtained can be used to calculate the electromagnetic transitions and other properties, as discussed in the following section.
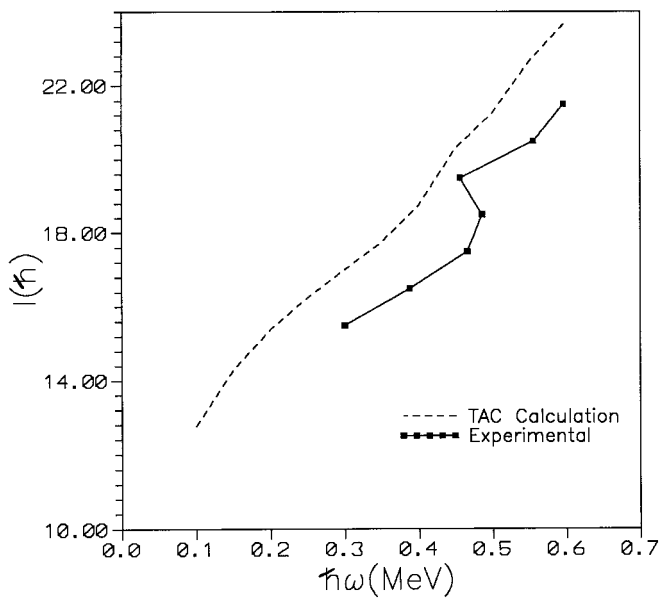
FIG. 3. Angular momentum vs rotational frequency for ^{105}Sn using the TAC model for the configuration $\pi(g_{9/2}^{-1}g_{7/2}) \otimes \nu[h_{11/2}^2(d_{5/2}g_{7/2})^1]$ and the deformation parameters $(\beta, \gamma) = (0.137, 10°)$ along with the experimental curve for the dipole band in ^{105}Sn.

Electromagnetic Properties of Magnetic Dipole Rotational Bands

A $\Delta I = 1$ structure and large intraband $B(M1)$ values immediately suggest that the MR bands are based on high-K proton configurations. In the strong coupling limit [15],

$$B(M1, I \rightarrow I') = \frac{3}{4\pi} K^2 (g_K - g_R)^2 |\langle I'K10|IK\rangle|^2, \quad (4)$$

where g_K is the proton g-factor and $g_R \approx Z/A$. When both K and $(g_K - g_R)$ are large, the $B(M1)$ value increases. However, the trend of the $B(M1)$ values with rotational frequency distinguishes a high-K band from a MR band.

The coupling scheme for the bandhead in a tilted axis representation is shown in Fig. 2a, with the proton angular momentum vector close to the nuclear symmetry axis (deformation-aligned) and the neutron angular momentum vector close to an axis perpendicular to it (rotation-aligned). Such a coupling gives rise to a large perpendicular component of the magnetic moment, $\mu^\perp = \mu_\pi^\perp + \mu_\nu^\perp$. Higher angular momentum states are generated by a gradual alignment of the neutron and proton blades with the total angular momentum $\vec{I}$. As $\vec{I}$ increases, $\mu^\perp$ decreases. Since the $B(M1)$ values are proportional to $|\mu^\perp|^2$, the shears mechanism predicts decreasing $B(M1)$ values with increasing spin along the band. The $B(M1)$ and $B(E2)$ values can be calculated in the TAC model by using the expressions [4, 6],

$$B(M1) = \frac{3}{8\pi} \big[\sin\theta \{ g_{l,\pi}\langle j_{\pi,3}\rangle_\omega + (g_{s,\pi} - g_{l,\pi})\langle s_{\pi,3}\rangle_\omega$$
$$+ g_{s,\nu}\langle s_{\nu,3}\rangle_\omega \} - \cos\theta \{ g_{l,\pi}\langle j_{\pi,1}\rangle_\omega$$
$$+ (g_{s,\pi} - g_{l,\pi})\langle s_{\pi,1}\rangle_\omega + g_{s,\nu}\langle s_{\nu,1}\rangle_\omega \} \big]^2 \quad (5)$$

and

$$B(E2) = \frac{15}{128\pi} (eQ_0 \sin^2\theta)^2, \quad (6)$$

where the average values of the components of j, the spin s, and the intrinsic electric quadrupole moment Q_0 are calculated from the TAC model configurations. The g's are the usual gyromagnetic factors. In Fig. 4, we show the results of our calculations for $B(M1)$ and $B(M1)/B(E2)$ values for the ^{105}Sn nucleus discussed in the previous section. We find that both $B(M1)$ and $B(M1)/B(E2)$ values decrease with increasing rotational frequency and hence with increasing angular momentum, thus proving the validity of the shears mechanism in the mass $A = 110$ region.

A comparison of the calculated values with the recently measured $B(M1)$ values in a series of Pb isotopes with $A = 193$–197 has confirmed the decrease in $B(M1)$ with increasing angular momentum [11]. This constitutes the strongest argument in favor of the shears mechanism in lead nuclei. It may be emphasized that whereas the ratios such as $B(M1)/B(E2)$ may be explained on the basis of principal axis cranking, the behavior of $B(M1)$ with angular momentum confirms that it is a new mode of excitation which requires the TAC.

Measurement of the g-factor is another sensitive test of a configuration. For example, the g-factor of the 2584-keV bandhead in ^{193}Pb was measured [16] to be 0.68 ± 0.03, which matches very well with the calculated value 0.71 ± 0.04 for the assigned configuration $[(\pi h_{9/2} \otimes i_{13/2})_{K^\pi=11^-} \otimes (\nu i_{13/2})^{-1}]_{K^\pi=29/2^-}$; other configurations do not reproduce the measured value.

Another useful quantity which is reported more often and which highlights the large strength of the M1 transitions is the ratio $B(M1)/B(E2)$. It can be obtained from experiment by using the expression [17]

$$\frac{B(M1)}{B(E2)} = \frac{0.6968E_{\gamma2}^5}{\lambda E_{\gamma1}^3(1 + \delta^2)}, \quad (7)$$

where $E_{\gamma1,\gamma2}$ are the respective γ-ray energies in MeV corresponding to the M1 ($\Delta I = 1$) and E2 ($\Delta I = 2$) transitions from a state I, λ is the γ-ray intensity ratio $[I(\gamma_2)/I(\gamma_1)]$, and δ is the mixing ratio for the $\Delta I = 1$ transition. Since observed M1 transitions are much stronger than the E2 transitions, it may be assumed that the $\Delta I = 1$ transitions are pure M1 transitions and therefore the mixing ratio may
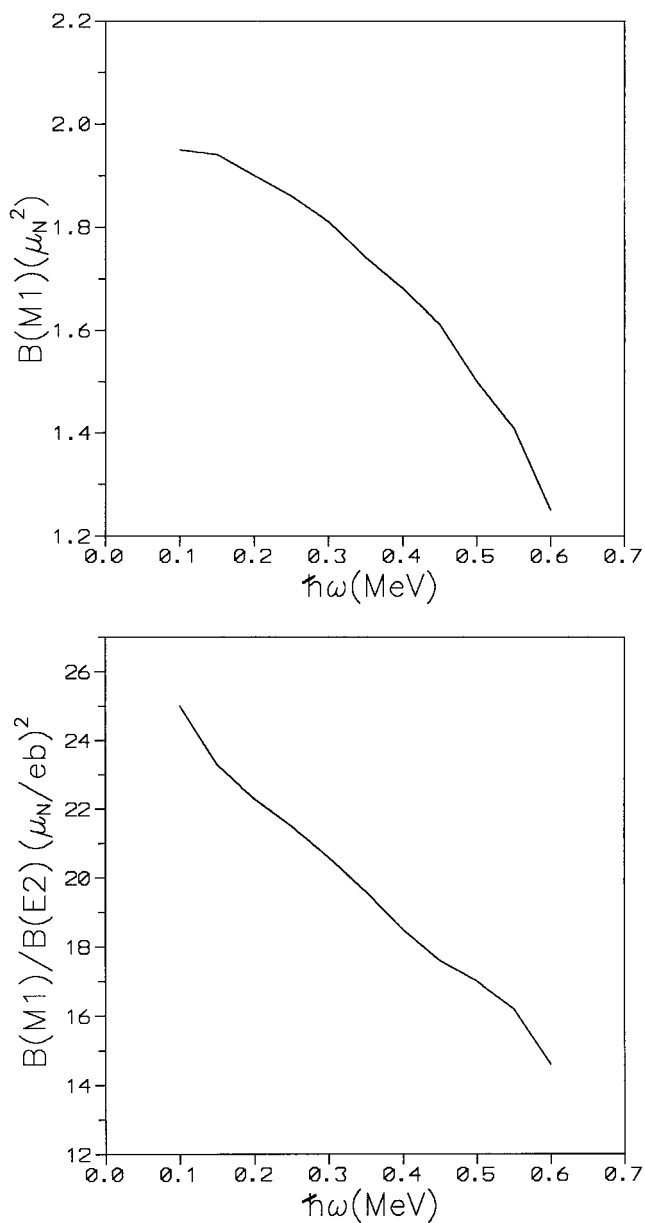
FIG. 4. The B(M1) (upper panel) and B(M1)/B(E2) values (lower panel) vs rotational frequency from the TAC model calculations for the configuration shown in Fig. 3.

be ignored. We tabulate this B(M1)/B(E2) ratio in the Table for a large number of cases. It turns out to be of the order of $10–100$ $(\mu_N/\text{eb})^2$ as compared to a value less than 1 $(\mu_N/\text{eb})^2$ in normally deformed nuclei.

Moments of Inertia, Alignment, and Backbending

The kinematic moment of inertia $\Im^{(1)} = \hbar I/\omega = \hbar^2 I/E_\gamma(I \rightarrow I - 1)$ and the dynamic moment of inertia $\Im^{(2)} = \hbar dI/d\omega = \hbar^2/\Delta E_\gamma(I)$ are plotted in Fig. 5 for some

typical cases from the $A = 80, 110, 135,$ and 195 mass regions. Here $\Delta E_\gamma(I) = E_\gamma(I \rightarrow I - 1) - E_\gamma(I - 1 \rightarrow I - 2)$. We notice many similarities in the four plots from each mass region. The $\Im^{(1)}$ values (solid lines) generally decrease with increasing angular momentum, a trend opposite to what one observes in normal deformed rotational bands where $\Im^{(1)}$ generally rises with increasing angular momentum. This is indicative of a large contribution to the total angular momentum from a source other than collective. Also the $\Im^{(2)}$ values are typically considerably smaller than $\Im^{(1)}$, again indicating a large contribution to the total angular momentum from alignment; the very large fluctuations in $\Im^{(2)}$ values shown in some MR bands are due to a backbending in these bands. More recently, the behavior of $\Im^{(1)}$ and $\Im^{(2)}$ as a function of angular momentum has also been shown to be consistent with the $P_2(\theta)$ type of residual interaction between protons and neutrons [18].

For rotational bands in normal deformed nuclei, the moment of inertia is directly proportional to the B(E2) values, and hence the ratio $\Im^{(2)}/B$(E2) is expected to be roughly constant. For MR bands, this ratio is, on average, more than a factor of 10 larger than in well deformed nuclei, which shows that only a fraction of the inertia is generated by the rotation of the deformed core. It should be noted, however, that ratios $\Im^{(2)}/B$(E2) as large as 10 can also come about for a normal rotor in the presence of pairing and having a small deformation.

A kind of singularity or sharp rise is observed in the value of $\Im^{(2)}$ at angular momenta where backbending occurs, which is normally attributed to a bandcrossing with a further alignment of the $i_{13/2}$ quasineutron pair in Pb nuclei and an alignment of the $h_{11/2}$ neutron pair in the mass 110 and 135 regions. For example an upbend at $\hbar\omega \sim 0.38$ MeV in band 2 of ^{196}Pb having configuration $\pi(h_{9/2} \otimes i_{13/2}) \otimes \nu(i_{13/2})^{-2}$ is attributed to a second $i_{13/2}$ quasineutron pair crossing [19]. Thus after the crossing, the configuration becomes $\pi(h_{9/2} \otimes i_{13/2}) \otimes \nu(i_{13/2})^{-4}$. A similar bandcrossing is also noticed in band 3 of ^{198}Pb but at a higher frequency; the shift in frequency may be interpreted as this band having some pairing prior to crossing. It is also possible to interpret the backbending as the crossing of two shears bands. When a second shears band crosses the first shears band, the shears angle opens up again from a small value (near 0°) to a large value (near 90°). The experimental evidence in favor of such a crossing would be a sudden rise in the B(M1) value near the crossing frequency. It would be very interesting to make such measurements.

Regular and Irregular Bands

While most of the bands are nearly regular (not considering backbending as an irregularity), some of the bands appear quite irregular. It may be pointed out that with better statistics in experiments, the order of transitions has been
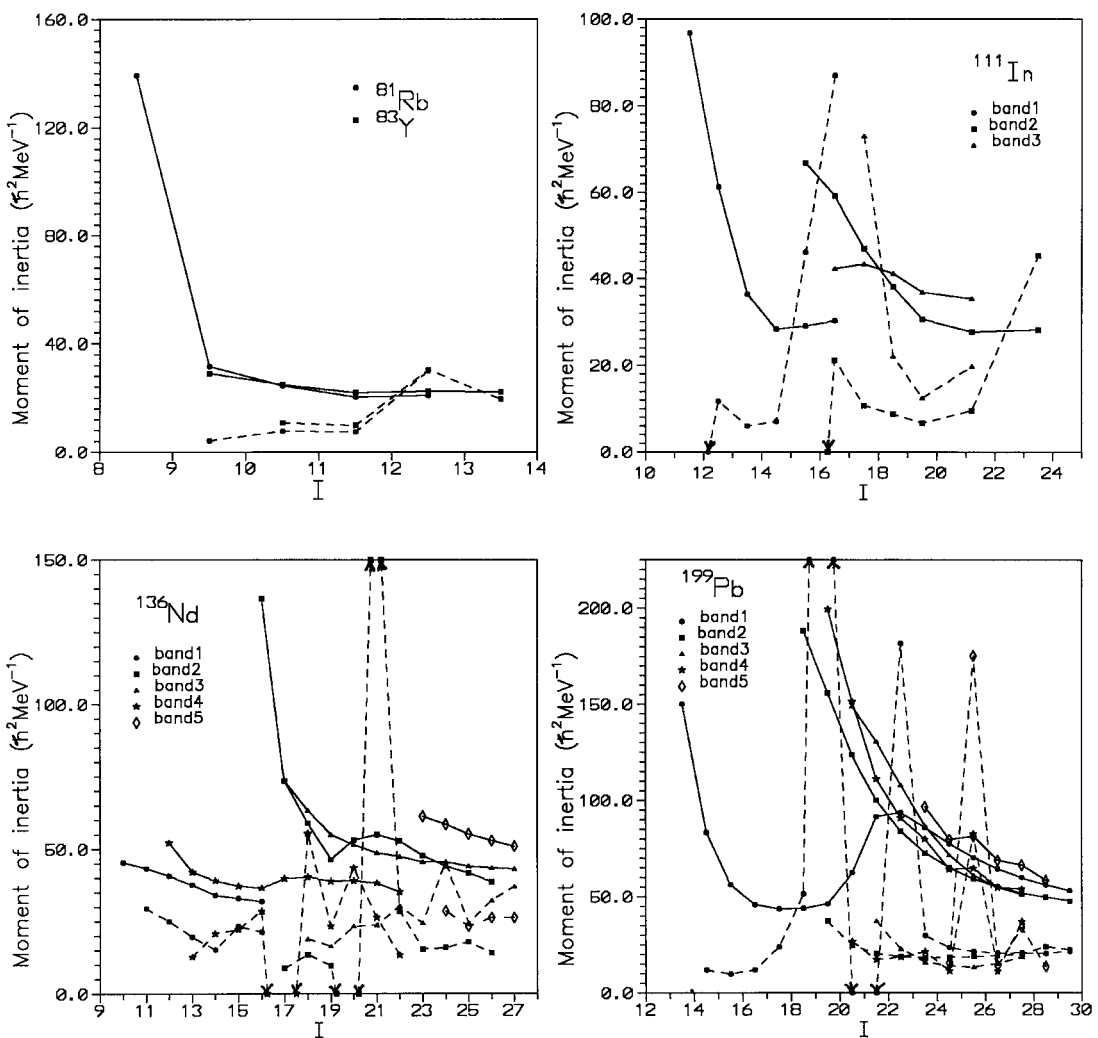
FIG. 5. Kinematic (solid lines) and dynamic (dashed lines) moments of inertia vs spin plotted for five nuclei from the $A = 80$, 110, 135, and 195 mass regions.

changed in many cases, thereby making some irregular bands regular. Also, it may be noted that signature splitting in a band must be distinguished from the irregular nature of a $\Delta I = 1$ band. This distinction may be achieved by dividing a $\Delta I = 1$ band into two $\Delta I = 2$ bands, then analyzing the levels within the $\Delta I = 2$ subbands for regularity and bandcrossing. For example, band 3 of ^{196}Pb, which otherwise looks quite irregular, on dividing into two bands can be interpreted as a rotational structure with alignment taking place around the 1237-keV level [19].

Signature Splitting

The TAC model mixes states of good signature. It is therefore expected that MR bands may not have a signature splitting. We find that 14 of the 42 MR bands experimentally observed in the Pb nuclei display a signature splitting.

We did not include a few other cases because it was difficult to make a judgment in those cases where only three or four transitions are known. In Fig. 6, we plot $\Delta E_\gamma(I)$ vs I for 6 of the 14 cases; a signature splitting is evident in all the cases. It is interesting to note that 2 cases, namely band 2 of ^{195}Pb and band 4 of ^{199}Pb, also exhibit a signature inversion. Such phenomena of signature splitting and signature inversion have been observed and studied in normal deformed even–even [20], odd–A, and odd–odd nuclei [21] and can be explained by using the particle-rotor model [22, 23].

An odd–odd nucleus with the odd proton and the odd neutron in appropriate orbitals is the simplest system for simulating the shears mechanism. Accordingly we have used the two-quasiparticle-plus-rotor model for a deformation-aligned proton particle in an $h_{9/2}$, $9/2[514]$ orbit and a rotation-aligned neutron hole in an $i_{13/2}$,
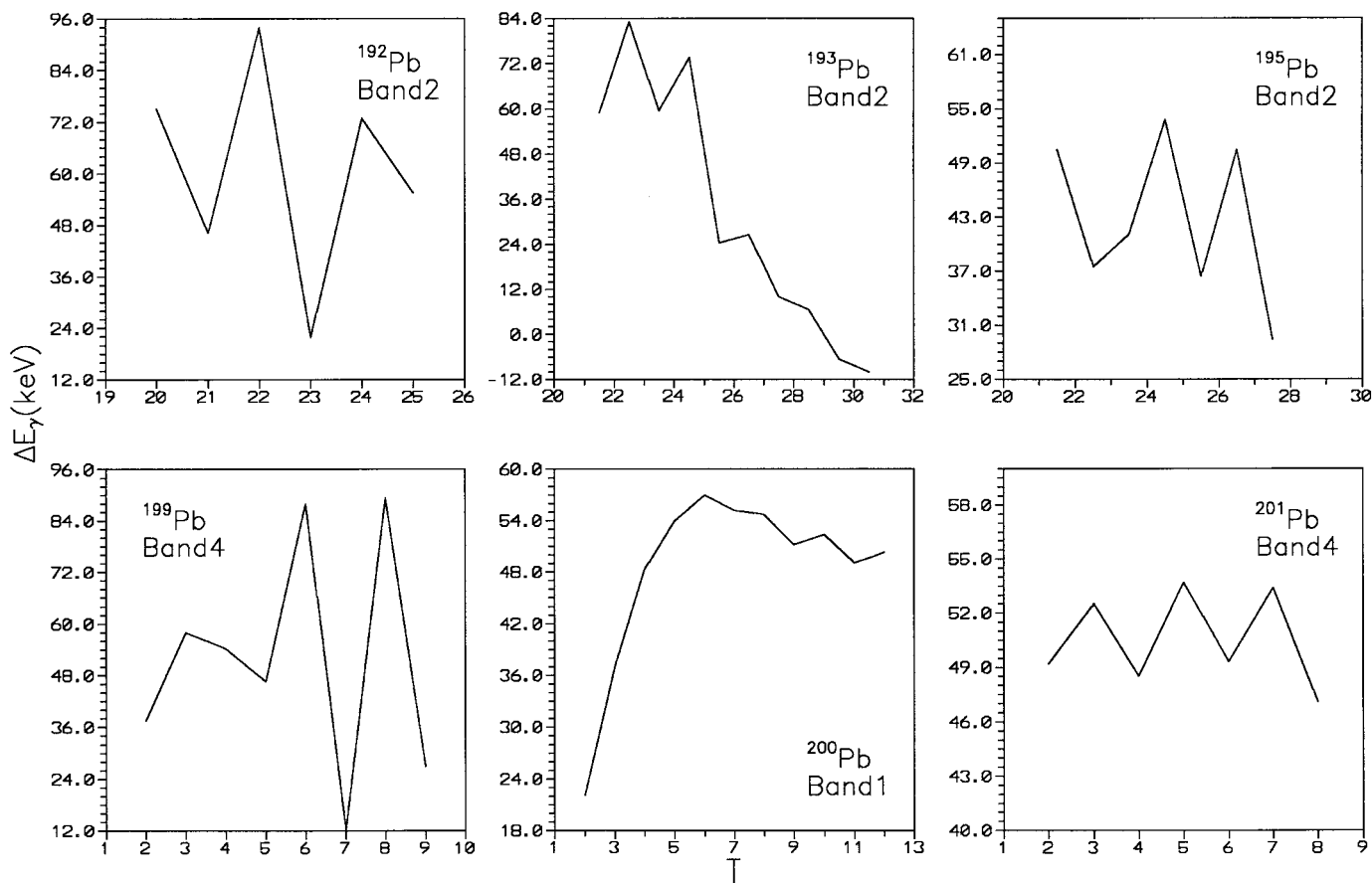
FIG. 6. Signature splitting in some MR bands in Pb isotopes as observed in the experimental data. The spins are uncertain in the three cases in the bottom panels.

1/2[600] orbit at a small oblate deformation ($\epsilon = -0.1$), and calculated energies and the aligned angular momenta, etc. Our calculations [24] show that the band based on this configuration develops a strong signature splitting at $I = 16$. The signature splitting persists even for the band based on the $h_{9/2}$, $9/2[514] \otimes i_{13/2}$, $7/2[604]$ configuration. However, this signature splitting disappears when the deformation is increased to, say, $\epsilon = -0.25$. These calculations also indicate that the shears mechanism is more valid at small deformations. Similar conclusions regarding the validity of the shears mechanism have also been reached by Macchiavelli et al. [25]. Since signature splitting is also prominent at small deformation, it is not unusual to observe signature splitting in MR bands, which is a small deformation phenomenon. In Fig. 7, we show the geometry of the particle angular momenta and their alignments at lower spins where splitting is absent and at higher angular momenta where splitting is present. The diagrams reveal that the shears mechanism is active at the lower spins. At higher spins ($I > 16$), the states belonging to different signatures clearly align along different directions, thus diluting the shears mechanism. We may therefore infer that the presence

of a large signature splitting may be linked with a dilution of the shears mechanism.

Identical Bands

Observation of identical bands in superdeformed nuclei brought this phenomenon, which is also present to some extent in normal deformed nuclei [26, 27], into sharp focus. Some MR bands also appear to have identical transition energies. An example is band 2 of ^{199}Pb and band 1 of ^{200}Pb. The bands differ in their configuration by a quasineutron orbital $f_{5/2}$, $1/2[521]$. An interpretation in terms of a decoupling of a pseudo-spin $\tilde{\Lambda} = 0$ quasineutron originating from $p_{3/2}$ and $f_{5/2}$ Nilsson orbitals has been suggested [5]; it requires a decoupling parameter $a = 1$. However, no identical band has been found in a similar situation in ^{201}Pb and ^{202}Pb. This phenomenon therefore remains to be investigated in MR bands.

Conclusions

In this paper, we have presented experimental data and other evidence taken from the literature which appear to
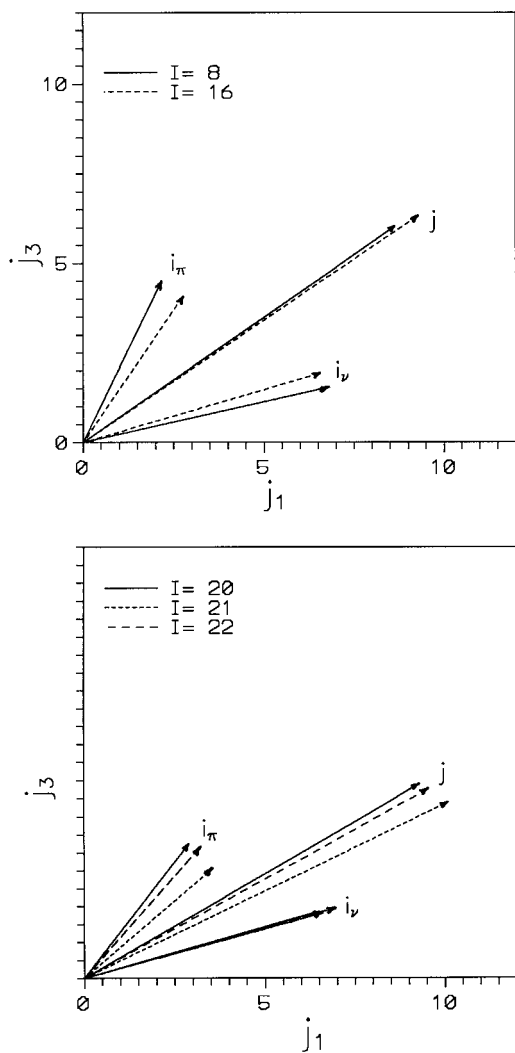
FIG. 7. Geometry of particle angular momenta at $I = 8$ and 16 (upper panel), and at three consecutive angular momenta for $I = 20, 21,$ and 22, which lie in the region of signature splitting (lower panel), for small oblate deformation $\epsilon_2 = -0.1$.

other features of MR bands such as signature effects are also discussed. Preliminary results from the two-particle–rotor model are given to check the applicability of the shears mechanism when signature splitting occurs. It may be pointed out that MR is just one of the several new modes of rotation that are being talked about [1]. For example, it is possible to construct both blades of the shears from the same type of particles (either protons or neutrons). While a regular pattern of levels would still be formed, these will be connected by weak E2 transitions (antimagnetic rotation). Observation of a "pure" MR band based on a perfectly spherical configuration is another challenge for the experimentalists. Another mode where the blades of the shears close with decreasing excitation rather than open has also been predicted. It would indeed be interesting to observe these new modes of rotation in experiments.

Acknowledgments

References for Introduction

1. R. M. Clark and R. Wadsworth, Physics World **11,** 25 (1998)

2. P. Van Duppen et al., Phys. Rev. Lett. **52,** 1974 (1984)

3. M. G. Porquet et al., J. Phys. G **20,** 765 (1994)

4. S. Frauendorf, Nucl. Phys. A **557,** 259c (1993)

5. G. Baldsiefen et al., Nucl. Phys. A **574,** 521 (1994)

6. S. Frauendorf, Z. Phys. A **358,** 163 (1996)

7. S. Frauendorf, in *Proceedings of the Workshop on Gammasphere Physics, Berkeley, 1995* (World Scientific, Singapore, 1996), p. 272

8. C. M. Petrache et al., Nucl. Phys. A **617,** 249 (1997)

9. S. Frauendorf, J. Reif, and G. Winter, Nucl. Phys. A **601,** 41 (1996)

10. A. O. Macchiavelli et al., Phys. Rev. C **58,** R621 (1998)

11. R. M. Clark et al., Phys. Lett. B **440,** 251 (1998)

12. D. G. Jenkins et al., Phys. Rev. Lett. **83,** 500 (1999)

support the recently proposed concept of magnetic rotation. A total of 120 bands in 56 nuclei from four mass regions have been compiled from the literature. Some additional cases, namely ^{83}Y [28, 29], ^{83}Zr [30], ^{106}Cd [31], ^{103,105,107,109}In [32, 33], ^{117}I [34], ^{128}Ba [35], and ^{139}Pm [36], are also likely candidates of MR bands but have not been included in this Table due to the uncertain nature of the bands and insufficient information. The bands in the $A = 80$ and 135 regions and Hg nuclides included in the Table should also be treated with caution. The energies, spin, parity, configuration assignments, electromagnetic properties, and other important details of MR bands are listed in the Table. We have discussed very briefly the shears mechanism and experimental as well as theoretical evidence in its favor. Many

13. S. Frauendorf, TAC code, private communication

14. A. Gadea et al., Phys. Rev. C **55,** R1 (1993)

15. A. Bohr and B. R. Mottelson, *Nuclear Structure* (Benjamin, New York, 1975), Vol. II

16. S. Chmel et al., Phys. Rev. Lett. **79,** 2002 (1997)

17. H. Ejiri and M. J. A. de Voigt, *Gamma Ray and Electron Spectroscopy in Nuclear Physics* (Oxford Univ. Press, Oxford, 1987), p. 504

18. A. O. Macchiavelli et al., Phys. Rev. C **58,** 3746 (1998)

19. E. F. Moore et al., Phys. Rev. C **51,** 115 (1995)

20. A. Goel and A. K. Jain, Phys. Lett. B **337,** 240 (1994)

21. A. K. Jain and A. Goel, Phys. Lett. B **277,** 233 (1992)

22. A. Goel and A. K. Jain, Nucl. Phys. A **620,** 265 (1997)

23. A. K. Jain et al., Rev. Mod. Phys. **70,** 843 (1998)

24. Amita, A. K. Jain, A. Goel, and B. Singh, Pramana-J. Phys. **53,** 463 (1999)

25. A. O. Macchiavelli et al., Phys. Lett. B **450,** 1 (1999)

26. A. K. Jain, Z. Phys. A **317,** 117 (1984)

27. C. Baktash et al., Annu. Rev. Nucl. Part. Sci. **45,** 485 (1995)

28. F. Cristancho et al., Nucl. Phys. A **540,** 307 (1992)

29. C. J. Lister et al., Z. Phys. A **329,** 413 (1988)

30. D. Rudolph et al., Z. Phys. A **338,** 139 (1991)

31. P. H. Regan et al., Nucl. Phys. A **586,** 351 (1995)

32. S. K. Tandel et al., Phys. Rev. C **58,** 3738 (1998)

33. J. Kownacki et al., Nucl. Phys. A **627,** 239 (1997)

34. M. P. Waring et al., Phys. Rev. C **48,** 2629 (1993)

35. I. Wiedenhover et al., Phys. Rev. C **58,** 721 (1998)

36. N. Xu et al., Phys. Rev. C **36,** 1649 (1987)

293

POLICIES

Level Energies   The listed level energies are taken from the first reference given for a band. In cases where values given by the original authors are relative to the energy of an isomer, we have added the energy of the isomer (taken from the Evaluated Nuclear Structure Data File database at Brookhaven National Laboratory) to each of the energy levels.

Band Intensity   The quoted value represents the approximate intensity (as a percentage) of the population of a band in a reaction channel leading to that nucleus. The value is taken from the cited reference if quoted explicitly by the authors. Otherwise an approximate value is deduced by us from the authors' relative γ-ray intensity data (either numeric or graphic).

References   The references are listed in chronological order in terms of eight digit key numbers as assigned in the Nuclear Science References database at Brookhaven National Laboratory.

TABLE. **Magnetic Dipole Rotational Bands**

$^A_Z X_N$	Denotes the specific nuclide with
	X chemical symbol
	A mass number
	Z atomic number
	N neutron number
	A single blank row marks the end of entries for each band. The number in the first column denotes the band number.
E_{level}	Level energy in units of keV. Energies in parentheses denote tentative levels. Labels X, Y, Z, etc., indicate that absolute excitation energies are unknown due to lack of knowledge about linking transitions to the lower levels.
I^π	I denotes the level spin for each band member. π denotes the parity (+ or −). I^π given in parentheses denotes uncertain spin and/or parity assignments.
$E_\gamma(M1)$	γ-Ray energies in units of keV for the M1 ($\Delta I = 1$) transition $I \rightarrow I - 1$.
$E_\gamma(E2)$	γ-Ray energies in units of keV for the E2 ($\Delta I = 2$) transition $I \rightarrow I - 2$.
$B(M1)/B(E2)$	The ratio of reduced transition probabilities in units of $(\mu_N/eb)^2$ given with the uncertainties in the last digits in parentheses [Eq. (7), $\delta = 0$]. In some bands where only upper limits for the intensities of the E2 transitions are given the lower limits for $B(M1)/B(E2)$ are given.
References	The references follow key numbers as assigned in the Nuclear Science References database at Brookhaven National Laboratory. The data for a band have been taken from the first reference cited (printed bold). Information taken from other references is given under the column "Configurations and Comments."
Configurations and Comments	The quasiparticle configuration for a band is given wherever assigned by the original authors. π here is for protons and ν is for neutrons. s, p, d, f, g, h, and i are the orbitals. A positive integer in the superscript of the orbital denotes the number of particles while a negative integer denotes the number of holes in that orbital.
	The abbreviations in this item are explained below:
	DSM deformed shell model
	TAC tilted-axis cranking
	CSM cranked shell model
	TRS total Routhian surface
	PSM projected shell model
	IBFM interacting Boson–Fermion model
	FAL Fermi aligned
	HF Hartree–Fock
	BCS Pairing theory of Bardeen, Cooper, and Schrieffer
	CWS Cranked Woods–Saxon
(β_2, γ)	Deformation parameters.
Backbending	In a rotational band, the transition energies increase with increase in spin reflecting the $I(I + 1)$ behavior, but in some cases, e.g., in band 1 of ^{108}Cd, the moment of inertia increases drastically after the spin 16^-, and the transition energy decreases and again starts rising after 18^-. This phenomenon is known as backbending and is usually attributed to the crossing of two rotational bands due to the alignment of a pair of either kind of quasiparticles.
Regular band	A band where the excitation energy varies more or less smoothly with spin, though not necessarily as $I(I + 1)$.
Irregular band	A band where energy variation with spin is quite abrupt.

TABLE. Magnetic Dipole Rotational Bands

See page 295 for Explanation of Table

$^{77}_{35}Br_{42}$

	E_{level} keV	I^{π}	$E_{\gamma}(M1)$ keV	$E_{\gamma}(E2)$ keV	$B(M1)/B(E2)$ $(\mu_N/eb)^2$	References
1	2931.6	$17/2^-$				**1993Do14**
	3219.6	$(19/2^-)$	288.0			1993Sy03
	3609.9	$(21/2^-)$	390.3			1995Ta21
	4149.8	$(23/2^-)$	539.9			

Configurations and Comments:

1. Tentatively assigned as $\pi(g_{9/2}) \otimes \nu\{g_{9/2} \otimes (p_{1/2}p_{3/2}f_{5/2})^1\}$ from the alignment and DSM calculations.
2. Regular band.
3. Nuclear reactions: ^{75}As $(\alpha,2n\gamma)$, $E(\alpha)= 27$ MeV, ^{73}Ge $(^7Li, 3n\gamma)$ and ^{74}Ge $(^7Li, 4n\gamma)$, $E(^7Li)= 35$ MeV.

$^{79}_{35}Br_{44}$

	E_{level} keV	I^{π}	$E_{\gamma}(M1)$ keV	$E_{\gamma}(E2)$ keV	$B(M1)/B(E2)$ $(\mu_N/eb)^2$	References
1	2393.1	$13/2^-$				**1988Sc13**
	2580.4	$15/2^-$	187.3			1995Ta21
	2773.9	$17/2^-$	193.5			
	3088.3	$19/2^-$	314.4			
	3535.8	$21/2^-$	447.5			

Configurations and Comments:

1. Tentatively assigned as $\pi(g_{9/2}) \otimes \nu[g_{9/2}(p_{3/2}f_{5/2})^1]$
2. Regular band.
3. Nuclear reaction: ^{77}Se $(\alpha, np\gamma)$, $E(\alpha)= 27$ MeV, Band intensity $\sim 6\%$.

$^{81}_{35}Br_{46}$

	E_{level} keV	I^{π}	$E_{\gamma}(M1)$ keV	$E_{\gamma}(E2)$ keV	$B(M1)/B(E2)$ $(\mu_N/eb)^2$	References
1	2549.4	$(13/2^-)$				**1986Fu04**
	2668.5	$(15/2^-)$	119.1			1995Ta21
	2942.1	$(17/2^-)$	273.6			
	3333.5	$(19/2^-)$	391.4			
	3798.7	$(21/2^-)$	465.2			

Configurations and Comments:

1. Tentatively assigned as $\pi(g_{9/2}^2p_{3/2})$, but this may only be just one component.
2. Regular band.
3. Nuclear reaction: ^{80}Se $(\alpha, p2n\gamma)$, $E(\alpha)= 35$-48 MeV.

$^{79}_{36}Kr_{43}$

	E_{level} keV	I^{π}	$E_{\gamma}(M1)$ keV	$E_{\gamma}(E2)$ keV	$B(M1)/B(E2)$ $(\mu_N/eb)^2$	References
1	2857.0	$(17/2^-)$				**1990Sc07**
	3214.3	$19/2^-$	357			1994Jo08
	3585.5	$21/2^-$	371.2			1995Ta21
	4133.0	$23/2^-$	547.5			

Configurations and Comments:

1. Tentatively assigned as $\pi[g_{9/2} \otimes (p_{3/2}f_{5/2})^1] \otimes \nu(g_{9/2})$.
2. Regular band.
3. Nuclear reactions: ^{77}Se$(\alpha, 2n\gamma)$, ^{78}Se$(\alpha, 3n\gamma)$, and ^{68}Cu$(^{18}O, 3pn\gamma)$.

$^{79}_{37}Rb_{42}$

	E_{level} keV	I^{π}	$E_{\gamma}(M1)$ keV	$E_{\gamma}(E2)$ keV	$B(M1)/B(E2)$ $(\mu_N/eb)^2$	References
1	3309.4	$(19/2^-)$				**1993Ho15**
	3687.5	$(21/2^-)$	378.1			1995Ta21
	4152.2	$(23/2^-)$	464.7	842.8		1996Sm07
	4686.4	$(25/2^-)$	534.2			
	5287.4	$(27/2^-)$	601			

Configurations and Comments:

1. Tentatively assigned as $\pi(g_{9/2}) \otimes \nu[(g_{9/2}) \otimes (pf)^1]$ by comparison with the isotone ^{77}Br.
2. Regular band.
3. 601 keV M1 transition is from 1996Sm07.
4. Nuclear reactions: ^{63}Cu(^{19}F, 2pnγ) and ^{65}Cu(^{18}O, 4nγ), E(^{19}F) and E(^{18}O) = 65 MeV, Band intensity < 2%.

$^{81}_{37}Rb_{44}$

	E_{level} keV	I^{π}	$E_{\gamma}(M1)$ keV	$E_{\gamma}(E2)$ keV	$B(M1)/B(E2)$ $(\mu_N/eb)^2$	References
1	2636.0	$(15/2^-)$				**1994Do18**
	2697.2	$17/2^-$	61.0			1995Ta21
	2997.7	$19/2^-$	300.5			
	3427.5	$21/2^-$	429.8			
	3993.1	$23/2^-$	565.6	(996)		
	4529	$(25/2^-)$	599			

Configurations and Comments:

1. Tentatively assigned as $\pi(g_{9/2}) \otimes \nu[(g_{9/2}) \otimes (pf)^1]$
2. Regular band.
3. Nuclear reactions: ^{79}Br(α, 2nγ), E(α)= 27 MeV and ^{68}Zn(^{19}F, α2nγ), E(^{19}F) = 72 MeV.

$^{82}_{37}Rb_{45}$

	E_{level} keV	I^{π}	$E_{\gamma}(M1)$ keV	$E_{\gamma}(E2)$ keV	$B(M1)/B(E2)$ $(\mu_N/eb)^2$	Reference
1	2616	$11^{(-)}$				**1999Sc14**
	3027	$12^{(-)}$	411			1999Do02
	3499	$13^{(-)}$	473	883		
	4046	(14^-)	548	1018		
	4714	(15^-)	668	1215		
	5483	(16^-)	769	1437		

Configurations and Comments:

1. Tentatively assigned as $\pi[(g_{9/2})^2 \otimes (p_{3/2}f_{5/2})^1] \otimes \nu(g_{9/2})$.
2. $(\beta_2, \gamma) = (0.16, 20°)$ from TAC calculations.
3. Regular band.
4. $B(M1)/B(E2)$ values range from 10-25 $(\mu_N/eb)^2$.
5. Nuclear reaction: ^{76}Ge (^{11}B, 5nγ), E(^{11}B)= 50 MeV, band intensity ~ 20%.

$^{83}_{37}Rb_{46}$

	E_{level} KeV	I^{π}	$E_{\gamma}(M1)$ keV	$E_{\gamma}(E2)$ keV	$B(M1)/B(E2)$ $(\mu_N/eb)^2$	References
1	2314.0	$(13/2^-)$				**1980Ga17**
	2414.4	$(15/2^-)$	100.5			1995Ta21
	2596.7	$(17/2^-)$	182.0			
	2958.9	$(19/2^-)$	362.2			
	3363.8	$(21/2^-)$	404.9			

Configurations and Comments:

1. Tentatively assigned as a three qp band.
2. Regular band.
3. Nuclear reactions: ^{81}Br(α, 2nγ), E(α)= 19-25 MeV, ^{80}Se(^{6}Li, 3nγ), E(^{6}Li)= 23-29 MeV, ^{70}Zn(^{16}O, p2nγ), E(^{16}O)= 52 MeV and ^{74}Ge(^{12}C, p2nγ), E(^{12}C)= 35-49 MeV.

$^{84}_{37}$Rb$_{47}$

	E_{level} keV	I^π	E_γ(M1) keV	E_γ(E2) keV	B(M1)/B(E2) $(\mu_N/eb)^2$	References
1	3393	11$^{(-)}$				**1999Sc14**
	3720	12$^{(-)}$	327			
	4166	13$^{(-)}$	445	772		
	4714	14$^{(-)}$	548	996		
	5372	15$^{(-)}$	657	1206		
	6094	16$^{(-)}$	722	1381		
	6861	17$^{(-)}$	766	1489		

Configurations and Comments:

1. Tentatively assigned as $\pi[(g_{9/2})^2 \otimes (p_{3/2}f_{5/2})^1] \otimes \nu(g_{9/2})$.
2. $(\beta_2, \gamma) = (0.14, -15°)$ from TAC calculations.
3. Regular band.
4. B(M1)/B(E2) values range from 5-20 $(\mu_N/eb)^2$.
5. Nuclear reaction: ^{76}Ge (^{11}B, 3nγ), E(^{11}B)= 50 MeV, band intensity ~ 20%.

$^{85}_{37}$Rb$_{48}$

	E_{level} keV	I^π	E_γ(M1) keV	E_γ(E2) keV	B(M1)/B(E2) $(\mu_N/eb)^2$	References
1	3198.2	17/2$^{(-)}$				**1995Sc04**
	3813.1	19/2$^{(-)}$	614.9			1995Ta21
	4356.1	21/2$^{(-)}$	543.5			
	4940.0	(23/2$^-$)	583.9			

Configurations and Comments:

1. Tentatively assigned as $\pi(g_{9/2}^{-1}) \otimes \nu(g_{9/2}^{-1}f_{5/2}^{-1})$.
2. Irregular band.
3. Nuclear reaction: ^{82}Se(^{7}Li, 4nγ), E(^{7}Li)= 32 MeV.

$^{108}_{48}$Cd$_{60}$

	E_{level} keV	I^π	E_γ(M1) keV	E_γ(E2) keV	B(M1)/B(E2) $(\mu_N/eb)^2$	References
1	(5590.7)	(11$^-$)				**1993Th05**
	5641.0	12$^-$	(51)			1994Th01
	5762.2	13$^-$	121.2			
	6078.2	14$^-$	316.0		>25	
	6600.1	15$^-$	521.9		>118	
	7277.0	16$^-$	676.9		>164	
	7742.5	17$^-$	465.5		>218	
	8104.0	18$^-$	361.5		>91	
	8586.5	(19$^-$)	482.5		>35	
	9176.7	(20$^-$)	590.2			
	(9881.2)	(21$^-$)	(704.5)			
2	(7863.7)	(16)				**1993Th05**
	(8187.0)	(17)	323.3			
	(8545.7)	(18)	358.7			
	(8966.5)	(19)	420.8			

Configurations and Comments:

1. Tentatively assigned as $\pi(g_{9/2})^{-2}_{K=8} \otimes \nu[h_{11/2} (g_{7/2}$ or $d_{5/2})^3$ before and $\pi(g_{9/2})^{-2}_{K=8} \otimes \nu(h_{11/2}^3 (g_{7/2}$ or $d_{5/2})^1]$ after the band crossing.
2. Small prolate deformation suggested.
3. Lower limits on B(M1)/B(E2) are from the unobserved ΔI= 2 (E2) transitions.
4. Regular band with backbending at 17$^-$.
5. Mean lifetimes of 14$^-$ and 15$^-$ levels are <3 ps from 1994Th01.
6. Nuclear reaction: ^{96}Zr (^{16}O, 4nγ), E(^{16}O)= 74, 75 MeV, Band intensity ~ 3% and from 1994Th01: ^{100}Mo (^{12}C, 4nγ), E(^{12}C)= 54 MeV.

1. Regular band.
2. Band intensity < 2%.

$^{109}_{48}\text{Cd}_{61}$

	E_{level} keV	I^π	$E_\gamma(M1)$ keV	$E_\gamma(E2)$ keV	B(M1)/B(E2) $(\mu_N/eb)^2$	Reference
1	3354.5	21/2⁻				**1994Ju05**
	3549.5	23/2⁻	195.0			
	4030.5	25/2⁻	481.7			
	4630.5	27/2⁻	600.0			
	5279.5	29/2⁻	649.0	1249.0		
	5441.1	31/2⁻	161.6			
	5731.0	33/2⁻	289.9			
	6164.3	35/2⁻	433.3			
	6795.8	37/2⁻	631.5			
	7554.8	(39/2⁻)	759			
2	5560.9	(27/2)				**1994Ju05**
	5862.0	(29/2)	301.1			
	6241.0	(31/2)	379.0			
	6704.0	(33/2)	463.0			
	7244.6	(35/2)	540.6			
	7822.4	(37/2)	577.8			
	8429.4	(39/2)	607			

Configurations and Comments:

1. Tentatively assigned as $\pi(g_{9/2})^{-2} \otimes \nu(h_{11/2})$ by comparison with the similar bands in ^{108}Cd and ^{110}Cd.
2. $(\beta_2, \gamma) \sim (0.12, 3°)$ from CSM calculations.
3. B(M1)/B(E2) values range from ~ 40 $(\mu_N/eb)^2$ to ~ 150 $(\mu_N/eb)^2$.
4. Regular band with a backbending at 31/2.
5. Nuclear reactions: ^{100}Mo (^{13}C, 4nγ), E(^{13}C)= 44 MeV and ^{96}Zr (^{18}O, 5nγ), E= 73 MeV, Band intensity $\sim 4\%$.

Configurations and Comments:

1. Tentatively assigned as $\pi(g_{9/2})^{-2} \otimes \nu(d_{5/2} h_{11/2}^2)$ or $\pi(g_{9/2})^{-2} \otimes \nu(g_{7/2} h_{11/2}^2)$ from the properties of the band and its decay patterns.
2. B(M1)/B(E2) values ≥ 20 $(\mu_N/eb)^2$ for the two levels at 33/2 and 35/2.
3. Regular band.
4. Band intensity $\sim 2\%$.

$^{110}_{48}\text{Cd}_{62}$

	E_{level} keV	I^π	$E_\gamma(M1)$ keV	$E_\gamma(E2)$ keV	B(M1)/B(E2) $(\mu_N/eb)^2$	References
1	5759.7	13⁻				**1994Ju04**
	5985.3	14⁻	225.6			
	6355.3	15⁻	370.0			
	6963.8	16⁻	608.5		>58	
	7576.2	17⁻	612.4		>317	
2	6584.2	14				**1994Ju04**
	6879.2	15	295.0			
	7280.6	16	401.4			
	7758.5	17	477.9			
3	8015.8	17				**1994Ju04**
	8277.0	18	261.2			1999Cl03
	8594.6	19	317.6			
	8966.9	20	372.3			
	9429.4	21	462.5		>48	
	9990.4	22	561		>63	
	10664.2	23	673.8		>60	
	11450.2	24	786			

Configurations and Comments:

1. Tentatively assigned as $\pi(g_{9/2}^{-2}) \otimes \nu(h_{11/2}g_{7/2})$ or $\pi(g_{9/2}^{-2}) \otimes \nu(h_{11/2}d_{5/2})$ by comparison with a similar band in ^{108}Cd and from the alignments.
2. Prolate deformation.
3. Lower limits on B(M1)/B(E2) values are from the unobserved ΔI= 2 (E2) transitions.
4. Regular band.
5. Nuclear reactions: ^{96}Zr (^{18}O, 4nγ), E(^{18}O) = 73 MeV and ^{100}Mo (^{13}C, 3nγ), E(^{13}C) = 44 MeV, Band intensity $\sim 5\%$.

Configurations and Comments:

1. Tentatively assigned as $\pi(g_{9/2}^{-2}) \otimes \nu(h_{11/2}^2)$ or $\pi(g_{9/2}^{-1}p_{1/2}) \otimes \nu(h_{11/2}^2)$ depending on whether the band has positive or negative parity.
2. Prolate deformation.
3. Regular band.
4. Band intensity $\sim 1\%$.

Configurations and Comments:

1. Configuration may involve in addition to that of band 2, an aligned pair of neutrons in the $g_{7/2}$ orbital.
2. Prolate deformation.
3. Lower limits on B(M1)/B(E2) values are from the unobserved ΔI= 2 (E2) transitions.
4. Regular band.
5. Mean lifetimes of levels with spins from 20 to 23, as given in 1999Cl are 0.184(+18-22), 0.101(+15-18), 0.094(+14-18) and 0.092(+17 -23) ps, respectively.
6. B(M1) values for transitions from 372.3 to 673.8 keV, as given in 1999Cl are 5.40(+65-53) 5.13(+90-75), 3.06(+57-45) and 1.83(+46-34) μ_N^2 respectively.
7. Band intensity $\sim 2.5\%$.

$^{111}_{49}\text{In}_{62}$

	E_{level} keV	I^π	$E_\gamma(M1)$ keV	$E_\gamma(E2)$ keV	$B(M1)/B(E2)$ $(\mu_N/eb)^2$	Reference
1	3461.0	$19/2^+$				**1998Va03**
	3588.4	$21/2^+$	127.4			
	3707.2	$23/2^+$	118.8			
	3911.3	$25/2^+$	204.1			
	4282.6	$27/2^+$	371.3			
	4795.8	$29/2^+$	513.2	884.3	70(11)	
	5330.7	$31/2^+$	534.9	1048.4	34(3)	
	5877.1	$(33/2^+)$	546.4	1081.3	20(2)	
2	4932.0	$27/2^+$				**1998Va03**
	5166.8	$29/2^+$	234.8			
	5398.8	$31/2^+$	232.0			
	5678.1	$33/2^+$	279.3			
	6051.0	$35/2^+$	372.9			
	6538.1	$(37/2^+)$	487.1			
	7175.2	$(39/2^+)$	637.1			
	7917.1	$(41/2^+)$	741.9			
	8681.1	$(43/2^+)$	764.0			
3	X	$(31/2^-)$				**1998Va03**
	390.5+X	$(33/2^-)$	390.5			
	794.7+X	$(35/2^-)$	404.2			
	1244.3+X	$(37/2^-)$	449.6			
	1774.1+X	$(39/2^-)$	529.8			
	2354.6+X	$(41/2^-)$	580.5			

Configurations and Comments:

1. $\pi(g_{9/2}^{-1}) \otimes \nu(h_{11/2}^2)$ by comparison with a similar band in ^{110}Cd.
2. Small prolate deformation.
3. $B(M1)/B(E2) > 50$-100 $(\mu_N/eb)^2$ from unobserved $\Delta I = 2$ (E2) transitions.
4. Regular band with small backbending at 23/2.
5. Nuclear reaction : ^{96}Zr(^{19}F, 4nγ), E(^{19}F)= 72 MeV, Band intensity ~ 33%.

1. $\pi(g_{9/2}^{-1}) \otimes \nu(h_{11/2}^2 g_{7/2}^2)$ by comparison with a similar band in ^{110}Cd.
2. Small prolate deformation.
3. $B(M1)/B(E2) > 50$-100 $(\mu_N/eb)^2$ from unobserved $\Delta I = 2$ (E2) transitions.
4. Regular band with small backbending at 31/2.
5. Band intensity ~ 15%.

1. Tentatively assigned as $\pi(g_{9/2}^{-1}) \otimes \nu(h_{11/2}g_{7/2}d_{5/2})$ (configuration of a band in ^{110}Cd) coupled to an aligned $g_{7/2}$ or $h_{11/2}$ neutron pair.
2. I^π and level energies are lower limits as estimated from intensity and feeding considerations.
3. X~ 5500 keV.
4. $B(M1)/B(E2) > 50$-100 $(\mu_N/eb)^2$ from unobserved $\Delta I = 2$ (E2) transitions.
5. Regular band.
6. Band intensity ~ 9%.

$^{113}_{49}\text{In}_{64}$

	E_{level} keV	I^π	$E_\gamma(M1)$ keV	$E_\gamma(E2)$ keV	$B(M1)/B(E2)$ $(\mu_N/eb)^2$	Reference
1	2233.2	$(15/2^-)$				**1997Ch01**
	2396.4	$(17/2^-)$	163.2			
	2663.9	$(19/2^-)$	267.5			
	2853.6	$(21/2^-)$	189.7			
	3023.1	$(23/2^-)$	169.5			
	3280.0	$(25/2^-)$	256.9			
	3972.6	$(27/2^-)$	692.6			
	4715.0	$(29/2^-)$	742.4	1434.9	8(2)	
	5392.7	$(31/2^-)$	677.7	1418.6	17(6)	
2	3122.1	$(21/2^+)$				**1997Ch01**
	3213.9	$(23/2^+)$	91.8			
	3397.2	$(25/2^+)$	183.3			
	3788.1	$(27/2^+)$	390.9			
	4377.5	$(29/2^+)$	589.4	980.2	24(6)	
	5062.1	$(31/2^+)$	684.6	1274.2	71(14)	
	5790.3	$(33/2^+)$	728.2			

Configurations and Comments:

1. Tentatively assigned as $\pi(g_{9/2}^{-1}) \otimes \nu(g_{7/2}^{-1}h_{11/2})$.
2. Small prolate deformation (β_2=0.09).
3. Parity assignment is based on comparison with neighboring nuclei.
4. Irregular band.
5. Fully aligned configuration gives rise to I^π= $27/2^-$; I^π beyond this value is attributed to some collectivity.
6. Nuclear reaction : ^{110}Pd(^{7}Li, 4nγ), E(^{7}Li) = 40 MeV, Band intensity ~ 31%.

1. Tentative Configuration $\pi(g_{9/2}^{-1}) \otimes \nu(h_{11/2}^2)$.
2. Small prolate deformation (β_2=0.09).
3. Parity assignment is based on comparison with neighboring nuclei.
4. Regular band.
5. Band intensity ~ 15%.

$^{105}_{50}$Sn$_{55}$

	E_{level} keV	I^π	E_γ(M1) keV	E_γ(E2) keV	B(M1)/B(E2) $(\mu_N/eb)^2$	Reference
1	7043	29/2$^+$				**1997Ga01**
	7343	31/2$^+$	300			
	7730	33/2$^{(+)}$	388			
	8196	35/2$^{(+)}$	466			
	8682	37/2$^{(+)}$	486			
	9137	39/2$^{(+)}$	456			
	9692	41/2$^{(+)}$	555			
	10287	43/2$^{(+)}$	596			

Configurations and Comments:

1. Tentatively assigned as $\pi(g_{9/2}^{-1}g_{7/2})\otimes\nu(h_{11/2}^2 (d_{5/2}g_{7/2})^1)$ from TRS calculations.
2. Prolate deformation (β_2=0.137)
3. B(M1)/B(E2)>100$(\mu_N$/eb$)^2$ from the unobserved ΔI= 2 (E2) transitions.
4. Regular band with a backbending at 37/2.
5. Nuclear reaction : ^{50}Cr(^{58}Ni, 2pnγ), E(^{58}Ni)= 210 MeV, Band intensity ~ 20%.

$^{106}_{50}$Sn$_{56}$

	E_{level} keV	I^π	E_γ(M1) keV	E_γ(E2) keV	B(M1)/B(E2) $(\mu_N/eb)^2$	References
1	8011	15$^-$				**1999Je07**
	8558	16$^-$	547			1999JeAA
	9101	17$^-$	543			1998Je03
	9551	18$^-$	450		>160	
	10039	19$^-$	488		>250	
	10631	20$^-$	592		>200	
	11412	21$^-$	781		>35	
	12046	22$^-$	634			

Configurations and Comments:

1. $\pi(g_{7/2}g_{9/2}^{-1}) \otimes \nu((g_{7/2}d_{5/2})^3 h_{11/2})$ from TAC calculations.
2. (β_2, γ) = (0.11, -13°).
3. Level energies, spins and parities are from 1999JeAA.
4. Mean lifetimes of the five uppermost levels are 0.30(3), 0.43(5), 0.51(15), 0.22(2) and 0.22(+1-3) ps, respectively.
5. B(M1) values for the transitions from 450 to 599 keV are 2.06(+22-26), 1.12(+15-13), 0.54(+20-13), 0.54(+5-7) and 1.17(17) μ_N^2, respectively.
6. Regular band with backbending at the top of the band.
7. Nuclear reaction: ^{54}Fe(^{58}Ni, α2pγ), E(^{58}Ni) = 243 MeV.

	E_{level} keV	I^π	E_γ(M1) keV	E_γ(E2) keV	B(M1)/B(E2) $(\mu_N/eb)^2$	References
2	9236.1	17$^-$				**1998Je03**
	9637.8	18$^-$	401.7			
	10117.0	19$^-$	479.2		>155	
	10672.4	20$^-$	555.4		>290	
	11292.7	21$^-$	620.3		>220	
	11971.5	22$^-$	678.8			

Configurations and Comments:

1. $\pi(g_{7/2}g_{9/2}^{-1}) \otimes \nu((g_{7/2}d_{5/2})^3 h_{11/2})$ from TAC calculations.
2. (β_2, γ) = (0.11, -13°).
3. Regular band.

$^{108}_{50}Sn_{58}$

	E_{level} keV	I^{π}	$E_{\gamma}(M1)$ keV	$E_{\gamma}(E2)$ keV	B(M1)/B(E2) $(\mu_N/eb)^2$	References
1	6665	12⁻				**1998Je03**
	6885.0	13⁻	220.0			1999Je07
	7182.7	14⁻	297.7			
	7606.4	15⁻	423.7	720	30.0(25)	
	8116.3	16⁻	509.9	934	23.5(40)	
	8634.5	17⁻	518.2	1028	26.0(35)	
	9169.6	18⁻	535.1	1053	19.5(40)	
	9719.8	19⁻	550.2	1085	23(4)	
	10355.3	20⁻	635.5	1184	24(4)	
2	8103	16⁻				**1998Je03**
	8351.2	17⁻	248.2			
	8695.8	18⁻	344.6	(592)		
	9105.8	19⁻	410.0	753	15.4(40)	
	9579.4	20⁻	473.6	885	14.1(40)	
	10062.8	21⁻	483.4	956	20.2(50)	
	10572.2	22⁻	509.4	992	22.7(70)	

Configurations and Comments:

1. $\pi(g_{7/2}\, g_{9/2}^{-1}) \otimes \nu((g_{7/2}d_{5/2})^1\, h_{11/2})$ from TAC calculations.
2. Prolate shape $(\beta_2, \gamma) = (0.08, 0°)$ from 1999Je.
3. The mean lifetimes of levels with spins from 15 to 19 as given in 1999Je are 0.66(2), 0.23(1), 0.29(1), 0.44(+5-2) and 0.56(2) ps, respectively.
4. B(M1) values for the transitions from 424 to 550 keV are 1.05(3), 1.63(8), 1.16(5), 0.64(+4 -8) and 0.48(3) μ_N^2, respectively.
5. Regular band.
6. Nuclear reaction: ^{54}Fe(^{58}Ni, 4pγ), E(^{58}Ni) = 243 MeV.

1. $\pi(g_{7/2}\, g_{9/2}^{-1}) \otimes \nu(g_{7/2}^2\, (g_{7/2}d_{5/2})^1\, h_{11/2})$ from TAC calculations.
2. Prolate shape $(\beta_2, \gamma) = (0.11, 0°)$ from 1999Je.

$^{108}_{51}Sb_{57}$

	E_{level} keV	I^{π}	$E_{\gamma}(M1)$ keV	$E_{\gamma}(E2)$ keV	B(M1)/B(E2) $(\mu_N/eb)^2$	Reference
1	2154.6	7⁻				**1998Je09**
	2246.0	8⁻	91.4			
	2438.3	9⁻	192.3	283		
	2719.9	10⁻	281.6	474		
	3032.4	11⁻	312.5	595		
	3376.8	12⁻	344.4	657		
	3764.7	13⁻	387.9	732		
	4173.6	14⁻	408.9	797		
	4613.3	15⁻	439.7	849		
	5101.9	16⁻	488.6	929		
	5611.5	17⁻	509.6	999		
	6150.0	18⁻	538.5	1049		
	6719.6	19⁻	569.6	1109		
2	2753.4	10⁻				**1998Je09**
	3057.4	11⁻	304.0			
	3376.4	12⁻	319.0	623		
	3722.5	13⁻	346.1	665		
	4177.9	14⁻	455.4	801		
	4597.3	15⁻	419.4	874		
	5064.4	16⁻	467.1	886		
	5561.8	17⁻	497.4	964		
	6092.3	18⁻	530.5	1028		
	6645.2	19⁻	552.9	1084		
	7216.3	20⁻	571.1	1124		

Configurations and Comments:

1. $\pi[(g_{7/2},d_{5/2})^2\, g_{9/2}^{-1}] \otimes \nu(h_{11/2})$ from TAC calculations.
2. $(\beta_2, \gamma) = (0.116, 30°)$ from TAC calculations.
3. B(M1)/B(E2) values range from ~ 5 $(\mu_N/eb)^2$ to ~ 20 $(\mu_N/eb)^2$.
4. Regular band.
5. Nuclear reaction: ^{54}Fe (^{58}Ni, 3pnγ), E(^{58}Ni)= 243 MeV, Band intensity ~ 47%.

1. $\pi(h_{11/2}\, g_{7/2}\, g_{9/2}^{-1}) \otimes \nu(g_{7/2},d_{5/2})^1$ from TAC calculations.
2. $(\beta_2, \gamma) = (0.116, 10°)$ from TAC calculations.
3. B(M1)/B(E2) values range from ~ 5 $(\mu_N/eb)^2$ to ~ 25 $(\mu_N/eb)^2$.
4. Regular band with backbending at 15.
5. Band intensity ~ 19%.

302

$^{112}_{51}\text{Sb}_{61}$

	E_{level} keV	I^π	$E_\gamma(M1)$ keV	$E_\gamma(E2)$ keV	B(M1)/B(E2) $(\mu_N/eb)^2$	Reference
1	1675.1	7^-				**1998La14**
	1747.5	8^-	72.4			
	1949.7	9^-	202.2			
	2275.2	10^-	325.5	527.7	24(2)	
	2629.1	11^-	353.9	679.1	16.0(8)	
	3009.7	12^-	380.6	734.6	14.2(7)	
	3402.1	13^-	392.4	773.5	13.3(7)	
	3809.0	14^-	406.9	799.7	6.8(4)	
	4295.3	15^-	486.3	893.2	10.6(8)	
	4798.3	16^-	503.0	989.8	9.9(9)	
	5326.2	17^-	527.9	1030.8		
2	X	(10^+)				**1998La14**
	378.2+X	(11^+)	378.2			
	750.8+X	(12^+)	372.6	750.6	7.5(5)	
	1077.6+X	(13^+)	326.8	699.7	15.3(12)	
	1372.5+X	(14^+)	294.9	621.7	56(7)	
	1690.3+X	(15^+)	317.8	613.0	200(180)	
	2046.1+X	(16^+)	355.8	673.9	30(3)	
	2437.7+X	(17^+)	391.6	747.6	26(3)	
	2851.9+X	(18^+)	414.2			
	3284.4+X	(19^+)	432.5			

Configurations and Comments:

1. $\pi(g_{9/2}^{-1}) \otimes \nu(h_{11/2})$ from TRS calculations.
2. Regular band.
3. Nuclear reaction: ^{103}Rh (^{12}C, 3nγ), E(^{12}C)= 60 MeV and ^{90}Zr (^{31}P, 2αnγ), E= 150 MeV, Band intensity ~ 30%.

1. $\pi(g_{9/2}^{-1}) \otimes \nu((d_{5/2}g_{7/2})^1 h_{11/2}^2)$ from TRS calculations and by comparison with similar bands in neighboring isotopes.
2. Regular band with backbending at 12.
3. Band intensity ~ 6%.

$^{124}_{54}\text{Xe}_{70}$

	E_{level} keV	I^π	$E_\gamma(M1)$ keV	$E_\gamma(E2)$ keV	B(M1)/B(E2) $(\mu_N/eb)^2$	Reference
1	5051	(12)				**1999Sc20**
	5292	(13)	241			1997Lo12
	5554	(14)	262	502		
	5830	(15)	276	537		
	6156	(16)	326	602		
	6556	(17)	400	726		
	6987	(18)	431	831		
	7436	(19)	449	880		
	7932	(20)	496	944		
	8368	(21)	436	932		
	8914	(22)	546	982		
	9486	(23)	572	1118		
	9929	(24)	443	1016		

Configurations and Comments:

1. Tentatively assigned as $\pi(h_{11/2} \otimes (d_{5/2}g_{7/2})^1) \otimes \nu(h_{11/2} g_{7/2})$.
2. The observed B(M1)/B(E2) values start from 23.3 (3.3) $(\mu_N/eb)^2$ and decrease with increasing spin before the backbend.
3. Irregular band with backbending at 8368 keV level and at the top of the band.
4. Nuclear reaction: ^{110}Pd (^{18}O, 4nγ), E(^{18}O)= 86 MeV, Band intensity ~ 13%.

$^{132}_{56}Ba_{76}$

E$_{level}$ KeV	I$^\pi$	E$_\gamma$(M1) keV	E$_\gamma$(E2) keV	B(M1)/B(E2) (μ_N/eb)^2	Reference
1	4108.5	(10$^+$)				1989Pa17
	4312.3	(11$^+$)	203.8			
	4548.0	(12$^+$)	235.7			
	4883.0	(13$^+$)	335.0			
	5307.5	(14$^+$)	424.5			
2	4863.9	(11$^-$)				1989Pa17
	5033.6	(12$^-$)	169.7			
	5249.2	(13$^-$)	215.6			
	5557.1	(14$^-$)	307.9			
	5964.1	(15$^-$)	407			

Configurations and Comments:

1. Tentatively assigned as $\pi(h_{11/2}g_{7/2}) \otimes \nu(h_{11/2}d_{3/2})$ by considering the available orbits nearest to the Fermi surface.
2. Oblate shape ($\gamma \sim$ -60°).
3. Parities are from multipolarities of interband transitions.
4. Regular band.
5. Nuclear reaction: ^{122}Sn (^{13}C, 3nγ), E(^{13}C) = 57 MeV, Band intensity $\sim$ 1%.

1. $\pi(h_{11/2}g_{7/2}) \otimes \nu(h_{11/2}^2)$ by considering the available orbits nearest to the Fermi surface.
2. Oblate shape ($\gamma \sim$ -60°).
3. Parities are from multipolarities of interband transitions.
4. Mean lifetime of Bandhead = 12.5(3) ns.
5. Regular band.
6. Band intensity $\sim$ 3%.

$^{131}_{57}La_{74}$

E$_{level}$ keV	I$^\pi$	E$_\gamma$(M1) keV	E$_\gamma$(E2) keV	B(M1)/B(E2) (μ_N/eb)^2	Reference
1	2476.7	(19/2$^-$)				1989Hi02
	2544.0	(21/2$^-$)	67.3			
	2698.3	(23/2$^-$)	154.3			
	2934.4	(25/2$^-$)	236.1	389.9		
	3242.6	(27/2$^-$)	308.2	544.1		
	3609.2	(29/2$^-$)	366.6	675.6		
	4023.1	(31/2$^-$)	413.9	780.7		
	4478.5	(33/2$^-$)	455.4	869.8		
	4967.1	(35/2$^-$)	488.6	943.9		
	5489.3	(37/2$^-$)	522.2	1010		
	6037.1	(39/2$^-$)	547.8	1069		
	(6605.6)	(41/2$^-$)	(568.5)	(1115)		
	(7184.6)	(43/2$^-$)	(579)			
2	2120.5	21/2$^-$				1989Hi02
	2548.0	(23/2$^-$)	427.5			
	3017.3	(25/2$^-$)	469.3	896		
	3526.3	(27/2$^-$)	509	978		

Configurations and Comments:

1. Tentatively assigned as $\pi(h_{11/2}) \otimes \nu(h_{11/2}^2)$ from CSM calculations.
2. Collective oblate structure (γ = -60°).
3. B(M1)/B(E2) ratio is in the range of 10-50 (μ_N/eb)^2 and rises with increasing spin.
4. Regular band.
5. Nuclear reaction: ^{116}Cd(^{19}F, 4nγ), E(^{19}F) = 76 to 90 MeV, Band intensity $\sim$ 7%.

1. Tentatively assigned as $\pi(g_{7/2}) \otimes \nu(g_{7/2}h_{11/2})$ by comparison with the neighboring ^{128}Ba and ^{130}Ce isotopes.
2. Oblate shape suggested because of strong connection to band 1.
3. Bandhead is isomeric with a half life of 38(2) ns.
4. Regular band.

$^{135}_{58}Ce_{77}$

	E_{level} keV	I^π	$E_\gamma(M1)$ KeV	$E_\gamma(E2)$ keV	$B(M1)/B(E2)$ $(\mu_N/eb)^2$	Reference
1	3229.8	$23/2^+$				**1990Ma26**
	3431.9	$25/2^+$	202.1			
	3699.9	$27/2^+$	268.0			
	4128.2	$29/2^+$	428.3	696	>8	
	4486.4	$31/2^+$	358.2	786.8	23(7)	
	4979.3	$33/2^+$	492.9	851	>9	
	5428.5	$35/2^+$	449.2	942	>14	
	5942.5	$(37/2^+)$	514	963		
	6444.5	$(39/2^+)$	502	(1016)		
2	4183.8	$27/2^-$				**1990Ma26**
	4460.9	$29/2^-$	277.1			
	4830.9	$31/2^-$	370.0			
	5206.5	$33/2^-$	375.6	746	>6	
	5651.6	$35/2^-$	445.1	821	>19	
	6086.5	$37/2^-$	434.9	880	>24	
	6526.5	$39/2^-$	440.0	(875)	>13	
	6994.5	$41/2^-$	468.0	(908)	>6	
	7494.5	$(43/2^-)$	500	968		
3	4498.8	$27/2^-$				**1990Ma26**
	4637.9	$29/2^-$	139.1			
	4816.4	$31/2^-$	178.5		>4	
	5065.4	$33/2^-$	249.0		>6	
	5362.9	$35/2^-$	297.5		>13	
	5755.1	$37/2^-$	392.2		>18	
	6259.7	$39/2^-$	504.6		>19	
	6843.3	$(41/2^-)$	583.6		>21	
	7473.3	$(43/2^-)$	630		>22	

Configurations and Comments:

1. Tentatively assigned as $\pi(h_{11/2}g_{7/2}) \otimes \nu(h_{11/2})$ by comparison with the N=75 isotones.
2. Near prolate shape ($\gamma \sim 0°$).
3. Irregular band with backbending at I^π =31/2 and 35/2.
4. Small signature splitting.
5. Lower limits of B(M1)/B(E2) are from the unobserved ΔI =2 (E2) transitions.
6. Nuclear reaction : $^{122}Sn(^{18}O, 5n\gamma)$, $E(^{18}O)$ = 85 and 89 MeV, Band intensity ~ 17%.

1. Tentatively assigned as $\pi(h_{11/2}^2) \otimes \nu(h_{11/2})$ by comparison with the N=75 isotones.
2. Near prolate shape ($\gamma \sim 0°$).
3. Irregular band with backbending at 37/2.
4. Small signature splitting.
5. Lower limits of B(M1)/B(E2) are from the unobserved ΔI =2 (E2) transitions.
6. Band intensity ~ 10%.

1. Tentatively assigned as $\pi(h_{11/2}g_{7/2}) \otimes \nu(h_{11/2}^2 s_{1/2})$.
2. Collectively rotating oblate structure ($\gamma \sim -60°$).
3. Limits on B(M1)/B(E2) values are from the assumption that the unobserved ΔI =2 (E2) transitions are less than 1% intense as compared to the strongest transition in the level scheme.
4. Regular band.
5. Relative intensity ~ 6%.

$^{136}_{58}Ce_{78}$

	E_{level} keV	I^π	$E_\gamma(M1)$ keV	$E_\gamma(E2)$ keV	$B(M1)/B(E2)$ $(\mu_N/eb)^2$	Reference
1	5645.3	(14^-)				**1990Pa05**
	5809.3	15^-	164			
	5995.3	16^-	186.0			
	6283.4	17^-	288.1			
	6663.3	18^-	379.9			
	7099.8	19^-	436.5			
	7586.3	(20^-)	486.5			
	(8101.3)	(21^-)	(515)			
	(8626.3)	(22^-)	(525)			

Configurations and Comments:

1. $\pi(g_{7/2}h_{11/2}) \otimes \nu(h_{11/2}^2)$ by comparison with the nearby odd Z and doubly odd nuclei.
2. E2/M1 mixing ratios ($\delta_{E2/M1}$) are negative for two gamma transitions, implying an oblate shape for the band ($\gamma = -60°$).
3. $B(M1)/B(E2) > 10(\mu_N/eb)^2$.
4. Regular band.
5. Nuclear reaction: $^{122}Sn(^{18}O, 4n\gamma)$, $E(^{18}O)$ = 85 and 89 MeV, Band intensity ~ 25%.

TABLE. Magnetic Dipole Rotational Bands
See page 295 for Explanation of Table

$^{133}_{59}\text{Pr}_{74}$

	E_{level} keV	I^π	$E_\gamma(M1)$ keV	$E_\gamma(E2)$ keV	$B(M1)/B(E2)$ $(\mu_N/eb)^2$	Reference
1	2141.5	$(23/2^-)$				**1988Hi04**
	2290.7		149.2			
	2536.6		245.9			
	2863.6		327.0			
	3258.3		394.7			
	3706.1		447.8			
	(4202.5)		(496.4)			
2	3309.7					**1988Hi04**
	3475.1		165.4			
	3726.3		251.2			
	4063.1		336.8			
	4472.4		409.3			
	4944.1		471.7			
3	X					**1988Hi04**
	196.1+X		196.1			
	440.1+X		244.0			
	736.7+X		296.6			
	1087.6+X		350.9			
	1491.3+X		403.7			
	1945.7+X		454.4			
	(2444.1+X)		(498.4)			

Configurations and Comments:

1. $\pi(h_{11/2}) \otimes \nu(h_{11/2}^2)$ by comparison with the similar band in ^{131}La.
2. Collective oblate band ($\gamma = -60°$).
3. $B(M1)/B(E2) \geq 5$ $(\mu_N/eb)^2$, from estimates of upper limits for the $\Delta I = 2$ (E2) transitions.
4. Regular band.
5. Nuclear reaction: ^{118}Sn (^{19}F, 4nγ), seven different E(^{19}F) ranging over 72-104 MeV and ^{117}Sn (^{19}F, 3nγ), E(^{19}F) = 86.5 MeV, Band intensity ~ 10%.

Configurations and Comments:

1. The properties of the band suggest mixed proton and neutron configurations with $h_{11/2}$ neutrons.
2. $B(M1)$ values are expected to be large since no $\Delta I = 2$ (E2) transitions are reported.
3. Regular band.
4. Band intensity ~ 5%.

Configurations and Comments:

1. The properties of the band suggest mixed proton and neutron configurations with $h_{11/2}$ neutrons.
2. $B(M1)$ values are expected to be large since no $\Delta I = 2$ (E2) transitions are reported.
3. Regular band.
4. Band intensity ~ 3%.

$^{137}_{59}\text{Pr}_{78}$

	E_{level} keV	I^π	$E_\gamma(M1)$ keV	$E_\gamma(E2)$ keV	$B(M1)/B(E2)$ $(\mu_N/eb)^2$	Reference
1	3439.3	$25/2^-$				**1989Xu01**
	3550.8	$27/2^-$	111.5			
	3871.5	$29/2^-$	320.7			
	4212.8	$31/2^-$	341.3			
	4696.1	$33/2^-$	483.3			
	5174.3	$35/2^-$	478.2			
	5515.0	$37/2^-$	340.7			
	5923.2	$39/2^-$	408.2			
	6388.3	$(41/2^-)$	465.1			

Configurations and Comments:

1. Tentatively assigned as $\pi(h_{11/2}) \otimes \nu(h_{11/2}^2)$ by comparison with a similar band in ^{131}La.
2. Collective oblate shape ($\gamma \sim -60°$) determined by large negative A_2/A_0 coefficients.
3. $B(M1)/B(E2)$ values > 1$(\mu_N/eb)^2$.
4. Signature splitting with backbending at 35/2.
5. Nuclear reaction: ^{122}Sn (^{19}F, 4nγ), E(^{19}F)= 81 MeV, Band intensity ~ 28%.

$^{134}_{60}\text{Nd}_{74}$

	E_{level} keV	I^π	$E_\gamma(M1)$ keV	$E_\gamma(E2)$ keV	$B(M1)/B(E2)$ $(\mu_N/eb)^2$	Reference
1	2294.2	8^-				**1997Pe07**
	2721.1	9^-	426.9			
	3183.4	10^-	462.3	888.9		
	3654.7	11^-	471.3	933.2		
	4131.2	12^-	476.5	947.9		
	4593.5	(13^-)	462	938.8		
2	4514.5	$12^{(-)}$				**1997Pe07**
	4714.0	$13^{(-)}$	199.5			
	5000.7	$14^{(-)}$	286.7			
	5363.1	$15^{(-)}$	362.4	648.6		
	5790.4	$16^{(-)}$	427.3	790		
	6271.3	$17^{(-)}$	480.9	908.7		
	6787.5	$18^{(-)}$	516.2	997.1		
	7293.2	$19^{(-)}$	505.7	1022		
3	4985.5	14^-				**1997Pe07**
	5201.4	$15^{(-)}$	215.9			
	5457.1	$16^{(-)}$	255.7			
	5770.4	$17^{(-)}$	313.3	569.3		
	6138.4	$18^{(-)}$	368.0	681.6		
	6544.7	$19^{(-)}$	406.3	774.4		
	6936.5	$20^{(-)}$	391.9	798		
	7350.2	$21^{(-)}$	413.6	806		
	7814.1	(22^-)	463.9	878.0		
	8331.2	(23^-)	517.1	981.6		
	8896.9	(24^-)	565.7	1082.6		
	9510.9	(25^-)	614	1180.0		
	10167.9	(26^-)	657	1270.9		
	10861.9	(27^-)	694	1351.3		

Configurations and Comments:

1. A strong admixture of $\nu(h_{11/2}[9/2])$ with $\nu(g_{7/2}[7/2] \otimes h_{11/2}[7/2])$ is suggested from the PSM calculations.
2. Prolate shape ($\beta_2 = 0.17$).
3. $B(M1)/B(E2)$ values > 3 $(\mu_N/eb)^2$.
4. Regular band with backbending at the top of the band.
5. Nuclear reaction: ^{110}Pd (^{28}Si, 4nγ), E(^{28}Si) = 130 MeV, Band intensity ~ 6%.

1. $\pi(h_{11/2}^2) \otimes \nu(g_{7/2}[7/2] \otimes h_{11/2}[7/2])$ from the PSM calculations.
2. Prolate shape ($\beta_2 = 0.17$).
3. $B(M1)/B(E2)$ values are >10 $(\mu_N/eb)^2$.
4. Regular band with backbending at the top of the band.
5. Band intensity ~ 6%.

1. $\pi(h_{11/2}[11/2] \otimes g_{7/2}[5/2])_{K^\pi = 8^-}$ coupled to a neutron pair in one of the following configurations: $\nu(h_{11/2}^2)[3/2,5/2, K^\pi = 1^+]$, $\nu(h_{11/2}^2)[1/2,5/2, K^\pi = 2^+]$ and $\nu(h_{11/2}^2)[1/2,5/2, K^\pi = 3^+]$. The lowest lying of these mixed 4-qp configurations is assigned to this band.
2. Oblate shape ($\beta_2 = -0.17$).
3. $B(M1)/B(E2)$ values >10 $(\mu_N/eb)^2$.
4. Regular band with backbending at spin 20.
5. Band intensity ~ 6%.

$^{136}_{60}$Nd$_{76}$

	E_{level} keV	I^{π}	E_{γ}(M1) keV	E_{γ}(E2) keV	B(M1)/B(E2) $(\mu_N/eb)^2$	Reference	Configurations and Comments:
1	3782	$9^{(-)}$				**1996Pe06**	1. $\pi(h_{11/2}^2) \otimes \nu(h_{11/2} d_{3/2})$ from PSM
	4002	$10^{(-)}$	220				calculations.
	4256	$11^{(-)}$	254				2. The plotted B(M1)/B(E2) values lie around
	4550	$12^{(-)}$	294				10 $(\mu_N/eb)^2$ and decrease as the spin values
	4895	$13^{(-)}$	345				increase.
	5306	$14^{(-)}$	411				3. Regular band.
	5760	$15^{(-)}$	454				4. Nuclear reaction: ^{110}Pd (^{30}Si, 4nγ), E(^{30}Si) =
	6261	$16^{(-)}$	501				125 and 130 MeV.
2	6232	$15^{(+)}$				**1996Pe06**	1. $\pi(h_{11/2}^2) \otimes (\nu h_{11/2} - \nu f_{7/2})$ associated with prolate
	6349	$16^{(+)}$	117				shape, from PSM calculations.
	6580	$17^{(+)}$	231				2. Regular band with backbending at 20.
	6885	$18^{(+)}$	305				3. Mean lifetimes of levels with spins 23 and 24
	7294	$19^{(+)}$	409				are 0.09(4) and 0.06(3) ps, respectively,
	7670	$20^{(+)}$	376				indicating enhanced B(M1) rates.
	8051	$21^{(+)}$	381				4. The B(M1)/B(E2) values range from about
	8467	$22^{(+)}$	416				6-20 $(\mu_N/eb)^2$.
	8948	$23^{(+)}$	481				
	9492	$24^{(+)}$	544				
	10092	$25^{(+)}$	600				
	10763	$26^{(+)}$	671				
3	6010	16^+				**1996Pe06**	1. $\pi(h_{11/2}^2) \otimes (\nu h_{11/2} + \nu f_{7/2})$ associated with prolate
	6241	17^+	231				shape, from PSM calculations.
	6525	18^+	284				2. Regular band .
	6870	19^+	345	629			3. The B(M1)/B(E2) values range from about
	7258	20^+	388	733			6-20 $(\mu_N/eb)^2$ and exhibit a rising trend as
	7688	21^+	430	818			the spin increases.
	8151	22^+	463	893			
	8655	23^+	504	967			
	9181	24^+	526	1030			
	9748	25^+	567	1093			
	10346	26^+	598	1165			
	10971	27^+	625	1223			
	11650	28^+		1304			
	12338	29^+		1367			
4	3875	11^-				**1996Pe06**	1. $\pi(h_{11/2}^2) \otimes \nu(h_{11/2} g_{7/2})$ or $\pi(h_{11/2}^2) \otimes (\nu h_{11/2} +$
	4105	12^-	230				$\nu d_{3/2})$ associated with oblate shape, from PSM
	4414	13^-	309	539			calculations.
	4771	14^-	357	666			2. Regular band with backbending at spin 17.
	5173	15^-	402	759			3. The B(M1)/B(E2) values range from about
	5610	16^-	437	839			3-25 $(\mu_N/eb)^2$.
	6037	17^-	427	864			
	6482	18^-	445	872			
	6970	19^-	488	933			
	7481	20^-	511	999			
	8030	21^-	549	1060			
	8654	22^-	624	1173			
5	8381	$22^{(+)}$				**1996Pe06**	1. No definite configuration could be assigned
	8756	$23^{(+)}$	375				to this band but from energy considerations ,
	9166	$24^{(+)}$	410	785			$\pi(h_{11/2}^2 g_{7/2}^2)$ may be favored.
	9619	$25^{(+)}$	453	863			2. Regular band.
	10110	$26^{(+)}$	491				
	10639	$27^{(+)}$	529	1020			

$^{137}_{60}\text{Nd}_{77}$

	E_{level} keV	I^π	$E_\gamma(M1)$ keV	$E_\gamma(E2)$ keV	$B(M1)/B(E2)$ $(\mu_N/eb)^2$	Reference	Configurations and Comments:
1	3896.2	$27/2^-$				**1997Pe06**	1. $\nu(h_{11/2})^3$ from the IBFM calculations.
	4160.2	$29/2^-$	264				2. Regular band with backbending at 37/2.
	4514.1	$31/2^-$	353.9	617.9			3. Nuclear reaction: ^{110}Pd (^{30}Si, 3nγ), E(^{30}Si) = 125
	4909.9	$33/2^-$	395.8	749.7			MeV and ^{123}Sb (^{19}F, 5nγ), E(^{19}F) = 97 MeV,
	5372.7	$35/2^-$	462.8	858.6			Band intensity $\sim$ 10%.
	5813.1	$37/2^-$	440.4	903.2			
	6194.5	$39/2^-$	381.4	821.8			
	6669.6	$41/2^-$	475.1	856.5			
	7100.9	$43/2^-$	431.3	906.4			
	7652.3	$45/2^-$	551.4	982.7			
	8349.3	$47/2^-$	697	1248.4			
2	4822.5	$31/2^-$				**1997Pe06**	1. $\pi(h_{11/2}^2) \otimes \nu(h_{11/2})$ from the IBFM calculations.
	5108.3	$33/2^-$	285.8				2. Regular band with backbending at 43/2.
	5416.5	$35/2^-$	308.2				3. Band intensity $\sim$ 5%.
	5788.6	$37/2^-$	372.1				
	6263.9	$39/2^-$	475.3				
	6795.4	$41/2^-$	531.5				
	7314.7	$43/2^-$	519.3				
	7702.8	$45/2^-$	388.1				
	8197.6	$47/2^-$	494.8				
	8745.7	$(49/2^-)$	548.1				
	9337.9	$(51/2^-)$	592.2				
3	5596.8	$33/2^+$				**1997Pe06**	1. Tentatively assigned as $\pi(h_{11/2}^2) \otimes \nu(h_{11/2}^2)$
	5853.8	$35/2^+$	257				$\otimes \nu\, s_{1/2}(d_{3/2})$.
	6161.1	$37/2^+$	307.3				2. Regular band.
	6515.8	$39/2^+$	354.7				3. B(M1) values are of the order of 1 W.u.
	6916.2	$41/2^+$	400.4				4. Band intensity $\sim$ 1%.
	7339.4	$43/2^+$	423.2				
	7797.0	$45/2^+$	457.6				
	8325.2	$(47/2^+)$	528.2				
	8922.1	$(49/2^+)$	596.9				
	9568.6	$(51/2^+)$	646.5				
	10272.2	$(53/2^+)$	703.6				

$^{138}_{60}\text{Nd}_{78}$

	E_{level} keV	I^π	$E_\gamma(M1)$ keV	$E_\gamma(E2)$ keV	$B(M1)/B(E2)$ $(\mu_N/eb)^2$	Reference	Configurations and Comments:
1	5577.6	14				**1994De11**	1. Tentatively assigned as $\pi(h_{11/2}^2) \otimes \nu(h_{11/2}^2)$.
	5771.4	15	193.8				2. Small Prolate deformation ($\beta_2 \approx 0.12$).
	6002.2	16^+	230.8				3. Regular band with a small backbending at 19.
	6288.5	(17)	286.3				4. Nuclear reaction: ^{121}Sb(^{19}F, 4nγ), E(^{19}F) = 75
	6669.0	(18)	380.5				MeV, Band intensity $\sim$ 4%.
	7048.1	(19)	379.1				
	7564.8	(20)	516.7				
	8489.5	(21)	924.7				

TABLE. Magnetic Dipole Rotational Bands
See page 295 for Explanation of Table

$^{139}_{62}\text{Sm}_{77}$

	E_{level} keV	I^π	$E_\gamma(M1)$ keV	$E_\gamma(E2)$ keV	$B(M1)/B(E2)$ $(\mu_N/eb)^2$	References
1	3327.2	25/2⁻				**1996Ro04**
	3445.8	27/2⁻	118.6			1996Br33
	3710.8	29/2⁻	265.0	384.2		
	4048.1	31/2⁻	337.3	601.9	4.6(21)	
	4457.5	33/2⁻	409.4	746.6	5.6(25)	
	4930.1	35/2⁻	472.6	882.3	4.8(22)	
	5443.6	37/2⁻	513.5	986.2		
	5934.9	(39/2)	491.3	1005.0		
	6494.9	(41/2)	560.0	1051.4		

Configurations and Comments:

1. Tentatively assigned in 1996Br33 as $\pi(h_{11/2}^2) \otimes \nu(h_{11/2})$ from CSM calculations.
2. Nearly axially symmetric prolate shape ($\beta_2 = 0.116$), from 1996Br33.
3. B(M1)/B(E2) are from 1996Br33.
4. Regular band with backbending at 39/2.
5. Mean lifetimes of levels with spin values 31/2⁻, 33/2⁻ and 35/2⁻ are 0.60(21), 0.40(14) and 0.25(8) ps, respectively from 1996Br33.
6. Nuclear reactions: ^{110}Pd (^{34}S, 5nγ), E(^{34}S) = 150 and 165 MeV, Band intensity~ 11% and (1996Br33): ^{62}Ni (^{81}Br, p3nγ), E(^{81}Br) = 350 MeV.

$^{142}_{64}\text{Gd}_{78}$

	E_{level} keV	I^π	$E_\gamma(M1)$ keV	$E_\gamma(E2)$ keV	$B(M1)/B(E2)$ $(\mu_N/eb)^2$	Reference
1	4767	12				**1997Su11**
	4989	13	222			
	5182	14	193			
	5374	15	192			
	5608	16	234			
	5893	17	285			
	6267	18	374			
	6562	19	295	670	11.6(9)	
	7090	20	528			
	7556	21	466	993	9.7(12)	
2	5416	16⁺				**1997Su11**
	5716	17⁺	300			
	6076	18⁺	360			
	6457	19⁺	381			
	6883	20⁺	426			
	7016	21⁺	133			

Configurations and Comments:

1. The band probably has $\pi(h_{11/2}^2) \otimes \nu(h_{11/2}^{-2})$ component in the configuration.
2. Irregular band.
3. Nuclear reaction: ^{111}Cd(^{35}Cl, 1p3nγ), E(^{35}Cl) = 170 MeV.

Configurations and Comments:

1. The band probably has $\pi(h_{11/2}^2) \otimes \nu(h_{11/2}^{-2})$ component in the configuration.
2. Regular band with backbending at 21.

$^{144}_{64}\text{Gd}_{80}$

	E_{level} keV	I^π	$E_\gamma(M1)$ keV	$E_\gamma(E2)$ keV	$B(M1)/B(E2)$ $(\mu_N/eb)^2$	Reference
1	5370.7	14⁺				**1994Rz01**
	5723.6	15⁺	352.9			
	6214.2	16⁺	490.6			
	6619.0	17⁺	404.8			
	7014.6	18⁺	395.6			
	7419.1	19⁺	404.5			
	7923.5	20⁺	504.4			
	8221.7	(21⁺)	298.2			
	8540.4	(22⁺)	318.7			
	8993.8	(23⁺)	453.4			

Configurations and Comments:

1. $\pi(h_{11/2}^2)_{K=10}{}^+ \otimes \nu(h_{11/2}^{-2})$ from the FAL Coupling scheme.
2. Negative E2/M1 mixing ratios ($\delta_{E2/M1}$) imply an oblate shape ($\beta_2 \sim -0.12$).
3. Irregular band.
4. Nuclear reaction: ^{108}Pd (^{40}Ar, 4nγ), E(^{40}Ar) = 182 MeV, Band intensity ~ 15%.

$^{192}_{80}\text{Hg}_{112}$

E_{level} keV	I^π	$E_\gamma(M1)$ keV	$E_\gamma(E2)$ keV	$B(M1)/B(E2)$ $(\mu_N/eb)^2$	References
1	6879	$23^{(-)}$				**1994Le08**
	7036	$24^{(-)}$	157			
	7273	$25^{(-)}$	237	394		
	7517	$26^{(-)}$	244	480		
	7788	$27^{(-)}$	272	515		
	7927	$28^{(-)}$	139	(410)		
	8265	$29^{(-)}$	337	476		
	8545	$30^{(-)}$	280	617		
	8992	$31^{(-)}$	447	727		
	9446	$32^{(-)}$	454	900		
	9936	$33^{(-)}$	490	942		
	10467	$34^{(-)}$	(532)	1021		
2	6304	(22^+)				**1996Wi09**
	6433.8	(23^+)	129.8			1994Le08
	6710.1	(24^+)	276.3	405.9	1.7(+10-9)	
	7043.7	(25^+)	333.6	611	0.6(+∞-6)	
	7435.6	(26^+)	391.9	725.3	1.7(+42-10)	
	7960.0	(27^+)	524.4	915.6	6.7(+39-56)	
	8303.4	(28^+)	343.4	867.6	10.0(+∞-106)	
	8712.5	(29^+)	409.1	753.7	3.8(+∞-39)	
	8960.6	(30^+)	248.1	659.2	6.4(+110-43)	
	9195.4	(31^+)	234.8	483.2	8.7(+25-17)	
	9375.2	(32^+)	179.8	414.6	7.4(+24-18)	
	9665.2	(33^+)	290	470		
	10037.2	(34^+)	372			

Configurations and Comments:

1. $\pi(i_{13/2}h_{9/2}) \otimes \nu(i_{13/2}^4)$ or $\pi(i_{13/2}h_{9/2}h_{11/2}^2) \otimes \nu(i_{13/2}^2)$ based on 23^- or 25^- states from HF+BCS. calculations. For the upper part of the band a mixing with the $\pi(i_{13/2}h_{9/2}) \otimes \nu(i_{13/2}^6)$ configuration is suggested.
2. Irregular band.
3. B(M1)/B(E2) ratios lie around $5.5(\mu_N/eb)^2$.
4. Nuclear reaction: ^{160}Gd ($^{36}\text{S}, 4n\gamma$), $E(^{36}\text{S}) = 159$ MeV, Band intensity ~ 10%.

Configurations and Comments:

1. $\pi(h_{9/2}^2) \otimes \nu(i_{13/2}^4)$, $I=22^+$ or $\pi(h_{11/2}^2 h_{9/2}^2) \otimes \nu(i_{13/2}^2)$, $I=23^+$ from the HF+BCS calculations (1994Le08).
2. Small oblate deformation (1994Le08).
3. Mean lifetimes of the states with spins between (23^+) and (32^+) are 14.9(+50-39), 20.4(+40-52), 1.0(+10-16), 3.6(+19-10), 1.7(+14-15), 0.7(7), 0.2(+7-2), 1.3(6), 3.5(+6-5) and 2.2(5) ps, respectively.
4. Irregular band.
5. $B(M1) \sim 0.01 \mu_N^2$ in the lower spin region and jumps to $1.1 \mu_N^2$ in the high spin region of the band.
6. Band intensity ~ 12%.

$^{193}_{80}\text{Hg}_{113}$

E_{level} keV	I^π	$E_\gamma(M1)$ keV	$E_\gamma(E2)$ keV	$B(M1)/B(E2)$ $(\mu_N/eb)^2$	References
1	6418.7	$(53/2^-)$				**1995Fo13**
	6921.1	$(55/2^-)$	502.4			
	7275.8	$(57/2^-)$	354.7	857.1		
	7698.7	$(59/2^-)$	422.9	777.6		
	7837.5	$(61/2^-)$	138.8	561.8		
	8134.2	$(63/2^-)$	296.7	437.5		
	8392.0	$(65/2^-)$	257.8	556.5		
	8748.1	$(67/2^-)$	356.1	614.0		
	9218.7	$(69/2^-)$	470.6	826.6		
	9673.1	$(71/2^-)$	454.4	924.9		
	10287.6	$(73/2^-)$	614.5	1068.9		
	10850.6	$(75/2^-)$	(563)	1177.7		

Configurations and Comments:

1. Tentatively assigned as $\pi(h_{9/2}^2 h_{11/2}^{-2}) \otimes \nu(i_{13/2}^{-3})$ in addition to $p_{3/2}$ neutrons because of its negative parity.
2. Small oblate deformation ($\beta_2 \sim 0.15$).
3. B(M1)/B(E2) values lie in the interval $2 - 4$ $(\mu_N/eb)^2$.
4. Irregular band.
5. Nuclear reaction: ^{150}Nd ($^{48}\text{Ca}, 5n\gamma$), $E(^{48}\text{Ca}) = 213$ MeV, Band intensity ~ 20%.

TABLE. Magnetic Dipole Rotational Bands
See page 295 for Explanation of Table

2	5338.4	(47/2⁻)			**1995Fo13**	1. Tentatively assigned as $\pi(h_{9/2}^2 h_{11/2}^{-2}) \otimes \nu(i_{13/2}^{-3})$ in addition to $p_{3/2}$ neutrons because of its negative parity.
	5714.2	(49/2⁻)	(375.8)			
	6016.4	(51/2⁻)	(302.2)	678.0		2. Small oblate deformation ($\beta_2 \sim 0.15$).
	6400.3	(53/2⁻)				3. B(M1)/B(E2) values lie in the interval $2-4$ $(\mu_N/eb)^2$.
	6725.7	(55/2⁻)	325.4			
	6978.0	(57/2⁻)	252.3	577.6		4. Regular band with backbending at 57/2.
	7245.0	(59/2⁻)	267.0			5. Band intensity $\sim 6\%$.
	7559.7	(61/2⁻)	314.7	581.9		
	7919.3	(63/2⁻)	359.6	674.1		
	8330.3	(65/2⁻)	411.0	770.7		
	8757.2	(67/2⁻)	426.9	837.8		
3	5546.9	47/2⁽⁺⁾			**1995Fo13**	1. Tentatively assigned as $\pi(h_{9/2}^2 h_{11/2}^{-2}) \otimes \nu(i_{13/2}^3)$ from the CSM calculations.
	5831.4	49/2⁽⁺⁾	284.5		1993De42	
	6067.0	51/2⁽⁺⁾	235.6	520.1	1993Ro03	2. Small oblate deformation ($\beta_2 \sim 0.15$).
	6464.0	53/2⁽⁺⁾	397.0	632.6		3. B(M1)/B(E2) values lie in the interval $2-4$ $(\mu_N/eb)^2$.
	6839.4	55/2⁽⁺⁾	375.4	772.2		
	7037.0	57/2⁽⁺⁾	197.6			4. Irregular band.
	7197.4	59/2⁽⁺⁾	160.4			5. Band intensity $\sim 20\%$.
	7554.7	61/2⁽⁺⁾	357.3	517.6		
	7924.4	63/2⁽⁺⁾	369.7	726.9		
	8388.4	65/2⁽⁺⁾	464.0	833.6		
	8886.3	67/2⁽⁺⁾	497.9	962.0		
	9408.5	69/2⁽⁺⁾	522.2	1020.3		
	9922.6	71/2⁽⁺⁾	514.1	1036.3		

$^{195}_{80}\text{Hg}_{115}$

	E_{level} keV	I^π	$E_\gamma(M1)$ keV	$E_\gamma(E2)$ keV	B(M1)/B(E2) $(\mu_N/eb)^2$	Reference	Configurations and Comments:
1	7412.2	57/2⁻				**1998Ne01**	1. $\pi(h_{11/2}^2) \otimes \nu(i_{13/2}^{-4} f_{5/2}^{-1})$ from CSM calculations.
	7744.9	59/2⁻	332.7				2. Small oblate deformation.
	8067.5	61/2⁻	322.6	654.5			3. B(M1)/B(E2) ratios $\sim 2\ (\mu_N/eb)^2$.
	8456.7	63/2⁻	389.2	712.2			4. Irregular band with backbending at 61/2.
	8892.1	65/2⁻	435.4	825.1			5. Nuclear reaction: ^{192}Os (^{9}Be, 6nγ), E(^{9}Be) = 80 MeV, Band intensity $\sim 5\%$.
	9331.2	67/2⁻	439.1	875.7			
	9785.2	69/2⁻	454.0	893.4			
	10220.6	71/2⁻		889.4			
2	5174.7	43/2⁺				**1998Ne01**	1. $\pi(h_{11/2}^2) \otimes \nu(i_{13/2}^{-3})$ from CSM calculations.
	5308.1	45/2⁺	133.4				2. Small oblate deformation.
	5411.3	47/2⁺	103.2				3. B(M1)/B(E2) ratios lie around 2 $(\mu_N/eb)^2$.
	5687.7	49/2⁺	276.4				4. Irregular band.
	5893.6	51/2⁺	205.9	481.3			5. Band intensity $\sim 15\%$.
	6300.1	53/2⁺	406.5	611.5			
	6652.1	55/2⁺	352.0	758.3			
	7129.0	57/2⁺	476.9	828.3			
	7538.2	59/2⁺	409.2	886.1			
	8010.3	61/2⁺	472.1	882.0			
	8383.3	63/2⁺		845.1			
3	X					**1998Ne01**	1. This band has tentatively been assigned to the nucleus.
	171.8+X		171.8				2. Irregular band.
	443.3+X		271.5				3. Band intensity $\sim 3\%$.
	749.0+X		305.7	576.9			

$^{196}_{80}\text{Hg}_{116}$

	E_{level} keV	I^π	$E_\gamma(M1)$ keV	$E_\gamma(E2)$ keV	$B(M1)/B(E2)$ $(\mu_N/eb)^2$	Reference
1	6400+X	(22^+)				**1993Ce04**
	6557+X	(23^+)	157			
	6659+X	(24^+)	102	259		
	6916+X	(25^+)	257	359		
	7094+X	(26^+)	178	435		
	7462+X	(27^+)	368	547		
	7750+X	(28^+)	288	656		
	8211+X	(29^+)	461	749		
	8609+X	(30^+)	398	859		

Configurations and Comments:

1. $\pi(h_{9/2}^2 h_{11/2}^{-2}) \otimes \nu(i_{13/2}^{-2})$ from TRS calculations.
2. Small oblate shape $(\beta_2, \gamma) = (0.139, -72°)$.
3. $X \geq 0$ keV.
4. B(M1)/B(E2) values range from 0.5 - 3 $(\mu_N/eb)^2$
5. Irregular band.
6. Nuclear reaction: ^{192}Os $(^9$Be, 5n$\gamma)$, E(^{9}Be) = 65 MeV, Band intensity $\sim$ 19%.

$^{191}_{82}\text{Pb}_{109}$

	E_{level} keV	I^π	$E_\gamma(M1)$ keV	$E_\gamma(E2)$ keV	$B(M1)/B(E2)$ $(\mu_N/eb)^2$	Reference
1	2577.5+X	$(29/2^-)$				**1998Fo02**
	2811.5+X	$(31/2^-)$	234.0			
	3195.1+X	$(33/2^-)$	383.6			
	3604.4+X	$(35/2^-)$	409.3	792.9	23(5)	
	4030.5+X	$(37/2^-)$	426.1	835.5	20(5)	
	4377.2+X	$(39/2^-)$	346.7			
	4691.3+X	$(41/2^-)$	314.1			
	4929.9+X	$(43/2^-)$	238.6			
	5207.1+X	$(45/2^-)$	277.2			

Configurations and Comments:

1. Tentatively assigned as $\pi(h_{9/2}i_{13/2}s_{1/2}^{-2})_{K=11^-} \otimes \nu(i_{13/2}^{-1})$ below, and $\pi(h_{9/2}i_{13/2}s_{1/2}^{-2})_{K=11^-} \otimes \nu(i_{13/2}^{-3})_{K=33/2^+}$ above the bandcrossing.
2. $X \sim 72$ keV.
3. All E_{level} given here are approximate since E_{level} of $13/2^+$ state is $\sim$ 138 keV.
4. Regular band with backbending at 39/2.
5. Nuclear reaction: ^{173}Yb $(^{24}$Mg, 6n$\gamma)$, E(^{24}Mg) = 134.5 MeV, Band intensity $\sim$ 10%.

	E_{level} keV	I^π	$E_\gamma(M1)$ keV	$E_\gamma(E2)$ keV	$B(M1)/B(E2)$ $(\mu_N/eb)^2$	Reference
2	2428.7	$27/2^+$				**1998Fo02**
	2765.9	$(29/2^+)$	337.2			
	3141.4	$(31/2^+)$	375.5			
	3551.3	$(33/2^+)$	409.9			

Configurations and Comments:

1. Tentatively assigned as $\pi(h_{9/2}^2 s_{1/2}^{-2})_{K=8^+} \otimes \nu(i_{13/2}^{-1})$ or $\pi(i_{13/2}s_{1/2}^{-1})_{K=7^+} \otimes \nu(i_{13/2}^{-1})$.
2. All E_{level} given here are approximate since E_{level} of $13/2^+$ state is $\sim$ 138 keV.
3. Regular band.
4. Band intensity $\sim$ 7.5%.

$^{192}_{82}\text{Pb}_{110}$

	E_{level} keV	I^π	$E_\gamma(M1)$ keV	$E_\gamma(E2)$ keV	$B(M1)/B(E2)$ $(\mu_N/eb)^2$	Reference
1	4241.2	15^-				**1993Pl02**
	4370.1	16^-	128.9			
	4519.2	17^-	149.1		>2.38	
	4702.3	18^-	183.1		>7.69	
	4989.6	19^-	287.3		>6.67	
	5276.9	20^-	287.3		>16.67	
	5559.5	21^-	282.6		>11.11	
	5708.6	(22^-)	149.1	431.7	<20	

Configurations and Comments:

1. Tentatively assigned as $\pi(9/2[505] \otimes 13/2[606]) \otimes \nu(i_{13/2}^2)$ based on CSM-TRS calculations and by comparison with ^{191}Tl.
2. Small oblate deformation.
3. The limits on B(M1)/B(E2) are by assuming that the unobserved E2 transitions are at the most half intense than the 489.5 keV γ ray in band 2.
4. Regular band with backbending at spin 21.
5. Nuclear reaction: ^{173}Yb $(^{24}$Mg, 5n$\gamma)$, E(^{24}Mg) = 132 MeV.

	E_{level} keV	I^π	$E_\gamma(M1)$ keV	$E_\gamma(E2)$ keV	$B(M1)/B(E2)$ $(\mu_N/eb)^2$	Reference
2	4963.0	18^-				**1993Pl02**
	5087.1	19^-	124.1		>50	
	5286.3	20^-	199.2		>4	
	5531.7	21^-	245.4		>11.11	
	5871.0	22^-	339.3		>12.5	
	6232.1	23^-	361.1		>5.88	
	6666.0	(24^-)	433.9		>4	
	7155.5	(25^-)	489.5		>5.88	

Configurations and Comments:

1. Tentatively assigned as $\pi(7/2[514] \otimes 13/2[606]) \otimes \nu(i_{13/2}^2)$ from the CSM-TRS calculations and by comparison with ^{191}Tl.
2. Small oblate deformation.
3. The limits on B(M1)/B(E2) are by assuming that the unobserved E2 transitions are at the most half-intense than the 489.5 keV γ ray.
4. Regular band.

$^{193}_{82}$Pb$_{111}$

	E_{level} keV	I^π	$E_\gamma(M1)$ keV	$E_\gamma(E2)$ keV	B(M1)/B(E2) $(\mu_N/eb)^2$	References
1	2584.8+X	29/2⁻				**1996Du18**
	2686.9+X	31/2⁻	102.1			1996Ba54
	2939.2+X	33/2⁻	252.3			1997Ch33
	3320.7+X	35/2⁻	381.5	633.8	28(5)	
	3722.3+X	37/2⁻	401.6	783.1	22(4)	
	4136.1+X	39/2⁻	413.8	815.4	16(6)	
	4470.6+X	41/2⁻	334.5	748.3		
	4828.3+X	43/2⁻	357.7	692.3		
	5218.6+X	45/2⁻	390.3			
2	4297.7+X	(39/2⁺)				**1996Du18**
	4387.7+X	(41/2⁺)	90.0			1998Cl06
	4536.6+X	(43/2⁺)	148.9			
	4768.6+X	(45/2⁺)	232.0			
	5060.2+X	(47/2⁺)	291.6			
	5425.4+X	(49/2⁺)	365.2	656.8	15(3)	
	5815.0+X	(51/2⁺)	389.6	754.7	12(3)	
	6231.1+X	(53/2⁺)	416.1	805.6		
	6657.2+X	(55/2⁺)	426.1	842.2	15(3)	
	7089.9+X	(57/2⁺)	432.7	858.8		
	(7516.0+X)	(59/2⁺)	(426.1)			
	(7932.1+X)	(61/2⁺)	(416.1)			
3	4944.8+X	(43/2⁺)				**1996Du18**
	5169.1+X	(45/2⁺)	224.3			
	5436.6+X	(47/2⁺)	267.5			
	5762.8+X	(49/2⁺)	326.2			
	6145.2+X	(51/2⁺)	382.4			
4	5092.7+X	(45/2⁻)				**1996Du18**
	5331.8+X	(47/2⁻)	239.1			1996Ba54
	5597.4+X	(49/2⁻)	265.6			
	5926.9+X	(51/2⁻)	329.5			
	6302.5+X	(53/2⁻)	375.6			
	6715.4+X	(55/2⁻)	412.9			
	7154.6+X	(57/2⁻)	439.2			
5	5825.3+X	(49/2⁻)				**1996Du18**
	6001.6+X	(51/2⁻)	176.3			
	6285.3+X	(53/2⁻)	283.7			
	6597.2+X	(55/2⁻)	311.9			
	6927.6+X	(57/2⁻)	330.4			
	7312.1+X	(59/2⁻)	384.5			
	7713.6+X	(61/2⁻)	401.5			

Configurations and Comments:

1. $\pi(9/2[505] \otimes 13/2[606])_{K=11}^- \otimes \nu(i_{13/2})$ by Comparison with similar bands in neighboring Pb nuclei.
2. Oblate deformation.
3. X ~ 100 keV from systematics.
4. For bandhead $T_{1/2}$ = 9.4(7) ns and g factor = 0.68(3) (1997Ch33).
5. Regular band with backbending at 41/2.
6. Nuclear reaction: ^{168}Er (^{30}Si, 5nγ), E(^{30}Si) = 159 MeV, Band intensity ~ 17%.

1. Tentatively assigned as $\pi(9/2[505] \otimes 13/2[606])_{K=11}^- \otimes \nu(i_{13/2}^2 p_{3/2})$ by comparison with similar Bands in neighboring Pb nuclei.
2. Oblate deformation.
3. X ~ 100 keV from systematics.
4. The B(M1) values as given in 1998Cl06 for the transitions from 291 to 416 keV are 5.27(64), 4.32(+56-75), 4.01(+95-76) and 2.83(34) (μ_N^2), respectively.
5. The mean lifetimes of levels having spin values from 45/2 to 51/2 as given in 1998Cl06 are 0.33(4), 0.23(+4-3), 0.21(+4-5) and 0.25(3) ps, respectively.
6. Regular band with backbending at spin 59/2.
7. Band intensity ~ 7%.

1. $\pi(9/2[505] \otimes 13/2[606])_{K=11}^- \otimes \nu(i_{13/2}^2 f_{5/2})$ by comparison with similar bands in neighboring Pb nuclei.
2. Oblate deformation.
3. X ~ 100 keV from systematics.
4. Regular band.
5. Band intensity ~ 3%.

1. Tentatively assigned as $\pi(9/2[505] \otimes 13/2[606])_{K=11}^- \otimes \nu(i_{13/2})^3$ by comparison with similar bands in neighboring Pb nuclei.
2. Oblate deformation.
3. X ~ 100 keV from systematics.
4. Regular band.
5. Band intensity ~ 0.6%.

1. Tentatively assigned as $\pi(9/2[505] \otimes 13/2[606])_{K=11}^- \otimes \nu(i_{13/2})^3$ or $\pi(9/2[505] \otimes 13/2[606])_{K=11}^- \otimes \nu(i_{13/2}h_{9/2}^2)$ from HF+BCS calculations.
2. X ~ 100 keV from systematics.
3. Parity assignment is based on three M1 transitions to band 1.
4. Regular band.
5. Band intensity ~ 0.6%.

$^{194}_{82}\text{Pb}_{112}$

	E_{level} keV	I^π	E_γ(M1) keV	E_γ(E2) keV	B(M1)/B(E2) $(\mu_N/eb)^2$	References
1	4963.5	16^-				**1993Me12**
	5083.1	17^-	119.6			1994Po08
	5228.3	18^-	145.2			1995Ka19
	5424.4	19^-	197.1			1998Cl06
	5685.8	20^-	260.4			1998Ka59
	6022.2	21^-	336.4			
	6398.3	22^-	376.1			
	6814.9	23^-	416.6			
	7239.0	(24)	424.1			
	7681	(25)	442			
	8109	(26)	428			
2	4376	13^+				**1998Ka59**
	4506.4	14^+	130.4			1993Me12
	4643.4	15^+	137.0			1994Po08
	4806.7	16^+	163.3			1995Ka19
	5109.7	17^+	303.0			
	5506.9	18^+	397.2			
	5883.5	19^+	376.6	773.4	21(4)	
	6247.3	20^+	363.8	740.0	13(3)	
	6508.3	21^+	261			
	6720.9	22^+	212.6			
	6948.6	23^+	227.7			
	7216.0	(24)	267.4			
	7523.2	(25)	307.2			
	7884.8	(26)	361.6	(668)		
	8278.4	(27)	393.6	(754)		
	8699	(28)	421			
	9141	(29)	442			
	9603	(30)	462			
	10088	(31)	485			
3	4135.6	16^+				**1993Me12**
	(4298.2)	17^+	(162.6)			
	4531.3	18^+	233.1			
	4819.3	19^+	288.0			
	5167.1	20^+	347.8			
	5541.4	21^+	374.3			
	5938.4	(22)	397.0			

Configurations and Comments:

1. Tentatively assigned as $\pi(9/2[505]\otimes 13/2[606])$ $_{K=11^-} \otimes \nu(i_{13/2}^2)$ in 1994Po08 from the excitation energy, spin, mom. of inertia, alignments and from a comparison with the isotone ^{192}Hg.
2. The two topmost transitions are from 1995Ka19
3. Regular band with backbending at the top of the band.
4. The B(M1) values as given in 1998Cl06 for the transitions from 260 to 417 keV are 9.79(+255 -170), 5.86(+56-56), 5.13(+114-143) and 3.90 (87) (μ_N^2), respectively.
5. The mean lifetimes of levels having spin values from 20 to 23 as given in 1998Cl06 are 0.23(+4-6), 0.21(2), 0.18(+5-4) and 0.18(4) ps, respectively.
6. Nuclear reaction: ^{158}Gd $(^{40}$Ar, 4n$\gamma)$, E(^{40}Ar) = 178 MeV, Band intensity $\sim$ 25%.

1. Tentatively assigned as $\pi(9/2[505]\otimes 13/2[606])$ $_{K=11^-} \otimes \nu(f_{5/2}i_{13/2})$ before and $\pi(9/2[505] \otimes 13/2[606])_{K=11^-} \otimes \nu(f_{5/2}i_{13/2}^3)$ after the bandcrossing from the spin, parity and from a comparison with the isotone ^{192}Hg.
2. The ordering of levels up to 23^+ is from 1998Ka59 with the exception that 212.6 is assumed between the 227.7 and 261 keV transitions. The ordering above this is taken from 1993Me12, 1994Po08 and 1995Ka19.
3. Regular band with backbending at 19^+.
4. Nuclear reaction: ^{182}W(^{16}O, 4n$\gamma)$, E(^{16}O)= 95 MeV.

1. No definite configuration has been suggested for this band. From the decay pattern it appears that this is based on four-neutron excitation.
2. Regular band.
3. Band intensity $\sim$ 4%.

$^{195}_{82}\text{Pb}_{113}$

	E_{level} keV	I^π	E_γ(M1) keV	E_γ(E2) keV	B(M1)/B(E2) $(\mu_N/eb)^2$	References
1	2968.3	27/2⁻				**1996Ka15**
	3098.0	29/2⁻	129.7			1995Fa19
	3362.0	31/2⁻	264.0			
	3734.7	33/2⁻	372.7	637.0	16(4)	
	4119.9	35/2⁻	385.2	757.7	18(3)	
	4566.2	(37/2⁻)	446.3	832.0	13(3)	
	4966.8	(39/2⁻)	400.6			
2	5123.6	(39/2⁻)				**1996Ka15**
	5270.4	(41/2⁻)	146.8			1995Fa19
	5467.7	(43/2⁻)	197.3			1998Cl06
	5702.5	(45/2⁻)	234.8			
	5978.4	(47/2⁻)	275.9			
	6308.1	(49/2⁻)	329.7			
	6674.2	(51/2⁻)	366.1			
	7090.8	(53/2⁻)	416.6			
	7536.8	(55/2⁻)	(446.0)			
3	4465.6	(33/2⁻)				**1996Ka15**
	4560.4	(35/2⁻)	94.8			1995Fa19
	4693.9	(37/2⁻)	133.5			
	4866.5	(39/2⁻)	172.6			
	5108.1	(41/2⁻)	241.6			
	5412.9	(43/2⁻)	304.8			
	5770.9	(45/2⁻)	358.0	663.0	17(4)	
	6144.7	(47/2⁻)	373.8	732.0	23(5)	
	6529.5	(49/2⁻)	384.8	759.0	13(3)	
	6907.2	(51/2⁻)	377.7	763.0	10(3)	
	7281.2	(53/2⁻)	374.0			

Configurations and Comments:

1. $\pi(9/2[505] \otimes 13/2[606])_{k^\pi=11^-} \otimes \nu(i_{13/2})$ by comparison with the neighboring ^{194}Pb and ^{195}Tl.
2. Oblate shape
3. Parities are from 1995Fa19.
4. Irregular band with backbending at the top of the band.
5. Nuclear reaction: ^{184}W $(^{16}O, 5n\gamma)$, $E(^{16}O) = 113$ MeV, Band intensity ~ 5%.

1. $\pi(9/2[505] \otimes 13/2[606])_{k^\pi=11^-} \otimes \nu(i_{13/2}^3)$ by comparison with the neighboring ^{194}Pb and ^{195}Tl.
2. Oblate shape
3. Parities are from 1995Fa19.
4. Regular band.
5. The B(M1) values as given in 1998Cl06 for the transitions from 276 to 366 keV are 7.01(+200 -125), 6.14(88) and 4.48 (+41-61) (μ_N^2), respectively.
6. The mean lifetimes of levels having spin values from 47/2 to 51/2 as given in 1998Cl06 are 0.28(+5-8), 0.21(3) and 0.22(+3-2) ps, respectively.

1. $\pi(9/2[505] \otimes 13/2[606])_{K=11} \otimes \nu(i_{13/2}^2(f_{5/2}/p_{3/2})^1)$ at low spin and $\pi(9/2[505] \otimes 13/2[606])_{K=11} \otimes \nu(i_{13/2}^4(f_{5/2}/p_{3/2})^1)$ at high spin, by comparison with a similar band of ^{194}Pb.
2. Oblate shape ($\beta_2 \sim -0.15$).
3. Regular band with backbending at the top of the band.
4. Parities are from 1995Fa19.
5. Band intensity ~ 15%.

$^{196}_{82}\text{Pb}_{114}$

	E_{level} keV	I^{π}	$E_{\gamma}(M1)$ keV	$E_{\gamma}(E2)$ keV	$B(M1)$ μ_N^2	References
1	X					**1996Ba53**
	164.4+X		164.4			1993Hu01
	372.9+X		208.5			1995Mo01
	622.8+X		250.3			
	931.9+X		309.1			
	1307.7+X		375.1			
	1712.2+X		404.4			
2	5155.0	$16^{(-)}$				**1995Mo01**
	5262.6	$17^{(-)}$	107.6			1993Hu01
	5400.2	$18^{(-)}$	137.6			1996Ba53
	5604.3	$19^{(-)}$	204.1			
	5872.7	$21^{(-)}$	268.4			
	6205.1	$21^{(-)}$	332.4			
	6572.3	$22^{(-)}$	367.2	698.7	≥ 2.3	
	6964.4	$23^{(-)}$	392.1	759.3	3.7(+49-16)	
	7362.3	$24^{(-)}$	397.9	790.3	4.4(+39-18)	
	7770.7	$25^{(-)}$	408.4	806.1	1.8(+7-4)	
	8104.5	(26)	333.8			
	8476.4	(27)	371.9			
	8813.1	(28)	336.7			
	9171.7	(29)	358.6			
	9614.2	(30)	442.5			
3	Y					**1996Ba53**
	192.9+Y		192.9			1993Hu01
	507.5+Y		314.6	507.6		1995Mo01
	882.0+Y		374.5	689.2		1998Cl06
	1237.4+Y		355.4	730.0		
	1578.9+Y		341.5	696.8		
	1822.6+Y		243.7	585.2		
	2032.5+Y		209.9			
	2272.0+Y	25	239.5			
	2558.2+Y	26	286.2		3.9(+10-6)	
	2897.4+Y	27	339.2		3.2(+13-12)	
	3295.1+Y	28	397.7		3.0(+10-6)	
	3743.7+Y	29	448.6		2.0(+4-3)	
	4234.2+Y		490.5		1.9(+5-3)	
	4760.9+Y		526.7			
4	Z					**1995Mo01**
	295.7+Z		295.7			1996Ba53
	638.5+Z		342.8			
	1018.4+Z		379.9			
	1431.1+Z		412.7			
	1863.5+Z		432.4			

Configurations and Comments:

1. Configuration assignment could not be made as the spins and excitation energies could not be measured experimentally.
2. Regular band.
3. X ~ 5874 keV from systematics.
4. Nuclear reaction (1993Hu01) : ^{170}Er (^{30}Si, 4nγ), E(^{30}Si) = 142, 146 and 151 MeV and ^{176}Yb (^{26}Mg, 6nγ), E(^{26}Mg) = 138 MeV, Band intensity ~ 9%.

1. Tentatively assigned as $\pi(h_{9/2}i_{13/2}) \otimes \nu(i_{13/2}^{-2})$ from the CSM calculations.
2. Oblate deformation.
3. Regular band with backbending at spin 26.
4. B(E2) values are from 1996Ba53.
5. The mean lifetimes of levels having spin values from $23^{(-)}$ to $28^{(-)}$ are ≤0.4, 0.21(+15-12), 0.17(+12 -8), 0.39(11), 0.47(+10-14) and 0.23(9) ps, respectively.
6. Top five transitions are from 1996Ba53. Above $25^{(-)}$ there is a forking with another path having 395.4, 422.1, 404.1 and 428.5 keV transitions.
7. Band intensity ~ 15% from 1993Hu01.

1. The band is likely to be based on the $\pi(h_{9/2}s_{1/2})$ quasiproton configuration (1995Mo01).
2. Oblate deformation.
3. Spins are from 1998Cl06.
4. Regular band with backbending at 1237.4+X level.
5. The B(M1) values are from 1995Mo01.
6. The B(M1) values as given in 1998Cl06 for the transitions from 286 to 490 keV are 9.57(+201 -151), 7.05(+166-124), 5.28 (106), 4.52 (+70-104) and 2.59(58) (μ_N^2), respectively.
7. The mean lifetimes as given in 1995Mo01, of five uppermost levels are 0.35(+20-10), 0.41(8), 0.25(6), 0.27(4) and 0.23(5) ps respectively.
8. The mean lifetimes of levels having spin values from 25 to 29 as given in 1998Cl06 are 0.19(+3-4), 0.17(+3-4), 0.15(3), 0.13(+3-2) and 0.18(4) ps, respectively.
9. Band intensity ~ 30% from 1993Hu01.

1. Configuration assignment could not be made as the spins and excitation energies could not be measured experimentally.
2. Regular band.
3. Nuclear reaction (1995Mo01) : ^{170}Er (^{30}Si, 4nγ) E(^{30}Si) = 142 MeV, Band intensity ~ 6%

$^{197}_{82}$Pb$_{115}$

	E_{level} keV	I^π	$E_\gamma(M1)$ keV	$E_\gamma(E2)$ keV	B(M1)/B(E2) $(\mu_N/eb)^2$	References
1	3283.8	27/2⁻				**1999Po13**
	3436.3	29/2⁻	152.5			1995Ba35
	3706.8	31/2⁻	270.5			1992Ku06
	4065.9	33/2⁻	359.1	629.8	17(4)	1994Cl01
	4435.7	35/2⁻	369.8	729.0	23(3)	1998Cl06
	4820.7	37/2⁻	385.0	754.9	15(2)	
	5185.9	39/2⁻	365.2	750.2	15(2)	
	5479.7	41/2⁻	293.8	659.2	28(4)	
	5707.3	43/2⁻	227.6	521.7	26(7)	
	5952.7	45/2⁻	245.4	473.2		
	6237.9	47/2⁻	285.2	531.0		
	6565.1	49/2⁻	327.2	612.4		
	6904.0	51/2⁻	338.9	666.1		
	7257.3	53/2⁻	353.3	692.1		
	7660.1	55/2⁻	402.8	756.0		
	8120.4	57/2⁻	460.3	862.8		
	8635.5	59/2⁻	515.1	975.1		
	9198.1	61/2⁻	562.6	1077.4		
	9794.1	63/2⁻	596.0	1158.1		
	10405.8	65/2⁻	611.7	1207.4		

Configurations and Comments:

1. $\pi(h_{9/2}i_{13/2})_{K=11}^- \otimes \nu(i_{13/2}^{-1})$ below and $\pi(h_{9/2}i_{13/2}s_{1/2}^{-2}) \otimes \nu(i_{13/2}^{-3})$ above the band crossing , by comparison with the similar band in neighboring ^{199}Pb and from the TAC model calculations.
2. Regular band showing a backbend at 41/2.
3. B(M1)/B(E2) values are from 1994Cl01. Since we are choosing ordering from 1999Po13, some B(M1)/B(E2) ratios of 1994Cl01 are left out.
4. The mean lifetimes for the transitions from 152.6 to 293.8 keV as given in 1994Cl01 are 3.1(7), 2.8(4), 1.3(3), 1.3(3), 1.1(3) 1.3(3) ps, respectively and that for transitions from 285 to 353 as given in 1998Cl06 are 0.40(2), 0.29(+3-2), 0.17(+2-1) and 0.17(+2-1) ps, respectively.
5. The B(M1) values as given in 1994Cl01 for the transitions from 152 to 294 keV are 0.76(+22 -14), 0.31(+6-5), 0.38(+11-8), 0.34(+11-7), 0.35 (+14-8), 0.34(+11-8) and 0.59(+17-12) W.u., respectively and that for transitions from 285 to 353 keV as given in 1998Cl06 are 4.59(23), 4.53(+31-47), 7.05(+41-83) and 6.35 (+37-75) (μ_N^2), respectively.
6. Nuclear reaction: ^{186}W (^{16}O, 5nγ) E(^{16}O) = 97 MeV, Band intensity ~ 18%.

	E_{level} keV	I^π	$E_\gamma(M1)$ keV	$E_\gamma(E2)$ keV	B(M1)/B(E2) $(\mu_N/eb)^2$	References
2	4794.6	37/2⁺				**1999Po13**
	4907.0	39/2⁺	112.4			1995Ba35
	5058.3	41/2⁺	151.3			1992Ku06
	5258.9	43/2⁺	200.6			1993Hu08
	5525.6	45/2⁺	266.7			1994Cl01
	5862.3	47/2⁺	336.7			1998Cl06
	6266.2	49/2⁺	403.9	740.7	24(4)	
	6712.3	51/2⁺	446.1	849.9	17(3)	
	7179.4	53/2⁺	467.1	913.3	32(5)	
	7613.1	55/2⁺	433.7	900.6		
	7984.5	57/2⁺	371.4			
	8372.1	59/2⁺	387.6			
	8794.7	61/2⁺	422.6			
	9246.4	63/2⁺	(451.7)			
	9723.5	65/2⁺	(477.1)			

1. $\pi(h_{9/2}i_{13/2})_{K=11}^- \otimes \nu(i_{13/2}^{-2}f_{5/2}^{-1})$ below and $\pi(h_{9/2}i_{13/2})_{K=11}^- \otimes \nu(i_{13/2}^{-4}f_{5/2}^{-1})$ above the bandcrossing from the TAC model calculations.
2. B(M1)/B(E2) values are from 1994Cl01.
3. The mean lifetimes for the transitions from 151.3 to 266.7 keV as given in 1994Cl01 are 1.8(8), 0.9(4) and 1.2(3) ps, and from 337 to 467 as given in 1998Cl06 are 0.17(3), 0.13(+3 -2), 0.16(2) and 0.28(+5-6) ps, respectively.
4. The B(M1) values as given in 1994Cl01 for the transitions from 151 to 267 keV are 1.32(+132 -44), 2.08(+125-57) and 1.01(+67-29) W.u., respectively, and that for transitions from 337 to 467 keV, as given in 1998Cl06 are 7.18(127), 5.88(+90-136), 3.72 (47) and 1.90(+41-34) (μ_N^2), respectively.
5. Regular band showing a backbending at 55/2.
6. Band intensity ~ 7%.

	E_{level} keV	I^π	$E_\gamma(M1)$ keV	$E_\gamma(E2)$ keV	B(M1)/B(E2) $(\mu_N/eb)^2$	References
3	X					**1995Ba35**
	162.7+X		162.7			1999Po13
	381.5+X		218.8			
	646.2+X		264.7			
	962.8+X		316.6			
	1325.9+X		363.1			
	1717.0+X		391.1			

1. Spin values could not be assigned due to the nonobservation of linking transitions to the lower lying states.
2. X ~ 5200 keV.
3. Regular band.
4. Band intensity ~ 6(2)%.

$^{198}_{82}\text{Pb}_{116}$

	E_{level} keV	I^π	$E_\gamma(M1)$ keV	$E_\gamma(E2)$ keV	$B(M1)/B(E2)$ $(\mu_N/eb)^2$	References	Configurations and Comments:
1	X	(20^+)				**1993Cl05**	1. Tentatively assigned as $\pi(h_{9/2}i_{13/2})_{K=11}^- \otimes \nu(i_{3/2}^{-4})$ from CWS calculations.
	206.8+X	(21^+)	206.8			1992Wa20	2. Nearly oblate shape $(\beta_2, \gamma) \sim (0.15, -60°)$
	444.9+X	(22^+)	238.1			1994Cl01	3. I^π's are from 1992Wa20, 1993Cl05 gives the
	725.1+X	(23^+)	280.2	(518)	>50	1997Cl03	tentative bandhead spin as 22 or 23.
	1051.4+X	(24^+)	326.3	607	32(3)		4. B(M1)/B(E2)'s except the first one are from
	1426.4+X	(25^+)	375.0	701	21(2)		1994Cl01.
	1848.3+X	(26^+)	421.9	797	26(3)		5. The mean lifetimes for the transitions from
	2312.5+X		464.2	886	34(3)		206.8 to 506.2 keV as given in 1994Cl01 are
	2818.7+X		506.2	970	27(3)		2.1(4), 0.85(30), 1.1(6), 0.58(15), 0.36(10),
	3369.0+X		550.3	1056	30(3)		0.20(4), 0.099(25) and 0.052(11) ps,
	3960.7+X		591.7	1142	21(3)		respectively.

6. B(M1) values for the transitions from 207 to 506 keV as given in 1994Cl01 are 0.75(+18-12) 1.5(+8-4), 0.8(+10-3), 1.1(+5-3), 1.2(+5-3), 1.6 (+5-3), 2.6(+9-5) and 3.7(+11-9) W.u., respectively.

7. Regular band.

8. Nuclear reaction: ^{186}W (^{17}O, 5nγ) E(^{17}O) = 92 and 98 MeV, Band intensity ~ 8%.

	E_{level}	I^π	$E_\gamma(M1)$	$E_\gamma(E2)$	$B(M1)/B(E2)$	References	Configurations and Comments:
2	Y					**1993Cl05**	1. Tentatively assigned as $\pi(h_{9/2}^2) \otimes \nu(i_{13/2}^{-3}p_{3/2}^{-1})$.
	114.1+Y		114.1				2. Small oblate deformation.
	270.0+Y		155.9				3. Regular band.
	485.8+Y		215.8	(372)	14(4)		4. Band intensity ~ 2%.
	769.6+Y		283.8	(499)	13(4)		
	1113.9+Y		344.3				
	1533.1+Y		419.2				
	2010.3+Y		477.2	(896)	30(8)		
	2495.1+Y		484.8				

	E_{level}	I^π	$E_\gamma(M1)$	$E_\gamma(E2)$	$B(M1)/B(E2)$	References	Configurations and Comments:
3	Z	(18^-)				**1993Cl05**	1. Tentatively assigned as $\pi(h_{9/2}^2) \otimes \nu(i_{13/2}^{-3}f_{5/2}^{-1})$.
	113.9+Z	(19^-)	113.9			1992Wa20	2. Small oblate deformation.
	269.9+Z	(20^-)	156.0	(270)	10(3)	1994Cl01	3. I^π's are from 1992Wa20. 1993Cl05 gives the
	485.2+Z	(21^-)	215.3			1997Cl03	tentative bandhead spin around 18-22.
	763.9+Z	(22^-)	278.7	(494)	30(9)	1998Kr20	4. Last six B(M1)/B(E2)'s are from 1994Cl01.
	1106.7+Z	(23^-)	342.8	622	13(4)		5. The mean lifetimes for the transitions from
	1496.2+Z	(24^-)	389.5	732	26(3)		156.0 to 476.2 keV as given in 1994Cl01 are
	1919.3+Z	(25^-)	423.1	812	24(2)		2.7(9), 1.8(5), 2.1(5), 1.14(23), 0.72(10),
	2363.9+Z	(26^-)	444.6	867	25(3)		0.46(10), 0.24(4), 0.22(6), and 0.27(7) ps,
	2835.6+Z	(27^-)	471.7	917	23(2)		respectively and B(M1) values for these
	3311.8+Z	(28^-)	476.2	948	17(2)		transitions are 0.67(+34-17), 0.83(+32-18), 0.45
	3840.8+Z		529.0				(+12-9), 0.48(+11-8), 0.55(+11-8), 0.69(+26

-12), 1.07(+38-17), 0.99(+49-19) and 0.74(+34 -14) W.u., respectively.

6. The mean lifetimes for the transitions from 156 to 342.8 keV as given in 1998Kr20 are 0.63(10), 0.70(+10-20), 0.34(+15-10) and 0.20(+20-10) ps and the B(M1) values for these transitions are 6.2(+11-9), 3.8(+15-5), 4.9(+20-15) and 4.9(+48-28) μ_N^2 respectively.

7. Regular band.

8. Band intensity ~ 10%.

TABLE. Magnetic Dipole Rotational Bands
See page 295 for Explanation of Table

4	U				**1993Cl05**	1. Tentatively assigned as $\pi(h_{9/2}i_{13/2}) \otimes \nu(i_{13/2}^{-3} f_{5/2}^{-1})$.
	123.4+U	123.4				2. Small oblate deformation.
	283.2+U	159.8				3. Regular band.
	487.6+U	204.4	(364)	19(4)		4. Band intensity ~ 4%.
	752.5+U	264.9				
	1090.3+U	337.8	(603)	14(3)		
	1499.4+U	409.1	(747)	21(8)		
	1952.4+U	453.0				
		(495)				

5	V				**1993Cl05**	1. Suggested proton configuration: $\pi(h_{9/2}s_{1/2})$, neutron configuration not indicated.
	220.8+V	220.8				2. Very small oblate deformed structure.
	461.2+V	240.4	(462)	10(3)		3. Irregular band with backbending at 997.7+V level.
	742.9+V	281.7	(523)	18(6)		4. Band intensity ~ 4%.
	997.7+V	254.8	(537)	8(3)		
	1330.0+V	332.3				
	1718.0+V	388.0	(720)	8(3)		
	2110.0+V	392.0				

$^{199}_{82}\text{Pb}_{117}$

	E_{level} keV	I^π	E_γ(M1) keV	E_γ(E2) keV	B(M1)/B(E2) $(\mu_N/eb)^2$	References	Configurations and Comments:
1	3604.2	$(25/2^-)$				**1995Ne09**	1. $\pi(h_{9/2}i_{13/2})_{K=11}^- \otimes \nu(i_{13/2}^{-1})$ below and $\pi(h_{9/2}i_{13/2})_{K=11}^- \otimes \nu(i_{13/2}^{-3})$ above the bandcrossing from the TAC model calculations.
	3694.1	$(27/2^-)$	89.9			1999Po13	
	3868.0	$(29/2^-)$	173.9			1994Ba43	
	4143.4	$(31/2^-)$	275.4			1997Cl03	
	4502.8	$(33/2^-)$	359.4	634.8			2. Small oblate deformation $(\beta_2,\gamma) \sim (0.1, -70°)$
	4904.1	$(35/2^-)$	401.3	760.8			3. Mean lifetimes of states with spins from 43/2 to 49/2 are 0.37(+51-29), 0.31(+31-24), 0.17(+6-4) and 0.13(+4-3), and for the states with spins 51/2 to 57/2 as given in 1997Cl03 are 0.20(5), 0.16(+5-4), 0.15(+5-4) and 0.21(+6-5) ps, respectively.
	5324.8	$(37/2^-)$	420.7	822.1			
	5746.3	$(39/2^-)$	421.5	842.4			
	6074.9	$(41/2^-)$	328.6	750.1			
	6309.5	$(43/2^-)$	234.6				
	6549.6	$(45/2^-)$	240.1				
	6823.4	$(47/2^-)$	273.8				4. B(M1) values for the transitions 234.6, 240.1 and 273.8 keV are 6.6(+25-38), 7.4(+24-38) and 10.6(+34-29) μ_N^2 and for the transitions from 363.1 to 508.3 keV as given in 1997Cl03 are 4.8(13), 4.4(+12-15), 3.0(+7-9) and 1.7(+4-5) μ_N^2, respectively.
	7139.7	$(49/2^-)$	316.3	590.1	35(+22-20)		
	7502.8	$(51/2^-)$	363.1	679.5	27(+18-14)		
	7914.1	$(53/2^-)$	411.3	774.6	27(+15-18)		
	8373.4	$(55/2^-)$	459.3	870.9	38(20)		5. Regular band with backbending at 41/2.
	8881.7	$(57/2^-)$	508.3	967.7			6. Nuclear reaction: ^{186}W $(^{18}$O, 5n$\gamma)$ E(^{18}O) = 92 and 94 MeV.
	9436.5	$(59/2^-)$	554.8	(1063)			

2	X	$(35/2^+)$				**1999Po13**	1. $\pi(h_{9/2}i_{13/2})_{K=11^-} \otimes \nu(i_{13/2}^{-2}f_{5/2}^{-1})$ below and
	98.2+X	$(37/2^+)$	98.2			1995Ne09	$\pi(h_{9/2}i_{13/2})_{K=11^-} \otimes \nu(i_{13/2}^{-4}f_{5/2}^{-1})$ above the
	223.2+X	$(39/2^+)$	125.0			1992Ba13	bandcrossing from the TAC model
	388.8+X	$(41/2^+)$	165.6			1994Ba43	calculations.
	603.4+X	$(43/2^+)$	214.6			1997Cl03	2. Small oblate deformation $(\beta_2,\gamma) \sim (0.1, -70°)$
	871.2+X	$(45/2^+)$	267.8				suggested in 1995Ne09.
	1194.3+X	$(47/2^+)$	323.1				3. Mean lifetimes of states with spins from 47/2 to
	1571.4+X	$(49/2^+)$	377.1	700.1	28(9)		55/2 are 0.19(+15-8), 0.14(+6-4), 0.10(+3-2),
	2001.7+X	$(51/2^+)$	430.3	807.1	49(28)		0.06(2) and 0.11(2) ps, respectively and that
	2483.6+X	$(53/2^+)$	481.9	912.4	52(20)		for spin 57/2 as given in 1997Cl03 is 0.14(+3-2)
	3015.6+X	$(55/2^+)$	532.0	1014.2	30(9)		4. B(M1) value for the transition 323.1 keV is
	3589.2+X	$(57/2^+)$	573.6	1105.7	34(10)		6.6(+47-29) μ_N^2 from 1995Ne09.
	4207.4+X	$(59/2^+)$	618.5	1192.1	45(11)		5. B(M1)/B(E2) values are from 1992Ba13.
	4546.6+X	$(61/2^+)$	339.2				6. Regular band with backbending at spin 61/2.
	4932.5+X	$(63/2^+)$	385.9				7. Nuclear reactions: ^{192}Os (^{12}C, 5nγ), E(^{12}C) = 82
	5353.5+X	$(65/2^+)$	421.0				MeV, and ^{186}W (^{18}O, 5nγ), E(^{18}O) = 94 MeV,
	5806.9+X	$(67/2^+)$	453.4				Band intensity ~ 12%.
	6303.4+X	$(69/2^+)$	496.5				
	6845.9+X	$(71/2^+)$	542.5				
	7433.6+X	$(73/2^+)$	587.7				
3	Y	$(39/2^+)$				**1994Ba43**	1. Tentatively assigned as $\pi(h_{9/2}i_{13/2})_{K=11^-} \otimes$
	137.7+Y	$(41/2^+)$	137.7			1999Po13	$\nu(i_{13/2}^{-2} f_{5/2}^{-1})$ from the TAC model calculation.
	302.3+Y	$(43/2^+)$	164.6			1995Ne09	2. Small oblate deformation $(\beta_2,\gamma) \sim (0.1, -70°)$
	510.6+Y	$(45/2^+)$	208.3				3. The topmost transition is from 1999Po13.
	781.6+Y	$(47/2^+)$	271.0				4. Regular band.
	1123.6+Y	$(49/2^+)$	342.0				
	1540.6+Y	$(51/2^+)$	417.0				
	2023.3+Y	$(53/2^+)$	482.7	900.0			
	2560.1+Y	$(55/2^+)$	536.8	1019.6			
	3145.3+Y	$(57/2^+)$	585.2	1122.0			
4	Z					**1994Ba43**	1. Tentatively assigned as $\pi(h_{9/2}^2)_{K=8^+} \otimes \nu(i_{13/2}^{-3})$.
	97.7+Z		97.7			1999Po13	2. The estimated bandhead spin is 37/2 since it
	232.9+Z		135.2				populates states with spin around 33/2.
	426.1+Z		193.2				3. The two topmost transitions are from 1999Po13
	673.5+Z		247.4				4. Regular band with signature splitting and
	967.6+Z		294.1	541.4			backbending at the top of the band.
	1349.7+Z		382.1	676.2			
	1743.9+Z		394.2	776.4			
	2227.4+Z		483.5	877.6			
	2737.9+Z		510.5	994.2			
	3256.7+Z		518.8	1029.4			
	3594.9+Z		338.2				
5	U					**1994Ba43**	1. Tentatively assigned as $\pi(h_{9/2}^2)_{K=8^+} \otimes \nu(i_{13/2}^{-4} p_{3/2}^{-1})$.
	242.9+U		242.9				2. The estimated bandhead spin is 45/2 since it
	550.2+U		307.3				populates states with spin around 41/2.
	863.2+U		313.0	620.5			3. Regular band with signature splitting.
	1247.8+U		384.6	697.6			
	1661.8+U		414.0	798.7			
	2148.8+U		487.0	901.4			

TABLE. Magnetic Dipole Rotational Bands
See page 295 for Explanation of Table

$^{200}_{82}\text{Pb}_{118}$

	E_{level} keV	I^π	E_γ(M1) keV	E_γ(E2) keV	B(M1)/B(E2) $(\mu_N/eb)^2$	Reference
1	X					**1994Ba43**
	100.6+X		100.6			
	223.9+X		123.3			
	384.2+X		160.3			
	592.8+X		208.6			
	855.3+X		262.5			
	1174.8+X		319.5			
	1549.5+X		374.7			
	1978.9+X		429.4			
	2459.5+X		480.6			
	2992.5+X		533.0	(1014)		
	3574.6+X		582.1			
	4207.0+X		632.4	1214.3		
2	Y					**1994Ba43**
	212.5+Y		212.5			
	452.8+Y		240.3			
	736.1+Y		283.3			
	1065.7+Y		329.6			
	1445.8+Y		380.1			
	1884.6+Y		438.8			
3	Z					**1994Ba43**
	237.5+Z		237.5			
	518.8+Z		281.3			
	853.4+Z		334.6			
	1234.8+Z		381.4			
	1658.3+Z		423.5			

Configurations and Comments:

Band 1:
1. $\pi(h_{9/2}i_{13/2})_{K=11}^{-} \otimes \nu(i_{13/2}^{-2})$ from the TAC model calculation.
2. Small oblate deformation.
3. Tentative bandhead spin is around 17.
4. Regular band.
5. Nuclear reaction (1992Ba13): ^{192}Os (^{13}C, 5nγ) E(^{13}C) = 81 MeV, Band intensity ~ 12%.

Band 2:
1. Tentatively assigned as $\pi(h_{9/2}i_{13/2})_{K=11}^{-} \otimes \nu(i_{13/2}^{-3} p_{3/2}^{-1})$ from the TAC model calculation.
2. Tentative bandhead spin is around 23.
3. Regular band.
4. Band intensity ~ 7%.

Band 3:
1. Tentatively assigned as $\pi(h_{9/2}i_{13/2})_{K=11}^{-} \otimes \nu(i_{13/2}^{-3} f_{5/2}^{-1})$ from the TAC model calculation.
2. Tentative bandhead spin is around 23.
3. Regular band.

$^{201}_{82}\text{Pb}_{119}$

	E_{level} keV	I^π	E_γ(M1) keV	E_γ(E2) keV	B(M1)/B(E2) $(\mu_N/eb)^2$	Reference
1	X					**1995Ba70**
	109.2+X		109.2			
	290.8+X		181.6			
	554.6+X		263.8			
	895.4+X		340.8			
	1299.4+X		404.0	744.6		
	1758.4+X		459.0	862.8		
	2264.1+X		505.7	964.7		
	2822.6+X		558.5			
2	6146.0+Y	35/2				**1995Ba70**
	6247.7+Y	37/2	101.7			
	6377.4+Y	39/2	129.7			
	6549.0+Y	41/2	171.6			
	6769.5+Y	43/2	220.5			
	7045.4+Y	45/2	275.9			
	7380.0+Y	47/2	334.6			
	7773.3+Y	49/2	393.3			
	8227.2+Y	51/2	453.9			

Configurations and Comments:

Band 1:
1. $\pi(h_{9/2}i_{13/2})_{K=11}^{-} \otimes \nu(i_{13/2}^{-1})$ by comparison with a similar band in ^{199}Pb.
2. Regular band.
3. Nuclear reaction: ^{192}Os (^{14}C, 5nγ), E(^{14}C) = 76 MeV, Band intensity ~ 11(4)%.

Band 2:
1. $\pi(h_{9/2}i_{13/2})_{K=11}^{-} \otimes \nu(i_{13/2}^{-2}p_{3/2}^{-1})$ by comparison with ^{199}Pb and TAC model calculations.
2. Small oblate deformation.
3. From 47/2 and above, there is a forking of the band with very close lying transitions having energies 333.1, 394.8 and 492.5 keV.
4. regular band.
5. Band intensity ~ 11(3)%.

TABLE. Magnetic Dipole Rotational Bands
See page 295 for Explanation of Table

	E_{level} keV	E_γ(M1) keV	E_γ(E2) keV	Reference	Configurations and Comments:
3	Z			1995Ba70	1. Tentatively assigned as $\pi(h_{9/2}i_{13/2})_{K=11}^-\otimes \nu(i_{13/2}^{-2}f_{5/2}^{-1})$, because of the similarity in the moment of inertia of the bands 2 and 3.
	139.6+Z	139.6			2. Regular band.
	315.4+Z	175.8			3. Band intensity $\sim$ 8(3)%.
	537.7+Z	222.3			
	814.1+Z	276.4			
	1146.4+Z	332.3			
	1534.5+Z	388.1			
	1975.8+Z	441.3	829.4		
	2467.5+Z	491.7	933.1		
	3007.3+Z	539.8	1031.4		
4	U			1995Ba70	1. Regular band.
	176.5+U	176.5			2. Band intensity $\sim$ 7(4)%.
	402.2+U	225.7			
	680.4+U	278.2			
	1007.1+U	326.7			
	1387.5+U	380.4			
	1817.2+U	429.7			
	2300.3+U	483.1			
	2830.5+U	530.2			
5	V			1995Ba70	1. Regular band.
	152.9+V	152.9			2. Band intensity $\sim$ 8(4)%.
	351.5+V	198.6			
	601.5+V	250.0			
	913.5+V	312.0			
	1287.9+V	374.4			
	1723.9+V	436.0			
	2217.3+V	493.4			

$^{202}_{82}\text{Pb}_{120}$

	E_{level} keV	I^π	E_γ(M1) keV	E_γ(E2) keV	B(M1)/B(E2) $(\mu_N/eb)^2$	Reference	Configurations and Comments:
1	X					1995Ba70	1. Tentatively assigned as $\pi(h_{9/2}i_{13/2})_{K=11}^-\otimes\nu(i_{13/2}^{-2})$ by comparison with the neighboring ^{201}Pb.
	161.5+X		161.5				2. Regular band.
	404.8+X		243.3				3. Nuclear reaction: ^{192}Os (^{14}C, 4nγ), E(^{14}C) = 76 MeV.
	737.7+X		332.9				
	1145.3+X		407.6				
	1611.8+X		466.5				
	2129.5+X		517.7				
2	Y					1995Ba70	1. This band is tentatively assigned to the nucleus because of its weaker intensity and the nonclarity of the coincidence relations. If it belongs to the nucleus, it probably has higher spin than band 1.
	183.0+Y		183.0				2. Regular band.
	423.1+Y		240.1				
	719.4+Y		296.3				
	1081.3+Y		361.9				
	1500.8+Y		419.5				
	1988.0+Y		487.2				

$^{198}_{83}\text{Bi}_{115}$

	E_{level} keV	I^π	$E_\gamma(M1)$ keV	$E_\gamma(E2)$ keV	$B(M1)/B(E2)$ $(\mu_N/eb)^2$	Reference
1	X					**1994Da17**
	165+X		165			
	416+X		251			
	731+X		315			
	1108+X		377			
	1517+X		409			

Configurations and Comments:

1. Tentatively assigned as $\pi(h_{9/2}\, i_{13/2}\, s_{1/2}^{-1})$ coupled to one or three $i_{13/2}$ neutron holes by comparison with a similar band in neighboring Pb isotopes.
2. B(M1)/B(E2) ratios are large due to the nonobservation of crossover E2 transitions.
3. Regular band.
4. Nuclear reaction: ^{186}W (^{19}F, 7nγ), E(^{19}F) = 115 and 105 MeV, Band intensity ~ 25% relative to the low lying 630 keV transition.

$^{199}_{83}\text{Bi}_{116}$

	E_{level} keV	I^π	$E_\gamma(M1)$ keV	$E_\gamma(E2)$ keV	$B(M1)/B(E2)$ $(\mu_N/eb)^2$	Reference
1	X					**1994Da17**
	184.4+X		184.4			
	400.2+X		215.8			
	642.0+X		241.8			
	923.2+X		281.2			
	1236.7+X		313.5			
	1590.3+X		353.6			
	1950.8+X		360.5			
	2316.7+X		365.9			

Configurations and Comments:

1. Tentatively assigned as $\pi(h_{9/2}\, i_{13/2}\, s_{1/2}^{-1})$ coupled to two $i_{13/2}$ neutron holes by comparison with a similar band in neighboring Pb isotopes.
2. The band depopulates around 37/2.
3. B(M1)/B(E2) ratios are large due to the nonobservation of crossover E2 transitions.
4. Regular band.
5. Nuclear reaction: ^{186}W (^{19}F, 6nγ), E(^{19}F) = 115 and 105 MeV, Band intensity ~ 20% relative to 495 keV 31/2$^-$→ 29/2$^-$ transition.

$^{200}_{83}\text{Bi}_{117}$

	E_{level} keV	I^π	$E_\gamma(M1)$ keV	$E_\gamma(E2)$ keV	$B(M1)/B(E2)$ $(\mu_N/eb)^2$	Reference
1	X					**1994Da17**
	193+X		193			
	431+X		238			
	720+X		289			
	1056+X		336			
	1432+X		376			
	1855+X		423			
2	Y					**1994Da17**
	199.0+Y		199.0			
	446.2+Y		247.2			
	740.7+Y		294.5			
	1083.8+Y		343.1			
	1475.2+Y		391.4			
	1918.8+Y		443.6			
	2417.8+Y		499.0			
	2970.7+Y		552.9			
	3577.7+Y		607.0			

Configurations and Comments:

1. Tentatively assigned as $\pi(h_{9/2}\, i_{13/2}\, s_{1/2}^{-1})$ coupled to one or three $i_{13/2}$ neutron holes by comparison with a similar band in neighboring Pb isotopes.
2. B(M1)/B(E2) ratios are large due to the nonobservation of crossover E2 transitions.
3. Regular band.
4. Nuclear reaction: ^{186}W (^{19}F, 5nγ), E(^{19}F) = 115 and 105 MeV, Band intensity ~ 20% relative to the low lying 326 keV transition.

Configurations and Comments:

1. Tentatively assigned as $\pi(h_{9/2}\, i_{13/2}\, s_{1/2}^{-1})$ coupled to one or three $i_{13/2}$ neutron holes by comparison with a similar band in neighboring Pb isotopes.
2. B(M1)/B(E2) ≥ 10 $(\mu_N/eb)^2$.
3. Regular band.
4. Band intensity ~ 30% relative to the low lying 326 keV transition.

$^{202}_{83}\text{Bi}_{119}$

	E_{level} keV	I^π	$E_\gamma(M1)$ keV	$E_\gamma(E2)$ keV	$B(M1)/B(E2)$ $(\mu_N/eb)^2$	Reference
1	X					**1993Cl02**
	164+X		164			
	423+X		259			
	775+X		352			
	1199+X		424			
	1680+X		481			
	2210+X		530			
	2780+X		570			
2	Y					**1993Cl02**
	180+Y		180			
	394+Y		214			
	659+Y		265			
	984+Y		325			
	1374+Y		390			
3	Z					**1993Cl02**
	250+Z		250			
	550+Z		300			
	907+Z		357			
	1320+Z		413			
	1785+Z		465			
	2302+Z		517			

Configurations and Comments:

Band 1.
1. Tentatively assigned as $\pi(h_{9/2}\,i_{13/2}\,s_{1/2}^{-1})$ coupled to one or two $i_{13/2}$ neutron holes by comparison with a similar band in neighboring Pb isotopes.
2. The estimated bandhead spin is about 10-16.
3. $B(M1)/B(E2) \geq 12\ (\mu_N/eb)^2$.
4. Regular band.
5. Nuclear reaction: $^{196}\text{Pt}\ (^{11}\text{B}, 5n\gamma)$, $E(^{11}\text{B}) = 75$ MeV, Band intensity ~ 15%.

Band 2.
1. Tentatively assigned as $\pi(h_{9/2}\,i_{13/2}\,s_{1/2}^{-1})$ or $\pi(h_{9/2}^2 s_{1/2}^{-1})$ coupled to one or two $i_{13/2}$ neutron holes by comparison with the similar band in neighboring Pb isotopes.
2. The estimated bandhead spin is about 10-16.
3. $B(M1)/B(E2) \geq 6\ (\mu_N/eb)^2$.
4. Regular band.
5. Band intensity ~ 4%.

Band 3.
1. Tentatively assigned as $\pi(h_{9/2}\,i_{13/2}\,s_{1/2}^{-1})$ coupled to one or two $i_{13/2}$ neutron holes by comparison with the similar band in neighboring Pb isotopes. The estimated bandhead spin is about 11-19.
2. $B(M1)/B(E2) \geq 5\ (\mu_N/eb)^2$.
3. Regular band.
4. Band intensity ~ 3%.

$^{203}_{83}\text{Bi}_{120}$

	E_{level} keV	I^π	$E_\gamma(M1)$ keV	$E_\gamma(E2)$ keV	$B(M1)/B(E2)$ $(\mu_N/eb)^2$	Reference
1	X					**1994Da17**
	175+X		175			
	421+X		246			
	759+X		338			
	1201+X		442			
	1718+X		517			
	2295+X		577			

Configurations and Comments:

1. Tentatively assigned as $\pi(h_{9/2}i_{13/2}s_{1/2}^{-1})$ coupled to two $i_{13/2}$ neutron holes by comparison with a similar band in neighboring Pb isotopes.
2. $B(M1)/B(E2)$ ratios are large due to the nonobservation of crossover E2 transitions.
3. Regular band.
4. Nuclear reaction: $^{198}\text{Pt}\ (^{11}\text{B}, 6n\gamma)$, $E(^{11}\text{B}) = 74$ MeV, Band intensity ~ 15% relative to the 689 keV transition.

$^{205}_{86}\text{Rn}_{119}$

	E_{level} keV	I^π	$E_\gamma(M1)$ keV	$E_\gamma(E2)$ keV	$B(M1)/B(E2)$ $(\mu_N/eb)^2$	Reference
1	1680+X	$(21/2^+)$				**1999No03**
	1796.7+X	$(23/2^+)$	116.7			
	1966.9+X	$(25/2^+)$	170.2			
	2124.8+X	$(27/2^+)$	157.9		2.0(2)	
	2246.0+X	$(29/2^+)$	121.2		>4	
	2494.0+X	$(31/2^+)$	248.0		>7	
	2861.7+X	$(33/2^+)$	367.7		>10	
	3164.1+X	$(35/2^+)$	302.4		>33	
	3452.3+X	$(37/2^+)$	288.2		>18	
	3653.6+X	$(39/2^+)$	201.3			
	4059.4+X	$(41/2^+)$	405.8			

Configurations and Comments:

1. The most likely configuration is the negative parity $\pi(h_{9/2}i_{13/2}) \otimes \nu(i_{13/2})$ from the TAC calculations. Since the observed parities are positive, the configuration $\pi(i_{13/2}^2) \otimes \nu(i_{13/2})$ is tentatively assigned.
2. Small oblate deformation, $\beta_2 \sim -0.1$.
3. X ~ 600 keV from systematics.
4. Irregular band.
5. Nuclear reaction: $^{170}\text{Er}\ (^{40}\text{Ar}, 5n\gamma)$, $E(^{40}\text{Ar}) = 183$ MeV, band intensity ~ 25%.

REFERENCES FOR TABLE

1980Ga17   W. Gast, K. Dey, A. Gelberg, U. Kaup, F. Paar, R. Richter, K. O. Zell and P. von Brentano, Phys. Rev. $\underline{C22}$, 469 (1980).

1986Fu04   L. Funke, J. Döring, P. Kemnitz, P. Ojeda, R. Schwengner, E. Will, G. Winter, A. Johnson, L. Hildingsson and Th. Lindblad, Z. Phys. $\underline{A324}$, 127 (1986).

1988Hi04   L. Hildingsson, C. W. Beausang, D. B. Fossan and W. F. Piel, Jr., Phys. Rev. $\underline{C37}$, 985 (1988).

1988Sc13   R. Schwengner, J. Döring, L. Funke, H. Rotter, G. Winter, A. Johnson and A. Nilsson, Nucl. Phys. $\underline{A486}$, 43 (1988).

1989Hi02   L. Hildingsson, C. W. Beausang, D. B. Fossan, R. Ma, E. S. Paul, W. F. Piel, Jr. and N. Xu, Phys. Rev. $\underline{C39}$, 471 (1989).

1989Pa17   E. S. Paul, D. B. Fossan, Y. Liang, R. Ma and N. Xu, Phys. Rev. $\underline{C40}$, 1255 (1989).

1989Xu01   N. Xu, C. W. Beausang, R. Ma, E. S. Paul, W. F. Piel, Jr., D. B. Fossan and L. Hildingsson, Phys. Rev. $\underline{C39}$, 1799 (1989).

1990Ma26   R. Ma, E. S. Paul, D. B. Fossan, Y. Liang, N. Xu, R. Wadsworth, I. Jenkins and P. J. Nolan, Phys. Rev. $\underline{C41}$, 2624 (1990).

1990Pa05   E. S. Paul, D. B. Fossan, Y. Liang, R. Ma, N. Xu, R. Wadsworth, I. Jenkins and P. J. Nolan, Phys. Rev. $\underline{C41}$, 1576 (1990).

1990Sc07   R. Schwengner, J. Döring, L. Funke, G. Winter, A. Johnson and W. Nazarewicz, Nucl. Phys. $\underline{A509}$, 550 (1990).

1992Ba13   G. Baldsiefen, H. Hübel, D. Mehta, B. V. Thirumala Rao, U. Birkental, G. Fröhlingsdorf, M. Neffgen, N. Nenoff, S. C. Pancholi, N. Singh, W. Schmitz, K. Theine, P. Willsau, H. Grawe, J. Heese, H. Kluge, K. H. Maier, M. Schramm, R. Schubart and H. J. Maier, Phys. Lett. $\underline{B275}$, 252 (1992).

1992Ku06   A. Kuhnert, M. A. Stoyer, J. A. Becker, E. A. Henry, M. J. Brinkman, S. W. Yates, T. F. Wang, J. A. Cizewski, F. S. Stephens, M. A. Deleplanque, R. M. Diamond, A. O. Macchiavelli, J. E. Draper, F. A. Azaiez, W. H. Kelly and W. Korten, Phys. Rev. $\underline{C46}$, 133 (1992).

1992Wa20   T. F. Wang, E. A. Henry, J. A. Becker, A. Kuhnert, M. A. Stoyer, S. W. Yates, M. J. Brinkman, J. A. Cizewski, A. O. Macchiavelli, F. S. Stephens, M. A. Deleplanque, R. M. Diamond, J. E. Draper, F. A. Azaiez, W. H. Kelly, W. Korten, E. Rubel and Y. A. Akovali, Phys. Rev. Lett. $\underline{69}$, 1737 (1992).

1993Ce04   B. Cederwall, M. A. Deleplanque, F. Azaiez, R. M. Diamond, P. Fallon, W. Korten, I. Y. Lee, A. O. Macchiavelli, J. R. B. Oliveira, F. S. Stephens, W. H. Kelly, D. T. Vo, J. A. Becker, M. J. Brinkman, E. A. Henry, J. R. Hughes, A. Kuhnert, M. A. Stoyer, T. F. Wang, J. E. Draper, C. Duyar, E. Rubel and J. deBoer, Phys. Rev. $\underline{C47}$, R2443 (1993).

1993Cl02   R. M. Clark, R. Wadsworth, F. Azaiez, C. W. Beausang, A. M. Bruce, P. J. Dagnall, P. Fallon, P. M. Jones, M. J. Joyce, A. Korichi, E. S. Paul and J. F. Sharpey-Schafer, J. Phys. $\underline{G19}$, L57 (1993).

1993Cl05   R. M. Clark, R. Wadsworth, E. S. Paul, C. W. Beausang, I. Ali, A. Astier, D. M. Cullen, P. J. Dagnall, P. Fallon, M. J. Joyce, M. Meyer, N. Redon, P. H. Regan, J. F. Sharpey-Schafer, W. Nazarewicz and R. Wyss, Nucl. Phys. $\underline{A562}$, 121 (1993).

1993De42   J. K. Deng, W. C. Ma, J. H. Hamilton, J. D. Garrett, C. Baktash, D. M. Cullen, N. R. Johnson, I. Y. Lee, F. K. McGowan, S. Pilotte, C. H. Yu and W. Nazarewicz, Phys. Lett. B319, 63 (1993).

1993Do14   J. Döring, L. Funke, R. Schwengner and G. Winter, Phys. Rev. C48, 2524 (1993).

1993Ho15   J. W. Holcomb, J. Döring, T. Glasmacher, G. D. Johns, T. D. Johnson, M. A. Riley, P. C. Womble and S. L. Tabor, Phys. Rev. C48, 1020 (1993).

1993Hu01   J. R. Hughes, Y. Liang, R. V. F. Janssens, A. Kuhnert, J. A. Becker, I. Ahmad, I. G. Bearden, M. J. Brinkman, J. Burde, M. P. Carpenter, J. A. Cizewski, P. J. Daly, M. A. Deleplanque, R. M. Diamond, J. E. Draper, C. Duyar, B. Fornal, U. Garg, W. Grabowski, E. A. Henry, R. G. Henry, W. Hesselink, N. Kalantar-Nayestanaki, W. H. Kelly, T. L. Khoo, T. Lauritsen, R. H. Mayer, D. Nissius, J. R. B. Oliveira, A. J. M. Plompen, W. Reviol, E. Rubel, F. Soramel, F. S. Stephens, M. A. Stoyer, D. Vo and T. F. Wang, Phys. Rev. C47, R1337 (1993).

1993Hu08   J. R. Hughes, J. A. Becker, M. J. Brinkman, E. A. Henry, R. W. Hoff, M. A. Stoyer, T. F. Wang, B. Cederwall, M. A. Deleplanque, R. M. Diamond, P. Fallon, I. Y. Lee, J. R. B. Oliveira, F. S. Stephens, J. A. Cizewski, L. A. Bernstein, J. E. Draper, C. Duyar, E. Rubel, W. H. Kelly, and D. Vo, Phys. Rev. C48, R2135 (1993).

1993Me12   D. Mehta, W. Korten, H. Hübel, K. Theine, W. Schimtz, P. Willsau, C. X. Yang, F. Hannachi, D. B. Fossan, H. Grawe, H. Kluge and K. H. Maier, Z. Phys. A346, 169 (1993).

1993Pl02   J. M. Plompen, M. N. Harakesh, W. H. A. Hesselink, G. Van't Hof, N. Kalantar-Nayestanaki, J. P. S. van Schagen, M. P. Carpenter, I. Ahmed, I. G. Bearden, R. V. F. Janssens, T. L. Khoo, T. Lauritsen, Y. Liang, U. Garg, W. Reviol and D. Ye, Nucl. Phys. A562, 61 (1993).

1993Ro03   N. Roy, J. A. Becker, E. A. Henry, M. J. Brinkman, M. A. Stoyer, J. A. Cizewski, R. M. Diamond, M. A. Deleplanque, F. S. Stephens, C. W. Beausang and J. E. Draper, Phys. Rev. C47, R930 (1993).

1993Sy03   G. N. Sylvan, J. E. Purcell, J. Döring, J. W. Holcomb, G. D. Johns, T. D. Johnson, M. A. Riley, P. C. Womble, V. A. Wood and S. L. Tabor, Phys. Rev. C48, 2252 (1993).

1993Th05   I. Thorslund, C. Fahlander, J. Nyberg, S. Juutinen, R. Julin, M. Piiparinen, R. Wyss, A. Lampinen, T. Lönnroth, D. Müller, S. Törmänen and A. Virtanen, Nucl. Phys. A564, 285 (1993).

1994Ba43   G. Baldsiefen, H. Hübel, W. Korten, D. Mehta, N. Nenoff, B. V. Thirumala Rao, P. Willsau, H. Grawe, J. Heese, H. Kluge, K. H. Maier, R. Schubart, S. Frauendorf and H. J. Maier, Nucl. Phys. A574, 521 (1994).

1994Cl01   R. M. Clark, R. Wadsworth, H. R. Andrews, C. W. Beausang, M. Bergstrom, S. Clarke, E. Dragulescu, T. Drake, P. J. Dagnall, A. Galindo-Uribarri, G. Hackman, K. Hauschild, I. M. Hibbert, V. P. Janzen, P. M. Jones, R. W. MacLeod, S. M. Mullins, E. S. Paul, D. C. Radford, A. Semple, J. F. Sharpey-Schafer, J. Simpson, D. Ward and G. Zwartz, Phys. Rev. C50, 84 (1994).

1994Da17   P. J. Dagnall, C. W. Beausang, R. M. Clark, R. Wadsworth, S. Bhattacharjee, P. Fallon, P. D. Forsyth, D. B. Fossan, G. deFrance, S. J. Gale, F. Hannachi, K. Hauschild, I. M. Hibbert, H. Hübel, P. M. Jones, M. J. Joyce, A. Korichi, W. Korten, D. R. LaFosse, E. S. Paul, H. Schnare, K. Starosta, J. F. Sharpey-Schafer, P. J. Twin, P. Vaska, M. P. Waring and J. N. Wilson, J. Phys. G20, 1591 (1994).

1994De11   G. de Angelis, M. A. Cardona, M. De Poli, S. Lunardi, D. Bazzacco, F. Brandolini, D. Vretenar, G. Bonsignori, M. Savoia, R. Wyss, F. Terrasi and V. Roca, Phys. Rev. C49, 2990 (1994).

1994Do18   J. Döring, R. Schwengner, L. Funke, H. Rotter, G. Winter, B. Cederwall, F. Lidén, A. Johnson, A. Atac, J. Nyberg and G. Sletten, Phys. Rev. C50, 1845 (1994).

1994Jo08   G. D. Johns, J. Döring, J. W. Holcomb, T. D. Johnson, M. A. Riley, G. N. Sylvan, P. C. Womble, V. A. Wood and S. L. Tabor, Phys. Rev. <u>C50</u>, 2786 (1994).

1994Ju04   S. Juutinen, R. Julin, M. Piiparinen, P. Ahonen, B. Cederwall, C. Fahlander, A. Lampinen, T. Lönnroth, A. Maj, S. Mitarai, D. Müller, J. Nyberg, P. Simecek, M. Sugawara, I. Thorslund, S. Törmänen, A. Virtanen and R. Wyss, Nucl. Phys. <u>A573</u>, 306 (1994).

1994Ju05   S. Juutinen, P. Simecek, C. Fahlander, R. Julin, J. Kumpulainen, A. Lampinen, T. Lönnroth, A. Maj, S. Mitarai, D. Müller, J. Nyberg, M. Piiparinen, M. Sugawara, I. Thorslund, S. Törmänen and A. Virtanen, Nucl. Phys. <u>A577</u>, 727 (1994).

1994Le08   Y. Le Coz, N. Redon, A. Astier, R. Beraud, R. Duffait, M. Meyer, F. Hannachi, G. Bastin, I. Deloncle, B. Gall, M. Kaci, M. G. Porquet, C. Schück, F. Azaiez, C. Bourgeois, J. Duprat, A. Korichi, N. Perrin, N. Poffe, H. Sergolle, J. F. Sharpey-Schafer, C. W. Beausang, S. J. Gale, M. J. Joyce, E. S. Paul, R. M. Clark, K. Hauschild, R. Wadsworth, J. Simpson, M. A. Bentley, A. G. Smith, H. Hübel, P. Willsau, G. De France, I. Ahmad, M. Carpenter, R. Henry, R. V. F. Janssens, T. L. Khoo and T. Lauritsen, Z. Phys. <u>A348</u>, 87 (1994).

1994Po08   M. G. Porquet, F. Hannachi, G. Bastin, V. Brindejonc, I. Deloncle, B. Gall, C. Schück, A. G. Smith, F. Azaiez, C. Bourgeois, J. Duprat, A. Korichi, N. Perrin, N. Poffe, H. Sergolle, A. Astier, Y. Le Coz, M. Meyer, N. Redon, J. Simpson, J. F. Sharpey-Schafer, M. J. Joyce, C. W. Beausang, R. Wadsworth and R. M. Clark, J. Phys. <u>G20</u>, 765 (1994).

1994Rz01   T. Rzaca-Urban, S. Utzelmann, K. Strähle, R. M. Lieder, W. Gast, A. Georgiev, D. Kutchin, G. Marti, K. Spohr, P. Von Brentano, J. Eberth, A. Dewald, J. Theuerkauf, I. Wiedenhöfer, K. O. Zell, K. H. Maier, H. Grawe, J. Heese, H. Kluge, W. Urban and R. Wyss, Nucl. Phys. <u>A579</u>, 319 (1994).

1994Th01   I. Thorslund, C. Fahlander, J. Nyberg, M. Piiparinen, R. Julin, S. Juutinen, A. Virtanen, D. Müller, H. Jensen and M. Sugawara, Nucl. Phys. <u>A568</u>, 306 (1994).

1995Ba35   G. Baldsiefen, S. Chmel, H. Hübel, W. Korten, M. Neffgen, W. Pohler, U. J. van Severen, J. Heese, H. Kluge, K. H. Maier and K. Spohr, Nucl. Phys. <u>A587</u>, 562 (1995).

1995Ba70   G. Baldsiefen, P. Maagh, H. Hübel, W. Korten, S. Chmel, M. Neffgen, W. Pohler, H. Grawe, K. H. Maier, K. Spohr, R. Schubart, S. Frauendorf and H. J. Maier, Nucl. Phys. <u>A592</u>, 365 (1995).

1995Fa19   B. Fant, B. Cederwall, L. O. Norlin, R. Wyss, P. Fallon, C. W. Beausang, P. A. Butler, R. Roberts, A. M. Bruce, D. M. Cullen, S. M. Mullins, R. J. Poynter, R. Wadsworth, M. A. Riley, W. Korten and M. J. Piiparinen, Phys. Scr. <u>T56</u>, 245 (1995).

1995Fo13   N. Fotiades, S. Harissopulos, C. A. Kalfas, S. Kossionides, C. T. Papadopoulos, R. Vlastou, M. Serris, M. Meyer, N. Redon, R. Duffait, Y. Le Coz, L. Ducroux, F. Hannachi, I. Deloncle, B. Gall, M. G. Porquet, C. Schück, F. Azaiez, J. Duprat, A. Korichi, J. F. Sharpey-Schafer, M. J. Joyce, C. W. Beausang, P. J. Dagnall, P. D. Forsyth, S. J. Gale, P. M. Jones, E. S. Paul, J. Simpsons, R. M. Clark, K. Hauschild and R. Wadsworth, J. Phys. <u>G21</u>, 911 (1995).

1995Ka19   M. Kaci, M. G. Porquet, F. Hannachi, M. Aïche, G. Bastin, I. Deloncle, B. J. P. Gall, C. Schück, F. Azaiez, C. W. Beausang, R. Beraud, C. Bourgeois, R. M. Clark, R. Duffait, J. Duprat, K. Hauschild, H. Hübel, M. J. Joyce, A. Korichi, Y. Le Coz, M. Meyer, E. S. Paul, N. Perrin, N. Poffe, N. Redon, H. Sergolle, J. F. Sharpey-Schafer, J. Simpsons, A. G. Smith and R. Wadsworth, Acta Phys. Pol. <u>B26</u>, 275 (1995).

REFERENCES FOR TABLE continued

1995Mo01   E. F. Moore, M. P. Carpenter, Y. Liang, R. V. F. Janssens, I. Ahmad, I. G. Bearden, P. J. Daly, M. W. Drigert, B. Fornal, U. Garg, Z. W. Grabowski, H. L. Harrington, R. G. Henry, T. L. Khoo, T. Lauritsen, R. H. Mayer, D. Nisius, W. Reviol and M. Sterrazza, Phys. Rev. $\underline{C51}$, 115 (1995).

1995Ne09   M. Neffgen, G. Baldsiefen, S. Frauendorf, H. Grawe, J. Heese, H. Hübel, H. Kluge, A. Korichi, W. Korten, K. H. Maier, D. Mehta, J. Meng, N. Nenoff, M. Piiparinen, M. Schönhofer, R. Schubart, U. J. van Severen, N. Singh, G. Sletten, B. V. Thirumala Rao and P. Willsau, Nucl. Phys. $\underline{A595}$, 499 (1995).

1995Sc04   R. Schwengner, G. Winter, J. Reif, H. Prade, L. Käubler, R. Wirowski, N. Nicolay, S. Albers, S. Eber, P. von Brentano and W. Andrejtscheff, Nucl. Phys. $\underline{A584}$, 159 (1995).

1995Ta21   S. L. Tabor and J. Döring, Phys. Scr. $\underline{T56}$, 175 (1995).

1996Ba53   G. Baldsiefen, H. Hübel, W. Korten, U. J. van Severen, J. A. Cizewski, N. H. Medina, D. R. Napoli, C. Rossi Alvarez, G. Lo Bianco and S. Signorelli, Z. Phys. $\underline{A355}$, 337 (1996).

1996Ba54   G. Baldsiefen, M. A. Stoyer, J. A. Cizewski, D. P. McNabb, W. Younes, J. A. Becker, L. A. Bernstein, M. J. Brinkman, L. P. Farris, E. A. Henry, J. R. Hughes, A. Kuhnert, T. F. Wang, B. Cederwall, R. M. Clark, M. A. Deleplanque, R. M. Diamond, P. Fallon, I. Y. Lee, A. O. Macchiavelli, J. Oliveira, F. S. Stephens, J. Burde, D. T. Vo and S. Frauendorf, Phys. Rev. $\underline{C54}$, 1106 (1996).

1996Br33   F. Brandolini, M. Ionescu-Bujor, N. H. Medina, R. V. Ribas, D. Bazzacco, M. De Poli, P. Pavan, C. Rossi Alvarez, G. de Angelis, S. Lunardi, D. De Acuña, D. R. Napoli and S. Frauendorf, Phys. Lett. $\underline{B388}$, 468 (1996).

1996Du18   L. Ducroux, A. Astier, R. Duffait, Y. Le Coz, M. Meyer, S. Perries, N. Redon, J. F. Sharpey-Schafer, A. N. Wilson, R. Lucas, V. Méot, R. Collatz, I. Deloncle, F. Hannachi, A. Lopez-Martens, M. G. Porquet, C. Schück, F. Azaiez, S. Bouneau, C. Bourgeois, A. Korichi, N. Poffe, H. Sergolle, B. J. P. Gall, I. Hibbert and R. Wadsworth, Z. Phys. $\underline{A356}$, 241 (1996).

1996Ka15   M. Kaci, M. G. Porquet, F. Hannachi, M. Aïche, G. Bastin, I. Deloncle, B. J. P. Gall, C. Schück, F. Azaiez, C. W. Beausang, C. Bourgeois, R. M. Clark, R. Duffait, J. Duprat, K. Hauschild, M. J. Joyce, A. Korichi, Y. Le Coz, M. Meyer, E. S. Paul, N. Perrin, N. Poffe, N. Redon, H. Sergolle, J. F. Sharpey-Schafer, J. Simpsons, A. G. Smith and R. Wadsworth, Z. Phys. $\underline{A354}$, 267 (1996).

1996Pe06   C. M. Petrache, Y. Sun, D. Bazzacco, S. Lunardi, C. Rossi Alvarez, R. Venturelli, D. De Acuña, G. Maron, M. N. Rao, Z. Podolyak and J. R. B. Oliveira, Phys. Rev. $\underline{C53}$, R2581 (1996).

1996Ro04   C. Rossi Alvarez, D. Vretenar, Zs. Podolyak, D. Bazzacco, G. Bonsignori, F. Brandolini, S. Brant, G. de Angelis, M. De Poli, M. Ionescu-Bujor, Y. Li, S. Lunardi, N. H. Medina and C. M. Petrache, Phys. Rev. $\underline{C54}$, 57 (1996).

1996Sm07   D. H. Smalley, R. Chapman, P. J. Dagnall, C. Finck, B. Haas, M. J. Leddy, J. C. Lisle, D. Prevost, H. Savajols, A. G. Smith, Nucl. Phys. $\underline{A611}$, 96 (1996).

1996Wi09   P. Willsau, M. Neffgen, Y. Le Coz, H. Hübel, W. Korten, F. Hannachi, A. Korichi, M. G. Porquet, M. Kaci, N. Redon, M. Meyer, C. W. Beausang, E. S. Paul, J. Simpson and J. R. Hughes, Z. Phys. $\underline{A355}$, 129 (1996).

1997Ch01   R. S. Chakrawarthy and R. G. Pillay, Phys. Rev. $\underline{C55}$, 155 (1997).

1997Ch33   S. Chmel, F. Brandolini, R. V. Ribas, G. Baldsiefen, A. Görgen, M. de Poli, P. Pavan and H. Hübel, Phys. Rev. Lett. $\underline{79}$, 2002 (1997).

1997Cl03   R. M. Clark, S. J. Asztalos, G. Baldsiefen, J. A. Becker, L. Bernstein, M. A. Deleplanque, R. M. Diamond, P. Fallon, I. M. Hibbert, H. Hübel, R. Krücken, I. Y. Lee, A. O. Macchiavelli, R. W. MacLeod, G. Schmid, F. S. Stephens, K. Vetter, R. Wadsworth and S. Frauendorf, Phys. Rev. Lett. <u>78</u>, 1868 (1997).

1997Ga01   A. Gadea, G. de Angelis, C. Fahlander, M. De Poli, E. Farnea, Y. Li, D. R. Napoli, Q. Pan, P. Spolaore, D. Bazzacco, S. M. Lenzi, S. Lunardi, C. M. Petrache, F. Brandolini, P. Pavan, C. Rossi Alvarez, M. Sferrazza, P. G. Bizetti, A. M. Bizetti Sona, J. Nyberg, M. Lypoglavsek, J. Persson, J. Cederkäll, D. Seweryniak, A. Johnson, H. Grawe, F. Soramel, M. Ogawa, A. Makishima, R. Schubart and S. Frauendorf, Phys. Rev. <u>C55</u>, R1 (1997).

1997Lo12   G. Lo Bianco, Ch. Protochristov, G. Falconi, N. Blasi, D. Bazzaco, G. de Angelis, D. R. Napoli, M. A. Cardona, A. J. Kreiner and H. Somacal, Z. Phys. <u>A359</u>, 347 (1997).

1997Pe06   C. M. Petrache, R. Venturelli, D. Vretenar, D. Bazzacco, G. Bonsignori, S. Brant, S. Lunardi, M. A. Rizzutto, C. Rossi Alvarez, G. de Angelis, M. De Poli and D. R. Napoli, Nucl. Phys. <u>A617</u>, 228 (1997).

1997Pe07   C. M. Petrache, Y. Sun, D. Bazzacco, S. Lunardi, C. Rossi Alvarez, G. Falconi, R. Venturelli, G. Maron, D. R. Napoli, Zs. Podolyak and P. M. Walker, Nucl. Phys. <u>A617</u>, 249 (1997).

1997Su11   M. Sugawara, H. Kusakari, Y. Igari, K. Terui, K. Myojin, D. Nishimiya, S. Mitarai, M. Oshima, T. Hayakawa, M. Kidera, K. Furutaka and Y. Hatsukawa, Z. Phys. <u>A358</u>, 1 (1997).

1998Cl06   R. M. Clark, R. Krücken, S. J. Asztalos, J. A. Becker, B. Busse, S. Chmel, M. A. Deleplanque, R. M. Diamond, P. Fallon, D. Jenkins, K. Hauschild, I. M. Hibbert, H. Hübel, I. Y. Lee, A. O. Macchiavelli, R. W. MacLeod, G. Schmid, F. S. Stephens, U. J. van Severen, K. Vetter, R. Wadsworth and S. Wan, Phys. Lett. <u>B440</u>, 251 (1998).

1998Fo02   N. Fotiades, J. A. Cizewski, D. P. McNabb, K. Y. Ding, D. E. Archer, J. A. Becker, L. A. Bernstein, K. Hauschild, W. Younes, R. M. Clark, P. Fallon, I. Y. Lee, A. O. Macchiavelli and R. W. MacLeod, Phys. Rev. <u>C57</u>, 1624 (1998).

1998Je03   D. G. Jenkins, I. M. Hibbert, C. M. Parry, R. Wadsworth, D. B. Fossan, G. J. Lane, J. M. Sears, J. F. Smith, R. M. Clark, R. Krücken, I. Y. Lee, A. O. Macchiavelli, V. P. Janzen, J. Cameron and S. Frauendorf, Phys. Lett. <u>B428</u>, 23 (1998).

1998Je09   D. G. Jenkins, R. Wadsworth, J. Cameron, R. M. Clark, D. B. Fossan, I. M. Hibbert, V. P. Janzen, R. Krücken, G. J. Lane, I. Y. Lee, A. O. Macchiavelli, C. M. Parry, J. M. Sears, J. F. Smith and S. Frauendorf, Phys. Rev. <u>C58</u>, 2703 (1998).

1998Ka59   M. Kaci, M-G. Porquet, Ch. Vieu, C. Schück, A. Astier, F. Azaiez, C. Bourgeois, I. Deloncle, J. S. Dionisio, J. Duprat, F. Farget, B. J. P. Gall, D. Han, A. Korichi, Y. Le Coz, M. Pautrat, N. Perrin, D. Santos and H. Sergolle, Eur. Phys. J. <u>A3</u>, 201 (1998).

1998Kr20   R. Krücken, R. M. Clark, A. Dewald, M. A. Deleplanque, R. M. Diamond, P. Fallon, K. Hauschild, I. Y. Lee, A. O. Macchiavelli, R. Peusquens, G. J. Schmid, F. S. Stephens, K. Vetter and P. von Brentano, Phys. Rev. <u>C58</u>, R1876 (1998).

1998La14   G. J. Lane, D. B. Fossan, C. J. Chiara, H. Schnare, J. M. Sears, J. F. Smith, I. Thorslund, P. Vaska, E. S. Paul, A. N. Wilson, J. N. Wilson, K. Hauschild, I. M. Hibbert, R. Wadsworth, A. V. Afanasjev and I. Ragnarsson, Phys. Rev. <u>C58</u>, 127 (1998).

REFERENCES FOR TABLE continued

1998Ne01   N. Nenoff, G. Baldsiefen, H. Hübel, A. Görgen, W. Korten, M. A. Deleplanque, R. M. Diamond, P. Fallon, I. Y. Lee, A. O. Macchiavelli and F. S. Stephens, Nucl. Phys. A629, 621 (1998).

1998Va03   P. Vaska, D. B. Fossan, D. R. LaFosse, H. Schnare, M. P. Waring, S. M. Mullins, G. Hackman, D. Prévost, J. C. Waddington, V. P. Janzen, D. Ward, R. Wadsworth and E. S. Paul, Phys. Rev. C57, 1634 (1998).

1999Cl03   R. M. Clark, S. J. Asztalos, B. Busse, C. J. Chiara, M. Cromaz, M. A. Deleplanque, R. M. Diamond, P. Fallon, D. B. Fossan, D. G. Jenkins, S. Juutinen, N. Kelsall, R. Kruken, G. J. Lane, I. Y. Lee, A. O. Macchiavelli, R. W. MacLeod, G. Schmid, J. M. Sears, J. F. Smith, F. S. Stephens, K. Vetter, R. Wadsworth and S. Frauendorf, Phys. Rev. Lett. 82, 3220 (1999).

1999Do02   J. Döring, D. Ulrich, G. D. Johns, M. A. Riley and S. L. Tabor, Phys. Rev. C59, 71 (1999).

1999Je07   D. G. Jenkins, R. Wadsworth, J. A. Cameron, R. M. Clark, D. B. Fossan, I. M. Hibbert, V. P. Janzen, R. Krücken, G. J. Lane, I. Y. Lee, A. O. Macchiavelli, C. M. Perry, J. M. Sears, J. F. Smith and S. Frauendorf, Phys. Rev. Lett. 83, 500 (1999).

1999JeAA   D. G. Jenkins, Private Communication (1999).

1999No03   J. R. Novak, C. W. Beausang, N. Amzal, R. F. Casten, G. Cata Danil, J. F. C. Cocks, J. R. Cooper, P. T. Greenlees, F. Hannachi, K. Helariutta, P. Jones, R. Julin, S. Juutinen, H. Kankaanpää, H. Kettunen, R. Krücken, P. Kuusiniemi, M. Leino, Benyuan Liu, M. Muikku, A. Savelius, T. Socci, J. T. Thomas, N. V. Zamfir, Jing-ye Zhang and S. Frauendorf, Phys. Rev. C59, R2989 (1999).

1999Po13   W. Pohler, G. Baldsiefen, H. Hübel, W. Korten, E. Mergel, D. Robbach, B. Aengenvoort, S. Chmel, A. Görgen, N. Nenoff, R. Julin, P. Jones, H. Kanakaanpää, P. A. Butler, K. J. Cann, P. T. Greenlees, G. D. Jones and J. F. Smith, Eur. Phys. J. A5, 257 (1999).

1999Sc14   H. Schnare, R. Schwengner, S. Frauendorf, F. Dönau, L. Käubler, H. Prade, A. Jungclaus, K. P. Lieb, C. Lingk, S. Skoda, J. Eberth, G. de Angelis, A. Gadea, E. Farnea, D. R. Napoli, C. A. Ur and G. Lo Bianco, Phys. Rev. Lett. 82, 4408 (1999).

1999Sc20   I. Schneider, R. S. Chakrawarthy, I. Wiedenhöver, A. Schmidt, H. Meise, P. Petkov, A. Dewald, P. von Brentano, O. Stuch, K. Jessen, D. Weisshaar, C. Schumacher, O. Vogel, G. Sletten, B. Herskind, M. Bergström and J. Wrzesinski, Phys. Rev. C60, 014312-1 (1999).